

UNIVERSIDADE DO ALGARVE

*Molecular mechanisms of
desiccation tolerance in Fucus*

Catarina Figueiredo da Mota

Tese submetida para obtenção do grau de doutor

Doutoramento em Ciências do Mar, da Terra e do Ambiente,

Ramo Ciências do Mar, Especialidade em Biotecnologia Marinha

Tese orientada por:

Doutor Gareth A. Pearson

Prof. Doutora Ester A. Serrão

2016

Declaração de autoria de trabalho

Declaro ser a autora deste trabalho, que é original e inédito. Autores e trabalhos consultados estão devidamente citados no texto e constam da listagem de referências incluída.

Catarina Figueiredo da Mota

Acknowledgements

A presente Tese foi apoiada pela Fundação para a Ciência e a Tecnologia (F.C.T) através da Bolsa de Doutoramento SFRH/BD/74436/2010, financiada pelo Programa Operacional Potencial Humano do QREN Portugal 2007-2013 e por verbas do Orçamento de Estado do MCTES.

Agradeço o apoio dos projectos Extant EXCL/AAG-GLO/0661/2012, UID/Multi/04326/2013 (Plurianual), do projecto ASSEMBLE (Association of European Marine Biological Laboratories) e da Rede de Excelência “Marine Genomics Europe”.

FCT Fundação para a Ciência e a Tecnologia

MINISTÉRIO DA EDUCAÇÃO E CIÊNCIA



Water is the driver of Nature.

- Leonardo da Vinci

Water, the Hub of Life.

Water is its mater and matrix, mother and medium.

Water is the most extraordinary substance!

Practically all its properties are anomolous, which enabled life to use it as building material for its machinery.

Life is water dancing to the tune of solids.

- Albert Szent-Gyorgyi (1972)

Lição sobre a água

Este líquido é água.

Quando pura

é inodora, insípida e incolor.

Reduzida a vapor,

sob tensão e a alta temperatura,

move os êmbolos das máquinas que, por isso,

se denominam máquinas de vapor.

É um bom dissolvente.

Embora com excepções mas de um modo geral,

dissolve tudo bem, bases e sais.

Congela a zero graus centesimais

e ferve a 100, quando à pressão normal.

Foi neste líquido que numa noite cálida de Verão,

sob um luar gomoso e branco de camélia,

apareceu a boiar o cadáver de Ofélia

com um nenúfar na mão.

- António Gedeão



Table of Contents

Declaração de autoria de trabalho.....	ii
Acknowledgements.....	iii
Table of Contents.....	v
Table Index.....	1
Figure Index.....	2
Resumo em português.....	3
Termos-chave.....	4
Abstract.....	5
Keywords.....	6
Abbreviations.....	7
Chapter 1 – General introduction.....	11
1.1 – Life without water - tolerance to water limitation.....	11
1.2 – Some important definitions: desiccation, drought and dehydration.....	14
1.3 – The Intertidal zone.....	16
1.4 - Aim of the thesis.....	17
1.5 – References.....	18
Chapter 2 - Differentiation in fitness-related traits in response to elevated temperatures between leading and trailing edge populations of marine macrophytes.....	19
2.0 - Abstract.....	21
2.1 - Introduction.....	22
2.2 - Material and methods.....	26
Model species and sampling.....	26
Heat shock experiment and physiological measurements.....	27
2.3 - Results.....	29
Photosynthetic efficiency.....	29
Gene expression.....	33
2.4 - Discussion.....	35
2.5 – References.....	40
2.6 – Acknowledgements.....	44
Supporting information.....	44

Chapter 3 – Some don't like it hot: microhabitat-dependent thermal and water stresses in a trailing edge population	47
3.0 – Summary	47
3.1 - Introduction.....	49
3.2 - Material & Methods.....	52
Model species and study site.....	52
Laboratory HSR and stress resilience experiments	52
Air and seawater temperatures.....	53
In situ measurements and sampling	53
RNA extraction and qPCR.....	54
3.3 - Results.....	55
Laboratory HSR and physiological resilience	55
Microhabitat temperature profiles.....	57
HS gene expression profiles in natural stands of <i>F. vesiculosus</i>	58
Current temperature regimes and regional warming trends.....	60
3.4 - Discussion.....	63
The HSR of <i>Fucus vesiculosus</i>	63
Does microhabitat variation moderate thermal stress?	64
Thermal conditions at the southern edge; a chronic heat stress environment.....	65
3.5 - References.....	67
3.6 – Acknowledgements	70
Supporting information	70
Chapter 4 – Optimizing protein extraction and separation to study desiccation-tolerance in <i>Fucus</i> macroalgae	73
4.0 - Abstract.....	73
4.1 – Introduction	75
4.2 – Material and methods	78
<i>In situ</i> desiccation and sampling	78
Protein extraction methods for <i>Fucus</i> spp.	78
Method A – Phenol extraction for brown algae.....	79
Method B – Ethanol/phenol method.....	79
Method C – Protein extraction using RNeasy columns (QIAGEN)	80
Method D – Plant fractionated protein extraction kit	81

Protein quantification.....	82
SDS-PAGE	82
2-DE.....	82
Image Analysis.....	83
4.3 – Results	84
Protein extraction methods for <i>Fucus</i> spp.	84
TWC after field desiccation	87
2-DE separation and image analysis	88
4.4 - Discussion	92
Protein extraction methods for <i>Fucus vesiculosus</i>	92
Protein separation, image analysis and detection of differentially expressed spots	93
4.5 - References.....	95
4.6 – Acknowledgements	98
Supporting information	98
Chapter 5 – Desiccation <i>in situ</i> : the importance of seaweed canopies in modulating temperature and desiccation stress.....	101
5.1 – Introduction	101
5.2 – Material and methods	104
Study site and microhabitat selection	104
Temporal stability of the Top microhabitat	104
Emersion stress in Top and Bottom microhabitats	105
TWC, temperature and F_v/F_m determinations	105
Proteomic analysis	107
5.3 - Results.....	108
Temporal stability of the Top microhabitat	108
Differences between Top x Bottom canopy microhabitats: TWC (desiccation)	110
Differences between Top and Bottom canopy microhabitats: tissue temperature.....	111
Differences between Top and Bottom canopy microhabitats: F_v/F_m (recovery).....	112
Correlations between temperature, desiccation and recovery F_v/F_m	112
Protein expression changes between Top and Bottom microhabitats.....	118
5.4 - Discussion	120
5.5 – References	122
5.6 – Acknowledgements	123

Supporting information	123
Chapter 6 –Proteomic profiling of desiccation-related proteins in furoid algae	127
6.1 – Introduction	127
6.2 – Materials and methods	131
<i>Fucus vesiculosus</i> and <i>F. serratus</i> ; sampling of High shore vs Low shore tissue.....	131
<i>Fucus vesiculosus</i> and <i>F. spiralis</i> ; laboratory desiccation and recovery	131
Protein phenol extraction for DIGE	132
Protein quantitation and DIGE labelling.....	132
DIGE	132
Image analysis and experimental design.....	133
Protein Identification	134
Functional annotation.....	135
6.3 – Results	136
High shore versus Low shore analysis	136
Laboratory desiccation with related species	146
The proteome of <i>F. vesiculosus</i>	150
6.4 – Discussion	153
6.5 - References.....	156
6.6 – Acknowledgements	158
Supporting information	158
Chapter 7 – Final conclusions and future directions.....	161
7.1 – Global overview	161
7.2 – Conclusions	164
7.3 – Future directions.....	165

Table Index

Table 2.1 - PERMANOVA of <i>Fucus vesiculosus</i> Fv/Fm from northern and southern edges	30
Table 2.2 - PERMANOVA of <i>Fucus vesiculosus</i> Fv/Fm from the northern and southern edges	30
Table 2.3 - PERMANOVA of <i>Zostera marina</i> Fv/Fm from the northern and southern edges	31
Table 2.4 - PERMANOVA of <i>Zostera marina</i> Fv/Fm from the northern and southern edges	31
Table 2.5 - Summary statistical analysis table of <i>Fucus vesiculosus</i> gene expression.	34
Table 3.1 – Rates of change in sea surface temperature (SST) and mean minimum (Tm), average (T) and maximum (TM) air temperatures in the Faro region.	62
Table 4.1 – Protein yields obtained with different extraction protocols from <i>Fucus</i> tissues.	85
Table 4.2 – Average Tissue Water Content (TWC) of the desiccated algae (n = 3 tips per plant).	87
Table 4.3 – Small gel protein spots changing expression during recovery from desiccation.	90
Table 4.4 – Large gel protein spots changing expression during recovery from desiccation.	91
Table 5.1 – Percentage observations on the Top microhabitat per tip and per individual of <i>Fucus vesiculosus</i> .	108
Table 5.2 – Percentage observations on the Top microhabitat per tip and per individual of <i>F. serratus</i> .	109
Table 5.3 – Size and branching of the <i>Fucus serratus</i> and <i>F.vesiculosus</i> individuals.	109
Table 5.5 – Candidate differentially expressed protein spots between Top and Bottom microhabitats, in <i>F. serratus</i> (n=5).	118
Table 5.6 – Candidate differentially expressed protein spots between Top and Bottom microhabitats, for <i>F.vesiculosus</i> (n=6).	119
Table 6.1 – Sample labels and gel loading design of the DIGE experiments.	133
Table 6.2 – Protein changes between High and Low shore samples in <i>Fucus vesiculosus</i> (n=5).	137
Table 6.3 – Protein changes between High and Low shore samples in <i>Fucus serratus</i> (n=5).	138
Table 6.4 – Protein changes between High and Low shore samples (<i>F. serratus</i> and <i>F. vesiculosus</i> , n=10).	139
Figure 6.2 – Predicted size of the <i>F. serratus</i> proteins and their corresponding db sequences.	140
Table 6.5 – Annotation of <i>Fucus serratus</i> proteins from High and Low shore samples (Roscoff).	142
Table 6.6 – Pathway and superpathway representation of the total identified proteins.	145
Table 6.7 – Protein changes between Control and Recovery samples in <i>Fucus spiralis</i> (n=4).	147
Table 6.8 – Protein changes between Control and Recovery samples in <i>Fucus vesiculosus</i> (n=4).	147
Table 6.9 – Protein changes between Control and Recovery samples (mixed species, n=8).	148
Table 6.10 – Annotations of <i>Fucus spiralis</i> proteins from laboratory desiccation.	149
Table 6.11 –KEGG pathway hits from the proteome and the transcriptome of <i>Fucus</i> .	151

Figure Index

Figure 2.1 - Normalised maximum quantum yield (Fv/Fm) for the alga <i>Fucus vesiculosus</i> from the leading (Greenland, blue) and rear (Portugal, red) edge ...	38
Figure 2.2 - Normalised maximum quantum yield (Fv/Fm) for the seagrass <i>Zostera marina</i> from the leading (Greenland, blue) and trailing (Portugal, red) edge ...	41
Figure 2.3 - Expression of seven heat shock transcripts in response to control (10 °C) and elevated seawater temperatures (24, 28 and 32°C), ...	44
Figure 3.1 - <i>F. vesiculosus</i> response after 3 h of heat-shock at 24, 28, 32 and 36 °C and following 24 h recovery.	64
Figure 3.2 - Site maximum air temperatures, tidal cycle and microhabitat temperatures.	65
Figure 3.3 - Gene expression for 7 Hsp transcripts in the field microhabitats...	68
Figure 3.4 - Relationship between temperature and HSP20_2 expression for January and August field samples.	69
Figure 3.5 - Air and seawater temperatures in the Ria Formosa in 2012.	70
Figure 4.1 – SDS-PAGE profiles of <i>Fucus vesiculosus</i> extracted with the four protocols.	96
Figure 4.2 – Representative Coomassie-stained small gel. <i>F. vesiculosus</i> sample C3	97
Figure 4.3 – Representative Coomassie-stained large gel. <i>F. vesiculosus</i> sample C3	97
Figure 5.1 – Experimental setup for microhabitat characterization.	115
Figure 5.2 – Frequency on the Top microhabitat for <i>Fucus serratus</i> and <i>F. vesiculosus</i> .	118
Figure 5.3 – Tissue Water Content of the <i>Fucus serratus</i> and <i>F.vesiculosus</i> tips (n = 6) at the end of the low tide emersion between 24 and 30 May, 2013.	121
Figure 5.4 – Tissue temperatures on six Top and six Bottom <i>Fucus serratus</i> apical tips	121
Figure 5.5 – Tissue temperatures on Top and Bottom microhabitats.	122
Figure 5.6 – Tissue temperatures of <i>Fucus serratus</i> and <i>F.vesiculosus</i> microhabitats	122
Figure 5.7 – Recovery Fv/Fm on Top and Bottom microhabitats in May, 2013.	123
Figure 5.8 – Recovery Fv/Fm and TWC on Top and Bottom microhabitats in June, 2013.	123
Figure 5.9 – Recovery Fv/Fm and TWC on Top and Bottom microhabitats in June, 2013.	124
Figure 5.10 – Microhabitat differences in desiccation, recovery Fv/Fm and (peak) tissue temperature between Top (T) and Bottom (B) microhabitats.	125
Figure 5.11 – Correlation between microhabitat parameters: Tmax, TWC, Fv/Fm.	126
Figure 5.11 – Representative gel image of a Bottom sample from <i>F. serratus</i>	128
Figure 6.1 – Sample/dye combinations of the DIGE experiments.	140
Figure 6.2 – Predicted size of the <i>F. serratus</i> protein spots and their corresponding db sequences.	148

Resumo em português

Na zona entre marés existem diversas macroalgas (castanhas, verdes e vermelhas), pertencentes a três linhagens multicelulares independentes e pouco estudadas, contendo espécies tolerantes e espécies intolerantes à dessecação, o que faz delas bons modelos para o estudo da tolerância à dessecação.

Recentemente, a atenção dada à distribuição de *Fucus vesiculosus* sob efeito das alterações climáticas levou-nos a querer determinar os limites subletais máximos de temperatura desta alga castanha, utilizando indicadores fisiológicos e alterações da expressão genética para descrever a temperatura de indução e o perfil da resposta ao choque térmico em diversas populações desta espécie. Vimos que conhecer a temperatura ambiente não é suficiente para antecipar o choque térmico sentido pela alga, ao mesmo tempo que os microhabitats formados pelo tapete de algas vão influenciar a temperatura local e afectar a resposta ao choque térmico. Surpreendentemente, no microhabitat mais quente as algas aparentavam estar protegidas do choque térmico pela dessecação rápida e intensa.

Estudos de proteómica em algas castanhas foram facilitados recentemente graças a recursos genéticos, a sequenciação do genoma completo da espécie modelo, *Ectocarpus siliculosus*, numerosas sequências de transcriptos de *Fucus*, obtidas pelas novas técnicas de sequenciação e avanços técnicos no estudo de outros organismos com compostos secundários semelhantes que interferem com a qualidade e a quantidade das proteínas extraídas. Foi otimizado um protocolo de extracção de proteínas de algas do género *Fucus*, que foi utilizado para investigar a expressão diferencial de proteínas em resposta à dessecação tanto por 2DE convencional como por 2D-DIGE. Não foram detectadas alterações significativas nos perfis de proteínas na sequência da dessecação ou da rehidratação, o que sugere a importância de mecanismos constitutivos de tolerância, minimizando os custos metabólicos da expressão de novos genes, enquanto a dessecação protege do choque térmico.

Estudos de campo, em locais de intensa dessecação ou protegidos, após exposição consecutiva ao stress de emersão, e após dessecação em condições controladas no laboratório, todos falharam na identificação de alterações robustas na expressão de proteínas envolvidas na tolerância à dessecação. Caracterizámos o primeiro proteoma extraível de *F. vesiculosus*,

identificando as proteínas por LC-MS/MS e anotando utilizando as bases de dados de algas castanhas. Esta anotação foi bem-sucedida, apesar da fraca anotação funcional das proteínas de algas castanhas e da presença de múltiplas proteínas em alguns dos spots.

Termos-chave

Tolerância à dessecação, perfil proteômico, microhabitats, Electroforese Diferencial em gel (DIGE), *Fucus vesiculosos*, *Fucus serratus*, *Fucus spiralis*.

Abstract

Intertidal algae (brown, red and green) are three understudied and independent multicellular lineages possessing related intolerant and desiccation tolerant species, making them good models for desiccation tolerance research.

Recent focus on distribution of *Fucus vesiculosus* under climate change led us to determine the upper thermal limits of this brown algae, using physiological indicators and gene expression responses to describe the induction and thermal characteristics of the heat-shock response in diverse populations. Ambient temperatures were poor predictors of the heat-stress experienced by intertidal algae, instead the microhabitats created by the algal canopy modulated the local thermal environment and influenced the stress response. Surprisingly, in the hottest microhabitat algae appeared to be protected from thermal stress by fast and intense desiccation.

Proteomic research in brown algae has recently been facilitated by genomic resources, complete genome sequencing of model species and large-scale transcriptomic resources from *Fucus* species, and by technical advances in work on organisms with similar interfering compounds. We tested and optimized a protein extraction protocol suitable for intertidal *Fucus* algae and used it to investigate differential expression of proteins in response to desiccation, both by conventional 2DE and by DIGE. No significant changes of the protein profiles were detected after desiccation or rehydration, suggesting the importance of constitutive tolerance mechanisms, minimizing the metabolic cost of gene expression, while the desiccated state provides protection against heat stress.

Studies of distinct field environments (desiccation-prone or –protected), of sequential emersion stress exposure and of laboratory desiccation under controlled conditions, all failed to identify robust protein expression changes attributable to desiccation tolerance. We characterized the first extractable proteome of *F. vesiculosus* by LC-MS/MS identification and annotation against brown algal protein databases, with considerable success despite limited functional annotation in brown algae proteins, and the presence of multiple proteins in some spots.

Keywords

Desiccation tolerance, proteomic profiles, intertidal microhabitats, difference gel electrophoresis (DIGE), *Fucus vesiculosos*, *Fucus serratus*, *Fucus spiralis*.

Abbreviations

2D-DIGE, DIGE - Two-dimensional difference gel electrophoresis

2DE - Two-dimensional electrophoresis

Bis-Tris - (Bis(2-hydroxyethyl) aminotris (hydroxymethyl) methane)

BSA – Bovine Serum Albumin

CBB – Coomassie Brilliant Blue

CHAPS - 3-[(3-Cholamidopropyl)dimethylammonio]-1-propanesulfonate

Cy2, Cy3, Cy5 –fluorescent cyanine dyes (reactive NHS esters) for protein labelling

Des - Desiccation

DTT –DL-Dithiothreitol, threo-1,4-Dimercapto-2,3-butanediol

DW – Dry Weight

Fser – Fucus serratus

Fspir– Fucus spiralis

F_v/F_m –optimal quantum yield of PSII (ratio of variable to maximal fluorescence), the maximum photochemical efficiency of PSII reaction centres of dark adapted leaves

Fves– Fucus vesiculosus

IEF – IsoElectric Focusing (first dimension of protein separation by 2DE)

liqN₂ – liquid nitrogen

MW- Molecular Weight

pI – Isoelectric point

PSII – Photosystem II

PVP-40 – Polyvinylpyrrolidone with an average MW of 40,000 Da, a polymer of N-vinylpyrrolidone (1-ethenylpyrrolidin-2-one)

PTM – Post- translational modifications

Rec - Recovery

SDS - Sodium Dodecyl Sulfate,

SDS-PAGE - Sodium Dodecyl Sulfate-PolyAcrylamide Gel Electrophoresis

TCA - Trichloroacetic acid

Tris –Tris(hydroxymethyl)aminomethane; 2-Amino-2-(hydroxymethyl)-1,3-propanediol

TWC – Tissue Water Content

TGS buffer – Tris-Glycine-SDS electrophoresis buffer

Chapter 1

General introduction

Chapter 1 – General introduction

1.1 – Life without water - tolerance to water limitation

Water is essential for life as we know it. Living cells contain a large percentage of water, a small molecule with unusual properties that allows the myriad of biochemical reactions required to sustain life. From the very start, organic molecules are thought to have originated in an aqueous environment, and after a very long and extraordinary story of increasing diversification and complexity, water never lost its fundamental role in life.

Despite this universal dependence on water, not all cells are created equal. Water is the major constituent of living cells, and water balance is strictly regulated to maintain ionic balance, solute concentration and the hydration shell of biomolecules, preserving the structure of intracellular macromolecules and membranes. In the oceans, where life is thought to have arisen, obtaining water was probably not too hard (osmotic balance aside!), but many adjustments had to be made for living organisms to colonize dry land. Land plants and animals developed impermeable surfaces to decrease water loss, along with a large assortment of complex mechanisms to regulate their water content and osmotic balance. Animals can physiologically adjust the levels of water loss by transpiration and renal and digestive excretion, actively search for available water to drink and minimize exposure to extreme temperatures that promote higher evaporation. Vascular plants control stomatal opening and transpiration and developed elaborate root systems to collect water. Ultimately these mechanisms will all collapse if water cannot be obtained, but even minor improvements on growth, reproduction and survival during periods of water-shortage can translate in competitive advantages, selecting for increased tolerance in adverse environments. This should be particularly relevant where water is often unavailable, as arid and polar regions, but can also occur in the rocky intertidal, where many organisms of marine origin face a periodically emersed environment that some species learned to tolerate with remarkable success.

Given the importance of water balance for all cells, it is no surprise to find reports of major impacts of even small decreases in water content. In humans, loss of 20% of body fluids is considered severe dehydration, with serious health consequences. Dehydration is a major cause of death in children, mostly associated to diseases that cause fever or diarrhea. It is also a major health issue in elderly people that can have chronic dehydration for not feeling the need to drink enough to replace water loss. Drought has large social and economic impacts, and even short dry spells can have large effects on major agricultural crop yields. It is no surprise to find extensive research into the mechanisms involved in water balance and tolerance to water-limitation in a large diversity of organisms, mainly in vascular plants due to the economic impacts of drought. Aiming at developing new crop varieties more resistant to drought, high temperatures or salinity, of increasing concern in a warming world with a growing human population to feed, the molecular mechanisms associated to drought and desiccation tolerance have been extensively probed, not only in major crops and established model organisms but in species that present exceptional tolerance to these stresses. From our still limited knowledge, we know that even related organisms can cope with water shortages in distinct ways, and by comparing strategies used by diverse lineages we may start to understand their particular advantages and disadvantages and the impact they must have had on the evolution of the terrestrial biota. Desiccation tolerance is also of interest for cryogenics, since freezing damage caused by formation of ice crystals can be avoided by cryoprotectants that are typically sugar molecules involved in freezing-, desiccation- and osmotic-tolerance. Despite many advances, there are still many unanswered questions on the interplay of known protective mechanisms, and new players are still being identified, even in flowering plants.

There seems to be two major strategies to avoid lethality due to water limitation. Avoidance is a popular strategy: many organisms, like humans, cannot tolerate relatively mild dehydration so they must retain access to water sources to replenish unavoidable losses. Despite mechanisms to reduce water loss in transpiration, urine and faeces, an active human in very hot weather can dehydrate and die of heat-stroke in just a few hours, after the need to conserve water overrides the regulation of body temperature by evapo-transpiration. On the other extreme we find desiccation tolerant organisms that remain viable after having lost virtually all their tissue water, in a metabolic inactive state that is reverted by rehydration. Such organisms, often unicellular or microscopic, can remain inactive for extended periods

without water, during which many can endure extreme temperatures, radiation or vacuum (reviewed in Leprince & Buitink, 2015).

Desiccation tolerant organisms are not rare, and have been found in many taxa, but not all can endure dehydration in the same circumstances. In many cases only a specific life-stage (e.g. spores, seeds) can survive desiccation. While many organisms benefit from slower desiccation rates (days or weeks) (Oliver et al 2005, Gasulla et al, 2013) others can benefit from faster (hours) desiccation (Mota et al, 2014). Current knowledge on the underlying mechanisms is lacking or very limited in most phyla, not allowing these observations to be conciliated into a general framework.

Research on tolerance to water limitation (dehydration, drought or desiccation) and related topics (osmotic stress and freeze-tolerance) is mostly performed on vascular plants aiming to improve crop yields, but some advances have been made by comparative studies across taxa, and detailed examination of related organisms that differ on their desiccation-tolerance (Leprince & Buitink, 2015). Among the least studied groups, intertidal algae possess some unique characteristics: algae are marine organisms, lacking the mechanisms developed by terrestrial plants to regulate water contents (e.g. roots, vascular transport, cuticles and stomata), their water content equilibrates to surrounding air, so they can desiccate quickly during low tide emersion. High intertidal macroalgae that tolerate desiccation to very low water contents can be found on three distant taxa (brown, red and green algae), often alongside related species occurring lower in the intertidal that are sensitive to desiccation. Contrary to most other multicellular models, that require slow desiccation rates and extended recovery periods and often undergo only seasonal or infrequent drying, intertidal algae undergo frequent and swift desiccation and require fast recovery to maintain positive growth. We propose that brown intertidal algae from the genus *Fucus* are a good model in which to study desiccation tolerance. Fucales belong to an understudied and independently evolved multicellular lineage, whose recent radiation, producing related, co-distributed, intertidal species with distinct desiccation-tolerances, allows for a comparative framework to identify the development of desiccation tolerance. The identification of these mechanisms in brown algae, a taxon unrelated to traditional models, will allow further insights into the (convergent?) evolution in the three main algal groups, where current research also starts to provide some insight into the molecular mechanisms of tolerance to desiccation.

1.2 – Some important definitions: desiccation, drought and dehydration

Historically, much attention has been given to water limitation in agriculture, where the negative effects of drought on crop yields have induced research on drought-tolerance. Drought tolerance typically relies on the avoidance of water loss, which is quite distinct from desiccation tolerance, the ability to survive extensive tissue water loss and recover physiologic functions upon rehydration. While most vascular plants are desiccation-sensitive, regardless of their ability to obtain and conserve water (drought tolerance), some species (like resurrection plants) are desiccation-tolerant, using their ability to desiccate and recover after prolonged dormancy to survive drought conditions (Dinakar et al, 2013).

Research on cellular dehydration independently focused on other organisms capable of surviving in a dry (desiccated) state, but the extent of water loss sustained to consider an organism desiccation-tolerant varies across studies. In some cases, desiccation tolerance is equated to anhydrobiosis. Anhydrobiosis, or life without water, is the ability to survive desiccation in equilibrium with dry air, attaining a stable state of suspended animation, reversible simply by rehydration (Rebecchi et al, 2007). Metabolism is assumed to cease under 10% absolute water content (0.1g H₂O per g of dry mass), roughly equivalent to equilibration with air of 50% relative humidity at 20°C (Alpert et al, 2006), which probably is not enough water to form a monolayer around proteins and membranes (Billi and Potts, 2002, Alpert et al, 2006). In practice however, it can be difficult to confirm the complete cessation of all metabolism, or even to state when an organism is completely “dry”, because small amounts of water often remain in air-dried tissues. The water-threshold for desiccation tolerance also varies, e.g. Gasulla et al, 2013 consider a water content of between 0.5 and 0.3 g g dm⁻¹ (citing Alpert & Oliver 2002) resulting from drying to equilibrium with air at a relative humidity (RH) of 50%. This is because mass-based values, like absolute water content, ignore composition differences across species and tissues, and these thresholds often do not clearly express equilibrium water contents (Alpert & Oliver 2002).

Also the ability to recover depends on a number of factors, like desiccation rate, exposure to additional stressors and duration of the desiccated period, leading to conflicting characterization of desiccation-tolerant or sensitive species, depending on the experimental setup. For these reasons, in this work I will not define desiccation tolerance as anhydrobiosis, as I did not verify the suspension of all (detectable) metabolic functions, and despite apparent rapid air-drying for extended periods the absolute water content of *Fucus* apical tissue was

always well above 10% (of dry weight). Instead I will consider a gradient of desiccation-tolerance, where the more tolerant species fully recover after prolonged equilibration with dry air and suspension of metabolism, while sensitive species do not survive even mild air drying. In between, a range of organisms may be able to recover from considerable water loss, depending on a number of factors, including final water content, drying rate, the presence of additional stressors (light, temperature), or optimal conditions during recovery.

Likewise the words dehydration (and desiccation) will refer to a level of water loss from an organism or tissue, not restricted to a state of complete absence of tissue water. Cells or tissues will be said to dehydrate (or desiccate) even if they are not shown to be in equilibrium with the relative humidity in the air. This approach is more suited to studies in intertidal organisms, whose natural exposure to desiccation conditions is constrained by tidal regimes and local conditions, and the relative humidity in the frond microhabitat cannot be easily determined. Natural fluctuations of light, temperature and wind exposure may also be more relevant for the intensity of macroalgae dehydration upon emersion than relative humidity, since the thin exposed fronds quickly lose water during the initial hours, but tend to stabilize after reaching a threshold, retaining a small fraction of bound water, even when remaining exposed for prolonged periods.

Maintaining viability when desiccated is not trivial. As cells lose water, they shrink, which may cause the membranes to fold and detach from the cell wall. As less solvent is present, osmotic strength rises, proteins and other molecules tend to denature and aggregate and metabolism is disrupted, producing oxidants that will further damage macromolecules. And during the period of desiccation, that may be long, cells may be exposed to additional stressors, like UV radiation, causing more molecular damage. After desiccation, rehydration can be even more detrimental: rapid water uptake may cause the cell membranes to burst, and all the damaged, aggregated or oxidised molecules that have accumulated will now be free to interfere with the other cellular components, until they can all be repaired or removed. Antioxidants have been identified as important in rehydration in several organisms (Dinakar *et al.* 2012), as they can remove free radicals (like reactive oxygen species, ROS) that can initiate chain reactions damaging multiple cellular components (lipids, DNA, proteins).

Desiccation tolerant organisms must be able to lose water without sustaining irreversible damage. Cellular constituents must be stabilized, avoiding the loss of membrane integrity during cell shrinkage. Organelles like mitochondria and plastids, source of reactive radicals,

must be stabilized and efficient mechanisms should be in place to quench produced radicals and avoid detrimental chain reaction causing lasting cellular damage. Protein aggregation must be avoided, or stabilized and repaired shortly after rehydration. Diverse lineages use diverse strategies to achieve desiccation tolerance, and this work aims to elucidate them in intertidal brown algae, now that molecular resources are available for this poorly studied branch of photosynthetic eukaryotes.

1.3 – The Intertidal zone

The intertidal zone comprises an area that is submerged during high tides and left air-exposed during the low tides. This leaves organisms living in the intertidal zone to cope with this frequent shift between marine and terrestrial exposure, requiring an high tolerance to major abiotic stressors. In terrestrial organisms, it is the salinity that is detrimental to most plants, evolved relying on freshwater, and upper intertidal flora is characteristically salt-tolerant (halophytes). Marine algae face a similar challenge in estuarine areas, where freshwater inflow requires additional effort to maintain adequate osmotic balance within cells. Compared to subtidal environments, the intertidal is exposed to larger temperature shifts, since tidepools or shallower waters don't benefit from the large thermal buffering capability of large bodies of water. And when exposed to the air, the algae not only lose thermal stability, they also experience stronger solar irradiation and salinity shifts, when evaporation from pools leaves behind an hypersaline medium, or when rainwater pours down on the dehydrated fronds and fills the tidepools.

Intertidal algae are poikilohydric organisms, those that lack mechanisms to prevent water loss, so their tissue water equilibrates to the relative humidity of the surrounding medium. When submerged these algae remain fully hydrated, but when exposed to air (of low or moderate) relative humidity, at low tide, particularly in exposed (windy) areas, these algae will desiccate.

1.4 - Aim of the thesis

The main objective of this thesis was to understand the molecular basis of desiccation tolerance in the brown algal genus *Fucus*, via the identification of desiccation-responsive proteins involved in protection, regulation, stabilization and repair of desiccation-induced cellular damage. *Fucus* macroalgae are intertidal poikilohydric autotrophs, evolutionarily distant from the major models in desiccation-tolerance studies: angiosperms, particularly resurrection plants, bryophytes, tardigrades, rotifers and nematodes. Unlike these organisms, intertidal algae experience frequent desiccation cycles that potentiate high desiccation rates and fast recovery of photosynthesis, probably possessing novel desiccation-tolerance mechanisms adjusted to its intertidal lifestyle.

Our goals were to contrast the proteomic profiles under desiccation/rehydration with hydrated controls to identify differentially expressed proteins with a role in desiccation-tolerance. The functional characterization of these proteins would allow the identification of the mechanisms maintaining cellular integrity and metabolism despite severe water loss.

To address the issue of desiccation tolerance from a proteomic perspective, new methods for protein extraction and 2DE separation were adapted for *Fucus* brown algae and used to identify proteins responsive to desiccation. As initial proteomic profiling revealed only non-significant protein expression changes after desiccation/rehydration, additional experiments aimed to clarify whether desiccation-tolerance is constitutively expressed, derived from extended acclimation periods or responsive to environmental conditions over several days.

Functional characterization of the total extractable proteome of *F. vesiculosus* provided an array of information about the protein component of this algal tissue.

1.5 – References

- Alpert, P. & Oliver, M. J. (2002). Drying without dying. In: Black M, Pritchard HW (eds) Desiccation and survival in plants: drying without dying. CABI, Wallingford, pp 3 –4 6.
- Alpert, P. (2006). Constraints of tolerance: why are desiccation-tolerant organisms so small or so rare? *J. Exp. Biol.* 209, 1575-1584
- Billi, D., and M. Potts. (2002). Life and death of dried prokaryotes. *Res. Microbiol.*, 1537-12.
- Charron, A. J. & Quatrano R.A. (2009). Between a Rock and a Dry Place: The Water-Stressed Moss. *Molecular Plant*, 2 , (3) , 478 – 486
- Dinakar, C., Bartels, D. (2013). Desiccation tolerance in resurrection plants: new insights from transcriptome, proteome and metabolome analysis. *Frontiers in Plant Science* 4:482
- Dinakar, C., Djilianov, D., Bartels, D. (2012). Photosynthesis in desiccation tolerant plants: energy metabolism and antioxidative stress defense. *Plant Sci* 182: 29–41.
- Gasulla, F, Jain, R, Barreno, E, Guéra, A, Balbuena, TS, Thelen, J, Oliver, M (2013). The response of *Asterochloris erici* (Ahmadjian) Skaloud et Peksa to desiccation: a proteomic approach. *Plant Cell Environ* 36: 1363–1378. doi: 10.1111/pce.12065
- Holzinger, A. & Karsten, U. (2013). Desiccation stress and tolerance in green algae: consequences for ultrastructure, physiological, and molecular mechanisms. *Frontiers in Plant Science*, 4:327.
- Leprince O and Buitink J (2015) Introduction to desiccation biology: from old borders to new
- Oliver MJ, Velten J, Mishler BD (2005) Desiccation tolerance in bryophytes: a reflection of the primitive strategy for plant survival in dehydrating habitats. *Integrative and Comparative Biology* 45:788–799
- Oliver, M. J., Tuba, Z., & Mishler, B. D. (2000). The evolution of vegetative desiccation tolerance in land plants. *Plant Ecology*, 151(1), 85-100.
- Oliver, M.J., Velten, J. & Mishler, B.D. (2005). Desiccation Tolerance in Bryophytes: A Reflection of the Primitive Strategy for Plant Survival in Dehydrating Habitats?. *Integrative and Comparative Biology*; 45 (5): 788-799.
- Proctor, M. C. F. & Pence, V. C. (2002). Vegetative tissues: bryophytes, vascular resurrection plants and vegetative propagules. In: Black M, Pritchard HW (eds) Desiccation and survival in plants: drying without dying. CABI, Wallingford, pp 207
- Rebecchi, L., Altiero, T. and Guidetti, R. (2007). Anhydrobiosis: the extreme limit of desiccation tolerance. *Invertebr. Survival J.* 4, 65-81

Chapter 2

Differentiation in fitness-related traits in response to elevated temperatures between leading and trailing edge populations of marine macrophytes.

Chapter 2 - Differentiation in fitness-related traits in response to elevated temperatures between leading and trailing edge populations of marine macrophytes.

2.0 - Abstract

The nature of species distributions, including factors influencing shifting range margins and responses to rapid environmental change, are key subjects in ecology, evolution and conservation research. Populations at the limits of distribution are often at the forefront of climate-related environmental change. Despite research efforts, little is known about performance differences of fitness-related traits in leading versus trailing edge range populations. We tested whether fitness and adaptive potential differ between distributional leading and trailing range edge populations of two foundation marine macrophytes, the intertidal *Fucus vesiculosus* and the subtidal *Zostera marina*. The tolerance and resilience of edge populations to elevated seawater temperatures was compared in common garden experiments combining a comparative ecophysiological approach using photosynthetic indicators with heat shock protein (Hsp) gene expression studies. The southern (trailing) edge population of the intertidal species showed higher thermal tolerance and resilience while fitness at elevated temperatures was eroded at the leading edge of *F. vesiculosus*. In contrast, the subtidal seagrass *Z. marina* showed slightly reduced resilience at the trailing edge which might reflect low fitness-related genetic variability and restricted evolvability in these low-diversity edge populations. Our results confirm that differentiation of thermal stress response can occur between leading and trailing edges.

Manuscript in preparation:

Aschwin H. Engelen*, Catarina Mota*, Ester A. Serrao, Márcio Coelho, Núria Marbà, Dorte Krause-Jensen, Gareth A. Pearson (* Authors with equal contribution)

2.1 - Introduction

In the current context of climate change, predictions of future environmental scenarios often involve research on climate-related species distribution shifts. Predictive models typically rely on observed distributions to derive estimates of which environmental variables set the range limits of a particular species. Such modelling approaches implicitly assume a homogeneous behaviour, in which all populations of a species have the same tolerance response to environmental stressors. However, previous ecological, evolutionary and conservational studies have widely questioned the limits of adaptive evolution at range margins on one hand (Bridle & Vines 2006; Eckert *et al.* 2008), and the importance of rear-edge refugial populations for biodiversity on the other (Hampe & Petit 2005), implying that separate populations of a species can present distinct genetic and phenotypic features. There is qualified support for the expectation that peripheral populations tend to have low genetic diversity, originating from reduced population size and genetic drift in fragmented or heterogeneous habitats, while reduced gene flow may also result in high differentiation between isolated edge populations (Eckert *et al.* 2008). Rapid environmental change is expected to trigger ecological and evolutionary responses (Jump & Penuelas 2005; Parmesan 2006; Willi *et al.* 2006), which will particularly affect peripheral populations at range edges restricted by climate-related factors. The relative performance of fitness-related traits in peripheral populations is still poorly studied. At present, little is understood about the adaptive potential of marginal populations under predicted climate change scenarios, and how this may vary at leading versus trailing edges. The ‘abundant-center hypothesis’, widely accepted in biogeographical ecology, establishes a decline in abundance toward range edges. When gradients of abiotic stress shape species distributions this ‘benign center’ provides the most favourable conditions that progressively decline until the range limits, where the stress levels are too high to allow population persistence.

More recent empirical work, particularly some done in coastal marine systems (Sagarin & Gaines 2002, Helmuth *et al.* 2002, 2006; Sagarin & Somero 2006) has challenged this ‘abundant center’ view, replacing it with a complex view where variation in environmental factors (e.g. temperature, tides, light exposure) produces a mosaic of stress factors and their intensities (Helmuth *et al.* 2002; Williams & Dethier 2005). Steep vertical abiotic stress gradients have been widely described in intertidal habitats and are known to set the upper boundaries of species distributions (Connell 1972; Dring & Brown 1982; Chapman 1995;

Davison & Pearson 1996; Somero 2002; Davenport & Davenport 2005). These steep gradients may cause intertidal or shallow-water species to be particularly susceptible to climatic change (Southward *et al.* 1995; Hawkins *et al.* 2003), making them early warning indicators of disturbance. As climatic effects should be easiest to detect where abiotic factors, rather than biotic interactions, constrain a species' distribution, there is a strong argument for studying organisms whose range edge is set mainly by physical factors. Knowledge of how the ecology, genetics, and physiology of these intertidal or shallow-water organisms interplay with abiotic stress factors to shape their distribution range should help predict these ecosystem's responses to climate change.

Temperature is one of the main physical factors that determine the distribution of species. Biogeographic distributions of many macrophytes have been explained by temperature adaptation, phenotypic acclimation of performance and temperature tolerance (Eggert 2012). Most studies that link temperature and species distribution have focused on mean conditions over time (Easterling *et al.* 2000), whereas temperature extremes can substantially stress performance and restrict survival and reproduction (Helmuth *et al.* 2005). This is increasingly so in environments with large temperature fluctuations like in intertidal or shallow water habitats in the marine realm. Global climate change is characterised by both the change in mean variables and the increase in extreme events that strongly impact ecosystems and associated species (Easterling *et al.* 2000; Walther *et al.* 2002). Habitat foundation species, such as trees, and macrophytes, often form the basis for entire ecosystems that may depend on the stability and performance of a single species (Jones *et al.* 1994). When these extreme events, like heat waves, droughts, or heavy precipitation (Easterling *et al.* 2000) impact foundation species, in both marine and terrestrial habitats, they may severely disturb an entire ecosystem. Foundation species in the intertidal/shallow subtidal regions of northern hemisphere temperate coasts frequently include brown algae of the genus *Fucus* or seagrasses of the genus *Zostera* when either a hard or soft substrate is available, respectively. Stands of these bioengineer species can provide feeding, nursery habitat and shelter from some abiotic stressors, facilitating occupation by other species and thus enhancing diversity). While the seagrass root and rhizome systems stabilize sediments, the macrophyte canopy alters the hydrodynamic environment (reviewed in Madsen *et al.* 2001) and allows suspended particles to sediment (e.g. Terrados & Duarte 2000). Hence, the resilience and persistence of foundation species in the face of climate change is of particular interest and importance.

Resilience to desiccation and heat shock have been shown to differ between central and trailing edge populations of foundation macro algae as well as be species dependent. Central populations of *F. serratus* (UK) were more resilient to stress than southern edge populations from Portugal, which responded with greater induction of heat-shock genes and lower resilience to desiccation and heat-shock, unlike co-existing populations of the related *F. vesiculosus* whose range extends further south (Pearson *et al.* 2009). Heat stress responses of four other *F. serratus* populations (Norway, Denmark, Brittany and Spain) also indicated population-specific differences, suggesting higher resilience (after 1h heat shock (HS) at up to 32°C) and constitutive sHSP expression of the southern edge (Spain) population, but reduced fitness (Jueterbock *et al.* 2014). Southern edge populations of *F. serratus* thus seem maladapted and with lower fitness, placing them at greater risk of local extinction. The HS response of the Arctic *F. distichus* also revealed population differences, with the northernmost population showing greater induction of heat-shock genes (Smolina *et al.* 2016). Another *Fucus* species presenting lower resilience and a more restricted range is *F. radicans* that occurs in sympatry with *F. vesiculosus* in the Baltic Sea. Comparative heat-shock gene expression studies showed that *F. radicans* was more sensitive to mild heat-shock than co-existing *F. vesiculosus* (Lago-Leston *et al.* 2010). Overall, this suggests that functional traits may be significantly altered in marginal habitats, where changes in transcriptional regulation, low genetic diversity due to genetic drift, and other local genetic traits interplay with local ecological dynamics (Pearson *et al.* 2009). Therefore, changing climate conditions may threaten small, fragmented and/or marginal populations because of inherently reduced fitness and lower adaptive capacity. In *Z. marina*, transcription profiling of southern and northern European populations from contrasting thermal environments during and after a simulated heat wave showed that while gene-expression patterns during stress were similar in both populations (with up-regulation of proteins involved in cell wall modification, protein folding, synthesis of ribosomal chloroplast proteins, and heat shock proteins), transcription profiles diverged during the recovery phase (Franssen *et al.* 2011, 2014). Gene expression patterns of the southern population returned to control values immediately, whereas the induction of genes involved in protein degradation indicated impaired recovery of the northern population. In the intertidal seagrass *Nanozostera noltii* (formerly *Z. noltii*) in contrast, the transcription profiles of the northern population changed considerably during the 26°C simulated heat wave unlike those in southern population, and neither up-regulated HSP genes (Franssen *et al.* 2014). As a unifying concept for ecological genomics, Franssen *et al.*

(2011) propose “transcriptomic resilience, analogous to ecological resilience, as an important measure to predict the tolerance of individuals and hence the fate of local populations in the face of global warming.”

In this study, we tested the hypothesis that fitness and adaptive potential differ between distributional leading and trailing range edges by investigating the functional differentiation in the response to elevated seawater temperatures between leading and trailing edge populations of *F. vesiculosus* and *Z. marina*. In common garden experiments, both photosynthetic indicators and heat shock protein (Hsp) gene expression were used to test the resilience to elevated seawater temperatures of leading and trailing edge populations. Comparative ecophysiology combined with gene expression studies demonstrate both plastic and constitutive cellular responses to stress. Our results strongly support the idea that differentiation of a thermal stress response can occur between leading and trailing edges. However, whereas fitness at elevated temperatures was eroded at the leading edge of the sexually reproducing brown alga *F. vesiculosus* this was not the case for the strongly clonally reproducing seagrass *Z. marina*, where the trailing edge population showed slightly reduced resilience.

2.2 - Material and methods

Model species and sampling

Fucus vesiculosus is a dioecious key foundation brown algal species, important from exposed intertidal rocky shores to highly sheltered tidal marshlands. It occupies the mid- to high rocky intertidal from northern Norway to Morocco along the eastern Atlantic, and extends into brackish environments of the Baltic and the White Sea. Along western Atlantic shores, it is found in similar rocky/marshland habitats ranging from Arctic Canada to North Carolina (USA). Leading edge samples were collected in Greenland in front of the Greenland Institute of Natural Resources in Nuuk (64.196°N 51.703°W), whereas trailing edge populations were sampled during low tide at Alcochete, Portugal (38.4535°N 8.5714°W). Mean seawater surface temperatures range from a long-term minimum of -1.8 to a maximum of 6.5 °C in Nuuk, and at Alcochete from 13.9 to 18.9 °C (Seatemperature.org).

Zostera marina, or eelgrass is a marine angiosperm and the dominant seagrass in temperate shallow coastal waters of the northern hemisphere with a distribution on both Atlantic and Pacific coasts (den Hartog 1970; Phillips & Meñez 1988). Reproduction takes place both clonally through vegetative growth as well as sexually by seeds. In Europe, *Z. marina* is the only seagrass to extend into the Arctic Circle and has its eastern Atlantic southern limit in the Ria Formosa lagoon, Portugal (den Hartog 1970). Leading edge samples were collected in Kobbefjord near Nuuk, Greenland (64.161 °N 51.556 °W), whereas trailing edge populations were sampled during low tide from Culatra island in the Ria Formosa lagoon (36.5951°N 7.4941°W South Portugal). Mean seawater surface temperature in the lagoon ranges from 14.7 °C to 23.4 °C (Seatemperature.org), but can locally reach up to 36°C in shallow water (Massa *et al.* 2009). *Z. marina* meadows in the Ria Formosa have lower clonal diversity than at central locations, lower levels of expected heterozygosity and exhibit heterozygote excesses rather than deficits (Billingham *et al.* 2003). Samples were collected from a monospecific *Z. marina* stand in a channel system with water depths of 0.1-0.5 m during low tide.

All macrophytes were transported alive wrapped in paper towels moist with seawater, inside cool boxes. Those from Portugal were returned to the laboratory within three hours of collection, whereas macrophytes from Greenland were transported in four days. *Fucus* apical tips or *Z. marina* shoots (henceforth “tissue”) were cut and cultured in 5 L tanks of aerated

and filtered natural seawater at 10 °C for three days before the experiments, under ambient day length conditions and photosynthetic photon flux density (PPFD) of 200 $\mu\text{mol m}^{-2}\text{s}^{-1}$. Three-quarters of the seawater volume was replaced after two days during the acclimation period.

Heat shock experiment and physiological measurements

After acclimation, macrophyte responses to temperature stress were tested through exposure to elevated seawater temperature scenarios that could occur during tidal cycles. For the experiments, the tissue was exposed to seawater of 18, 24, 28 or 32 °C for three hours, at a PPFD of 200 $\mu\text{mol m}^{-2}\text{s}^{-1}$, after which it was transferred back to acclimation conditions for recovery during 21 h. Photoinhibition of PSII maximum quantum yield (F_v/F_m) was measured on two tissue subsamples from each of five replicate individuals per treatment with a chlorophyll fluorometer (Junior PAM, Walz, Germany) immediately after the 3 h exposure and 24 h recovery. F_v/F_m scales directly with the quantum efficiency of PSII photochemistry (Butler 1978), and its reduction from maximal values (about 0.8 in seagrasses, slightly lower in brown algae) is a sensitive and rapid screening tool for stress responses. The fast and simple measurement of F_v/F_m makes it a very useful stress indicator despite its limitations. Short-term impacts on F_v/F_m (measured immediately after the 3h HS) reflect photodamage but also the effects of protective mechanisms (photoprotection). After recovery in constant acclimation conditions, the long-term impacts (F_v/F_m decrease after 24h) are assumed to reflect only lasting photodamage from the high temperature exposure. Tolerance to the heat-stress is considered here as the ability to withstand the elevated temperatures without visible physiological impacts (at 3h HS), while resilience is the ability to recover from the high temperature effects avoiding long-term damage (after 24h Recovery). Tissue subsamples (two per individual) used in the physiological measurements were dark adapted for 5 min in leaf clip holders, and the remaining tissue directly frozen in liquid nitrogen and stored at -80 °C for RNA extraction. Baseline F_v/F_m values (10 °C), i.e., controls, were measured at 3 and 24 h. Controls were manipulated as for temperature treatments, but maintained at acclimation temperature. The heat shock experiments were conducted in programmed thermostatically controlled water baths within a walk-in climate chamber (Aralab 20000 EHF). F_v/F_m data were normalised within each population and sampling time (divided by the mean values of 10 °C controls, n = 5 individuals) to account for intrinsic differences and to allow comparisons of stress resilience across populations and species. The experimental design tested for

differentiation between marginality (Edge, fixed factor, two levels), and temperature (fixed factor, five levels).

For the gene expression study of *Fucus vesiculosus*, samples were collected before PAM measurements, flash frozen in liquid nitrogen and stored at -80 °C. Total RNA was extracted, DNase-treated and purified as described previously (Pearson *et al.* 2006; 2009), from triplicate samples from each edge (Greenland and Portugal), treatment phase (3h HS or 24h Recovery) and temperature (10, 24, 28 or 32 °C) combination. Total RNA (500 ng) was reverse-transcribed with SuperScript III RT (Invitrogen) and oligo-dT primer in two independent reactions that were then pooled. Quantitative PCR (qPCR) was performed in duplicate on an iCycler iQ Detection System (BioRad), as described previously (Mota *et al.* 2015). The resulting files were analysed using iQ5 software (BioRad), with manual threshold settings and efficiency correction. The resulting individual expression values, normalised to the geometric average of three reference genes (EF1, Sumo3, and tubulin) were used for further analysis.

The seven selected transcripts were identified from EST libraries for heat and desiccation stress in *F. vesiculosus* and *F. serratus* (Pearson *et al.* 2010), and belong to four functionally diverse HSP families: HSP90, HSP70, HSP20 and ClpB/HSP100. One HSP70 sequence is a plastid-encoded DnaK (hs447), while the other (hs696) is a putative HSP70 cytosolic chaperone (Fu *et al.* 2009). HSP20-2 is a small HSP (sHSP), a family which functions as ATP-independent chaperones preventing aggregation of misfolded proteins. sHSPs are typically only induced upon stress, quickly stabilizing denatured and aggregated proteins until they can be delivered to other chaperones for subsequent refolding by ATP-dependent chaperones such as the DnaK system or ClpB/DnaK (Wang *et al.* 2004). The Clp_7H01 transcript is a member of the casein lytic proteinase/ heat shock protein 100 (Clp/Hsp100) family with sequence similarities to a ClpB chaperone, involved in delivering protein aggregates to other chaperones for refolding.

Data were analysed using the non-parametric PERMANOVA module (Anderson 2001; McArdle & Anderson 2001) within Primer 6 software (Clarke & Gorley 2006) following Pearson *et al.* (2009). For each species and time (immediately after the heat shock or after recovery), the effects of Edge and Temperature were tested. Tests (distance-based homogeneity of dispersion, main effects and pair-wise) were made on a data matrix of Euclidean distances using 999 unrestricted permutations of raw data.

2.3 - Results

Photosynthetic efficiency

The maximum quantum yield of PSII was differentially impacted by exposure to elevated temperatures both between edge populations and between species, as assessed by the decrease in normalized F_v/F_m (Figs. 2.1 and 2.2).

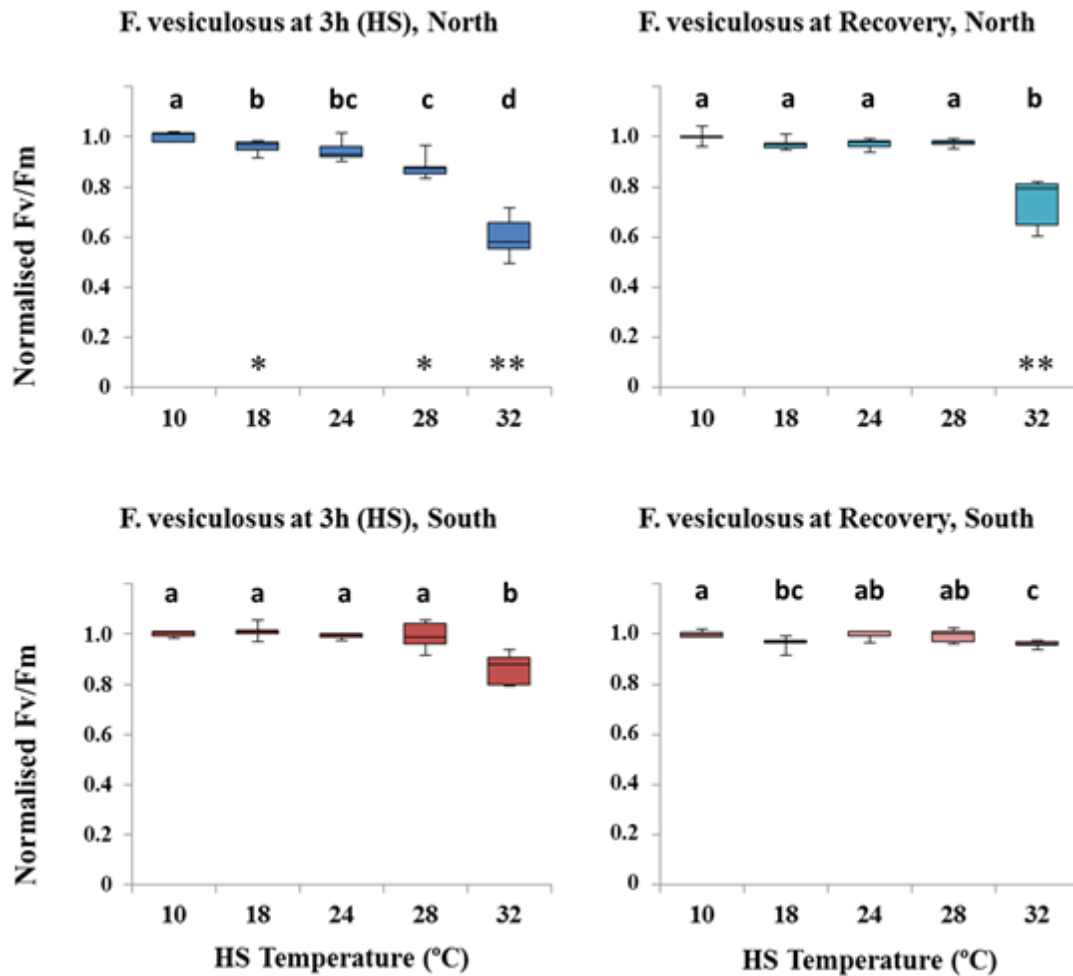


Figure 2.1 - Normalised maximum quantum yield (F_v/F_m) for the alga *Fucus vesiculosus* from the leading (Greenland, blue) and rear (Portugal, red) edge of distribution, directly after a 3 hour exposure (HS) to control (10°C) or elevated temperatures (18, 24, 28 and 32 °C) and after recovery at control temperatures. Boxplot horizontal lines show the median, boxes show the 50% quartiles, and the error bars display the range of the data (n=5). Asterisks show significant pair-wise differences between edges (* p<0.05; ** p<0.01) and different letters indicate significant pair-wise differences (p<0.05) between temperatures.

The response of Fv/Fm to 3h HS differed markedly between southern and northern edge *Fucus vesiculosus* populations. While the northern (leading) edge population showed a progressive decline from 18°C onwards, Fv/Fm in the southern (trailing) edge population remained unaffected by 3h HS up to 28°C, and decreased significantly only at 32°C. As a consequence, Fv/Fm was significantly lower in the northern compared with the southern population at all HS temperatures except 24°C (Fig. 2.1; Table 2.1). Population-specific differences in resilience (recovery capacity) were revealed at the highest HS temperature (32°C). While statistical tests indicated that Fv/Fm failed to fully recover in either population, the reduction was minimal in the southern edge population, and was significantly greater in the northern population (Fig. 2.1; Table 2.2). Overall, these results suggest clear variations in the thermal response of PSII between these two edge populations, which result in differential resilience to thermal stress.

Table 2.1 - PERMANOVA of *Fucus vesiculosus* Fv/Fm from northern and southern distribution edges (Ed: North and South) collected directly after exposure to different temperatures for 3 hours (Te: 10, 18, 24, 28 and 32 °C). Significant terms are shown in bold, based on 999 permutations.

Source	df	SS	MS	Pseudo-F	P(perm)
Ed	1	0.10998	0.10998	49.946	0.001
Te	4	0.48385	0.12096	54.934	0.001
EdxTe	4	0.10246	2.56E-02	11.633	0.001
Res	40	8.81E-02	2.20E-03		
Total	49	0.78437			

Table 2.2 - PERMANOVA of *Fucus vesiculosus* Fv/Fm from the northern and southern distribution edges (Ed: North and South) subjected to different temperatures for 3 hours (Te: 10, 18, 24, 28 and 32 °C) and collected 24 hours after return to control (10 °C) temperatures. Significant terms are shown in bold, based on 999 permutations.

Source	df	SS	MS	Pseudo-F	P(perm)
Ed	1	3.28E-02	3.28E-02	22.728	0.001
Te	4	0.15281	3.82E-02	26.498	0.001
EdxTe	4	9.39E-02	2.35E-02	16.279	0.001
Res	40	5.77E-02	1.44E-03		
Total	49	0.33713			

Maximum quantum yield in *Zostera marina* populations was less severely impacted by HS up to 32°C than in *F. vesiculosus*. The effects of HS were not different between populations (edge; Table 2.3), while the effects of temperature were clearer at 32°C in the northern population, in which inter-individual variation was lower (Fig. 2.2; Table 2.3). Neither population fully recovered (low resilience) following exposure at 32°C (Fig. 2.2) and PERMANOVA indicated significant differences during recovery due to the main effects temperature and edge, with no interaction (Table 2.4). The data therefore indicate that southern edge populations of *Z. marina* are slightly (but significantly, $p = 0.045$, see table 2.S2 on the appendix) less resilient to thermal stress than those at the northern leading edge (Fig. 2.2).

Table 2.3 - PERMANOVA of *Zostera marina* *Fv/Fm* from the northern and southern distribution edges (Ed: North and South) collected directly after exposure to different temperatures for 3 hours (Te: 10, 18, 24, 28 and 32 °C). Significant terms are shown in bold, based on 999 permutations.

Source	df	SS	MS	Pseudo-F	P(perm)
Ed	1	3.36E-05	3.36E-05	7.21E-03	0.929
Te	4	6.51E-02	1.63E-02	3.4875	0.014
EdxTe	4	2.31E-03	5.77E-04	0.12374	0.975
Res	40	0.18658	4.66E-03		
Total	49	0.25399			

Table 2.4 - PERMANOVA of *Zostera marina* *Fv/Fm* from the northern and southern distribution edges (Ed: North and South) subjected to different temperatures for 3 hours (Te: 10, 18, 24, 28 and 32 °C) and collected 24 hours after return to control (10 °C) temperatures. Significant terms are shown in bold, based on 999 permutations.

Source	df	SS	MS	Pseudo-F	P(perm)
Ed	1	2.96E-02	2.96E-02	5.2424	0.031
Te	4	5.84E-02	1.46E-02	2.5827	0.042
EdxTe	4	2.46E-02	6.14E-03	1.0867	0.380
Res	40	0.22602	5.65E-03		
Total	49	0.33857			

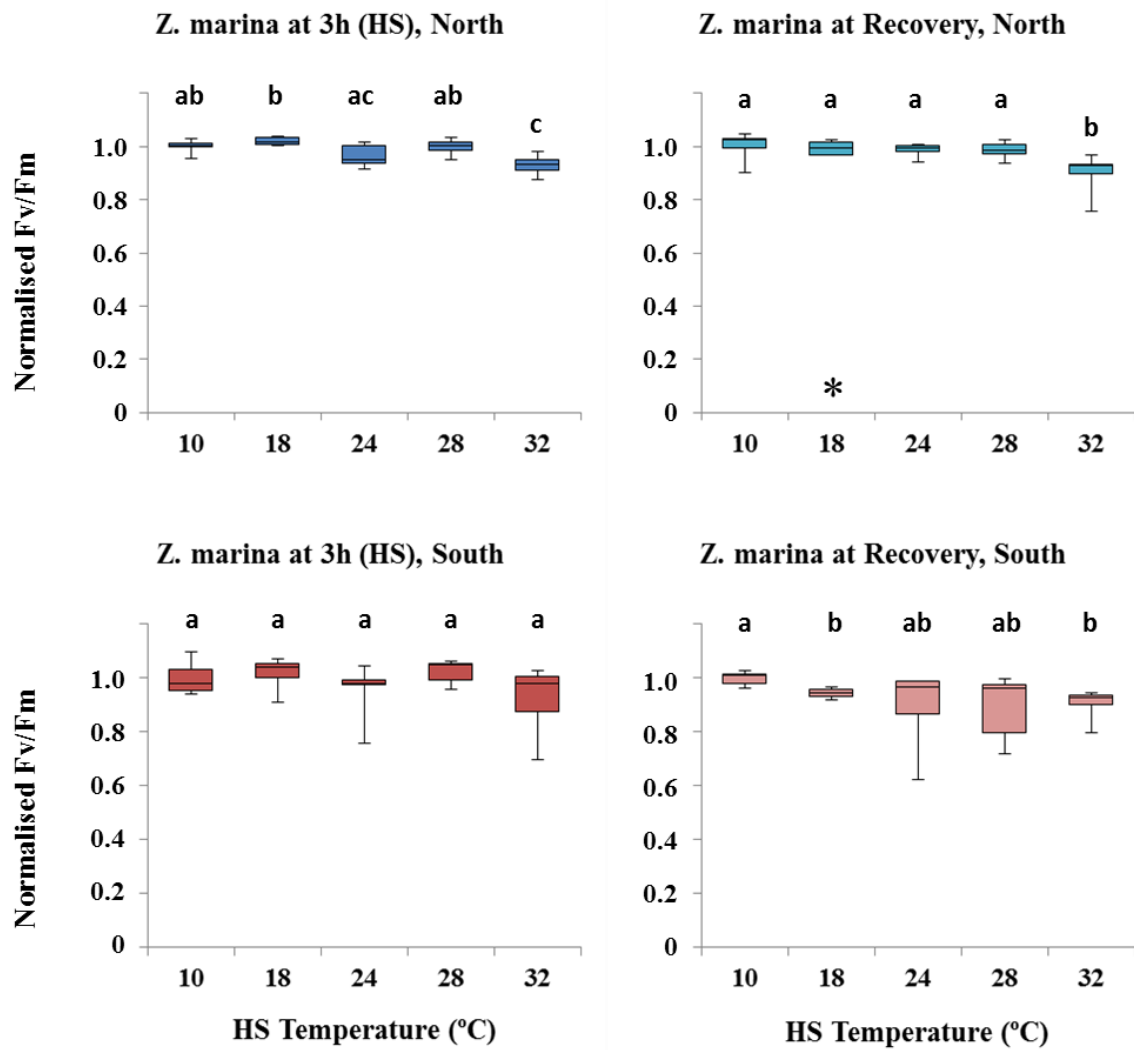


Figure 2.2 - Normalised maximum quantum yield (F_v/F_m) for the seagrass *Zostera marina* from the leading (Greenland, blue) and trailing (Portugal, red) edge of distribution, directly after a 3 hour exposure (HS) to control (10°C) or elevated temperatures (18, 24, 28 and 32°C) and after recovery at control temperatures. Boxplot horizontal lines show the median, boxes show the 50% quartiles, and the error bars display the range of the data (n=5). Asterisks show significant pair-wise differences between edges (* p<0.05) and different letters indicate significant pair-wise differences between temperatures (p<0.05).

Gene expression

Despite the diversity of expression patterns among the seven target genes, all displayed significant expression changes with temperature, as expected for putative HSP transcripts. Immediately after exposure to high temperatures (3h), most target genes showed increased expression levels (Figure 2.3a, b). Maximum expression occurred at 28°C in both edges, when most genes (five and six for Northern and Southern edge, respectively) showed increased expression. After 3h HS significant differences between edges were detected for 4 genes: induction of the small HSP (HSP20) at 28°C, and one HSP90 (HSP90_443) at 24°C were both higher in the North edge population. In contrast, after exposure to 32°C higher expression of two transcripts (HSP70_696 and HSP90_597) was found in the southern edge (asterisks in Fig. 2.3a). Significant interactions (Ed x Te) were only detected for HSP70_447, HSP90_443 and HSP20 (Table 2.5). The peak of HSP expression at 28°C likely reflects a tolerance threshold. Below 28°C, temperature rise induces a protective heat shock response, where HSP expression prevents or reduces the damaging effects of high temperature. Above this threshold, protective mechanisms likely no longer compensate for thermal damage and HSP expression is impaired. Damaged proteins that accumulated during heat stress will be processed (i.e., repaired or degraded) gradually during the recovery period, requiring extended HSP expression after severe stress. The absence of HSP over-expression after 24 h reflects either full recovery (no further need for additional HSPs), or that the stress was so intense that transcription is still impaired after this period (in this case *Fv/Fm* would likely be similarly impacted).

After 24 h recovery, gene expression had mostly returned to levels similar or below the controls, except for two genes that were still slightly elevated (under 10-fold) in the southern population (Figure 2.3c, d). Despite these similar patterns, significant differentiation between leading and trailing edge populations could be detected in five target genes and at all three HS temperatures (asterisks in Fig. 2.3c, d). Significant interactions (Ed x Te) were detected for HSP70_447, HSP90_597 and HSP90_870 (Table 2.5).

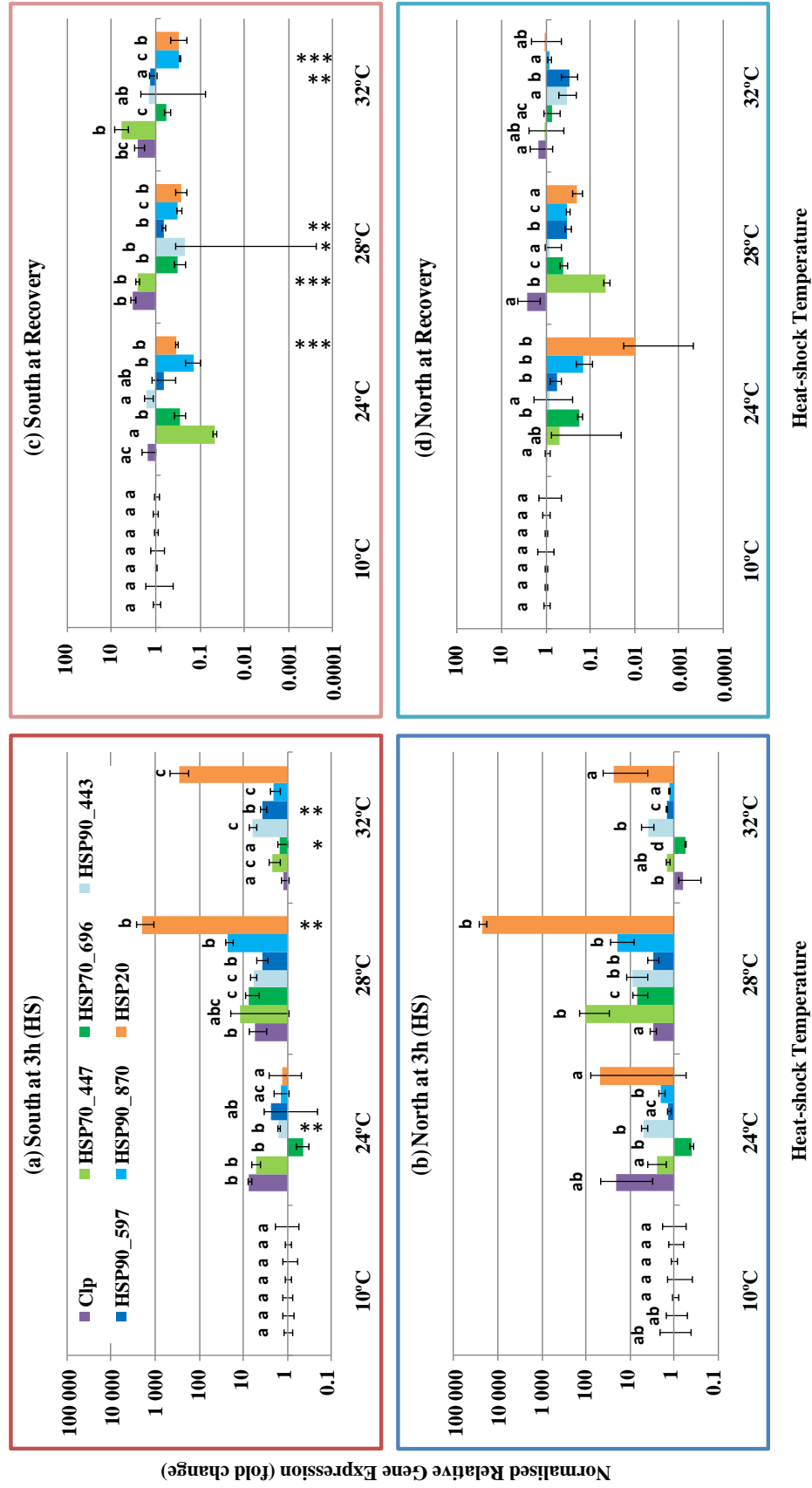
Unsurprisingly, most analyses exposed significant heterogeneity of dispersions, particularly for temperature, as relative gene expression (fold) changes often present large replicate variability, partly resulting from the strong switches (“on-off”) in gene expression, as well as underlying biological variation (Table 2.5). As with the *Fv/Fm* measurements, HSP gene expression supports the existence of edge specific differentiation in the induction of a heat

shock response. Although statistically supported by only one gene (HSP20), there was a trend towards greater HSP induction in the North edge population at 28°C, the temperature for peak HS response, while the same population was marginally less able to mount a HS response at 32°C, where *Fv/Fm* was also impacted.

Table 2.5 - Summary statistical analysis table of *Fucus vesiculosus* gene expression. For each transcript, data from the two sampling times were analysed separately for both fixed factors (Edge: North and South; Temperature: 10, 24, 28 and 32 °C) with the PERMANOVA module on Primer 6 using an Euclidean distance resemblance matrix and 999 permutations. PERMDISP is a distance-based test for homogeneity of multivariate dispersions. Significant *p*-values (0.05) are shown in bold.

P (perm)		PERMDISP		PERMANOVA		
Time	Gene	Temp	Edge	Edge	Temp	EdxTe
3h HS	Clp_HSP100	0.003	0.290	0.675	0.003	0.340
3h HS	HSP70_447	0.001	0.001	0.010	0.001	0.005
3h HS	HSP70_696	0.002	0.936	0.463	0.001	0.891
3h HS	HSP20	0.001	0.001	0.003	0.001	0.004
3h HS	HSP90_443	0.005	0.681	0.163	0.001	0.035
3h HS	HSP90_597	0.025	0.047	0.022	0.005	0.256
3h HS	HSP90_870	0.001	0.822	0.762	0.001	0.940
Recovery	Clp_HSP100	0.057	0.642	0.063	0.003	0.649
Recovery	HSP70_447	0.002	0.002	0.001	0.001	0.001
Recovery	HSP70_696	0.283	0.520	0.598	0.001	0.444
Recovery	HSP20	0.222	0.312	0.638	0.009	0.144
Recovery	HSP90_443	0.020	0.123	0.248	0.285	0.105
Recovery	HSP90_597	0.002	0.713	0.001	0.011	0.005
Recovery	HSP90_870	0.001	0.544	0.004	0.001	0.002

Figure 2.3 - Expression of seven heat shock transcripts in response to control (10 °C) and elevated seawater temperatures (24, 28 and 32°C), after 3h of HS and after recovery in the alga *Fucus vesiculosus* from the leading (North) and trailing (South) edge of distribution. Relative gene expression values were normalised to geometrical average of three reference genes and to a reference condition (each control at 10 °C). Bars show the mean, and error bars display the range of the data (n=3 biological replicates). Asterisks show significant pair-wise differences between edges (* p<0.05; ** p<0.01; *** p<0.001) and different letters indicate significant pair-wise differences between temperatures (p<0.05).



2.4 - Discussion

Our results support the differentiation of thermal stress responses between populations located at the leading and trailing edges. There were clear population differences in an intertidal furoid alga, although only minor differences were detected in a shallow subtidal seagrass species. Both species share similar latitudinal distributions, although their local vertical distribution and habitat is quite different, with the result that the intertidal species is usually exposed to a much more extreme range of thermal conditions (both emersed and submersed) compared with the subtidal species, which may only infrequently experience short-term changes in seawater temperatures.

The northern (leading edge) population of the intertidal species showed signs of eroded fitness at high temperatures, while the trailing edge seems adapted to peaks of water temperature approaching 30°C. Northern edge populations of *F. vesiculosus* were more affected by increasing temperatures, showing effects at lower temperatures (beyond 24°C) and stronger inhibitory effects at 32°C. The greater thermal tolerance and resilience of the trailing edge population is matched by a greater likelihood of experiencing heat stress events, since local temperatures are much higher at the southern edge.

Interestingly, these data suggest that the subtidal seagrass species may have lower fitness at the southern edge, although the temperatures used here were not high enough to cause strong physiological impacts. Higher temperatures or longer exposures might improve detection of potential edge differences. A 3 weeks simulated heat wave at 26°C revealed similar transcriptomic profiles between other northern (Denmark and USA) and southern (Italy and USA) populations of *Z. marina* during acute stress (indicating similar tolerance), but population differences increased during recovery (Jueterbock *et al.* 2016). Although in Jueterbock *et al.* 2016 the southern populations seemed more resilient, particularly due to the Mediterranean population, edge differences were also clearer during the recovery period. The same extended 26°C exposure revealed that the Mediterranean population of the intertidal seagrass *N. noltii* was more tolerant than the northern population (Franssen *et al.* 2014). The potentially lower resilience of the trailing edge population in this study (Portugal) may result from decreased genetic diversity from past population bottlenecks in this clonal species, due to habitat fragmentation, disturbance, or mass mortality events during heat waves that leave populations less able to adjust and respond to thermal shocks. The higher resilience of the

Mediterranean populations can be due to ancient differentiation and successful adaptation to warmer waters (Jueterbock *et al.* 2016).

The differential resilience to heat-shock of the two edge populations in *F. vesiculosus* raises two hypotheses: that the relative impact of climate warming may be different depending on the population involved, and that local adaptation could be responsible for those differences (although phenotypic plasticity and polymorphism could also play a role). These hypotheses are supported by the intraspecific differentiation between northern and southern edge populations in physiological and (to a lesser extent) gene expression responses to temperature shifts under common garden conditions. It has also been shown that southern and northern groups of *F. vesiculosus* form coherent phylogenetic groupings that could also support some degree of functional divergence (Cánovas *et al.* 2011). However, it is impossible in this case to definitively exclude the influence of the environment, or potential maternal effects that may influence the realised phenotype (Li & Brawley 2004; Marshall 2008).

Selection pressure favouring local adaptation can be counteracted by gene flow with populations from less selective habitats. Local adaptation is therefore expected to be more likely in species with strongly limited dispersal (although with many exceptions, Sanford & Kelly 2011), as is the case of *Fucus* species. *Zostera marina* is also a species with limited dispersal and distinct locally adapted populations existed until recently (Billingham *et al.* 2007). However, such adaptive traits have not prevented recent local seagrass extirpations at many southern edge sites (Diekmann & Serrao 2012, Cunha *et al.* 2013), as has also been the case for intertidal furoid species (Nicastro *et al.* 2013, Mota *et al.* 2015). The ongoing range contraction at the southern edge of these species might have influenced their current resilience to increasing temperatures. This may happen in two contrasting ways; the higher selective pressures would be expected to increase resilience and favour local adaptation. However, low genetic diversity at the range edges relative to central populations (Diekmann & Serrao 2012, Assis *et al.* 2014) can prevent local adaptation, by limiting the variation upon which selection operates, and can even result in reduced fitness (Pearson *et al.* 2009). Low genetic diversity (as allelic diversity) in northern populations of *Z. marina* is aggravated by the low genotypic richness (as the diversity of the clones or genotypes) found at these limit populations (Diekmann & Serrao 2012).

Despite the lower resilience of the northern *Fucus* species, inhabiting the more stressful intertidal habitat, both leading edge populations were only impacted at temperatures far

beyond those predicted for the polar regions in the future, and their range is thus expected to expand northwards with global change. Southern ranges will more likely face contractions, particularly for intertidal species, as high temperature peaks and heat waves become more frequent, imposing increasingly large fitness costs on the populations. Such sharp changes have indeed been recorded already (Cunha *et al.* 2013, Nicastró *et al.* 2013, Mota *et al.* 2015) and are predicted to continue in the future (Assis *et al.* 2014). Persistence of species in the face of climatic changes may be therefore dependent on the distribution of diversity between populations (Sanford & Kelly 2011). Species distribution models may therefore fail to fully capture species responses to climate change, since they assume that all populations within a species have similar constraints.

The expected distributional shifts (local extinctions and colonizations) of ecosystem structuring or foundational species will impact many other species. However, impacts are difficult to predict, as they depend on multiple factors, such as species-specific life-history traits, demography and adaptive potential of genetically differentiated populations. To predict critical points, it is important to consider both the expected temperature shifts and the thermal resilience of the resident populations. Northern (leading edge) populations face higher rates of SST increase, but trailing edge (Southern) populations may be at risk due to higher absolute SST values. By contrasting two species with similar latitudinal ranges, our study shows that leading and trailing edge populations can have different responses to thermal stress. Southern populations may be better adapted to elevated seawater temperatures whereas loss of resilience to high thermal stress may occur in polar edges. The causes for these distinct patterns and predictions between the two species models is not clear, although we raised the hypothesis that low fitness-related genetic variability might be restricting evolvability (*sensu* Pearson *et al.* 2009). Whether based on phenotypic plasticity or genetic local adaptation, the population differences that we report here have practical consequences besides suggesting possible susceptibility to climatic changes. Activities leading to admixture of such populations might result in outbreeding depression, a major concern for possible conservation management. Habitat restoration practices should take into account the possible occurrence of locally adapted genotypes and consider these a conservation priority as well as the best source for population restoration at similar habitats where populations have become extinct.

This study supported the hypothesis that fitness and resilience to elevated seawater temperatures can differ between leading (polar) and trailing (southern) range edges, of ecosystem-structuring, widespread, coastal macrophytes. However, the effects also differ between species, despite apparent similar climatic affinities, as shown here for the macroalga *Fucus vesiculosus* and the seagrass *Zostera marina*. By examining the resilience of two edge populations to a range of heat-shock temperatures, we raised predictions on how these may be impacted by climate warming, and hypotheses about the role of hypothetical local adaptation of populations. The thermal limits identified here are much higher than realistic levels expected for the near future at the northern edge, suggesting favourable conditions for northwards expansions with global change, in contrast with the recent southern range contractions recorded for these species. Any putative impacts of climate change on ranges of structural macrophytes are likely to have cascading consequences for many associated species.

2.5 – References

- Anderson, M.J. (2001). A new method for non-parametric multivariate analysis of variance. *Austral. Ecol.* 26: 32–46.
- Assis, J., Serrão, E.A., Claro, B., Perrin, C., Pearson, G.A. (2014). Climate-driven range shifts explain the distribution of extant gene pools and predict future loss of unique lineages in a marine brown alga. *Molecular Ecology* 23: 2797-2810.
- Billingham, M., Reusch, T.B., Alberto, F., Serrão, E.A. (2003). Is asexual reproduction more important at geographical limits? A genetic test of the seagrass *Zostera marina* in the Ria Formosa, Portugal. *Marine Ecology Progress Series* 265: 77-83.
- Billingham, M.R., Simões, T., Reusch, T.B.H., Serrão, E.A. (2007). Genetic substructure and intermediate optimal outcrossing distance in the marine angiosperm *Zostera marina*. *Marine Biology* 152: 793-801.
- Bridle, J.R. & Vines, T.H. (2006). Limits to evolution at range margins: When and why does adaptation fail? *Trends in Ecology and Evolution* 22: 140–147.
- Butler, W.L. (1978). Energy distribution in the photochemical apparatus of photosynthesis. *Annual Review of Plant Physiology* 29: 345–378.
- Cánovas, F.G., Mota, C.F., Serrão, E.A. & Pearson, G.A. (2011). Driving south: a multi-gene phylogeny of the brown algal family Fucaceae reveals relationships and recent drivers of a marine radiation. *BMC Evolutionary Biology*, 11: 371.
- Chapman, A.R.O. (1995). Functional ecology of fucoid algae: twenty-three years of progress. *Phycologia* 34: 1–32.
- Clarke, K.R. & Gorley, R.N. (2006). PRIMER v6 users manual and tutorial. PRIMER-E, Plymouth.
- Connell, J.H. (1972). Community interactions on marine rocky intertidal shores. *Annual Review of Ecology and Systematics*, 3: 169–192.
- Cunha, A.F., Assis, J.F. & Serrão, E.A. (2013). Seagrasses in Portugal: a most endangered marine habitat. *Aquatic Botany*, 104: 193-203.
- Davenport, J. & Davenport, J.L. (2005). Effects of shore height, wave exposure and geographical distance on thermal niche width of intertidal fauna. *Marine Ecology Progress Series*, 292: 41–50.
- Davison, I.R. & Pearson, G.A. (1996). Stress tolerance in intertidal seaweeds. *Journal of Phycology*, 32: 197–211.
- Den Hartog, C. (1970). *The Seagrasses of the World*, North- Holland, Amsterdam.
- Diekmann, O.E. & Serrão, E.A. (2012). Range-edge genetic diversity: locally poor extant southern patches maintain a regionally diverse hotspot in the seagrass *Zostera marina*. *Molecular Ecology*, 21: 1647–1657.
- Dijkstra, J., Boudreau, J. & Dionne, M. (2012). Species-specific mediation of temperature and community interactions by multiple foundation species. *Oikos* 121(5): 646-654.
- Dring, M.J. & Brown, F.A. (1982). Photosynthesis of intertidal brown algae during and after periods of emersion: A renewed search for physiological causes of zonation. *Marine Ecology Progress Series*, 8: 301–308.

- Easterling, D.R., Meehl, G.A., Parmesan, C., Changnon, S.A., Karl, T.R. & Mearns, L.O. (2000). Climate extremes: observations, modeling, and impacts. *Science* 289: 2068–2074.
- Eckert, C.G., Samis, K.E. & Loughheed, S.C. (2008). Genetic variation across species' geographical ranges: the central-marginal hypothesis and beyond. *Molecular Ecology*, 17: 1170–1188.
- Eggert, A. (2012). Seaweed responses to temperature. In: *Seaweed Biology: novel insights into ecophysiology, ecology and utilization*, Wiencke C, Bischof K (eds) Springer, p47-66.
- Franssen, S. U., Gu, J., Bergmann, N., Winters, G., Klostermeier, U. C., Rosenstiel, P., Bornberg-Bauer E. & Reusch, T. (2011). Transcriptomic resilience to global warming in the seagrass *Zostera marina*, a marine foundation species. *PNAS* 48: 19276- 19281.
- Franssen, S.U., Gu, J., Winters, G., Huylmans, A.-K., Wienpahl, I., Sparwel, M., Coyer, J.A., Olsen, J.L., Reusch, T.B.H. & Bornberg-Bauer, E. (2014). Genome-wide transcriptomic responses of the seagrasses *Zostera marina* and *Nanozostera noltii* under a simulated heatwave confirm functional types. *Marine Genomics* 15: 65–73.
- Fu, W.D., Yao, J.T., Wang, X.L., Liu, F.L., Fu, G. & Duan, D. (2009). Molecular cloning and expression analysis of a cytosolic Hsp70 gene from *Laminaria japonica* (Laminariaceae, Phaeophyta). *Marine Biotechnology* 11: 738–747.
- Hampe, A. & Petit, R.J. (2005). Conserving biodiversity under climate change: the rear edge matters. *Ecology Letters*, 8: 461–467.
- Hawkins, S.J., Southward, A.J. & Genner, M.J. (2003). Detection of environmental change in a marine ecosystem – evidence from the western English Channel. *The Science of the Total Environment*, 310: 245–256.
- Heck, K. L., Jr. & L. B. Crowder. (1991). Habitat structure and predator-prey interactions in vegetated aquatic ecosystems. Pages 281–299 in S. S. Bell, E. D. McCoy, and E. R. Mushinsky, editors. *Habitat structure of objects in space*. Chapman and Hall, London, UK.
- Helmuth, B., Harley, C.D.G., Halpin, P.M., O'Donnell, M., Hofmann, G.E. & Blanchette, C.A. (2002). Climate change and latitudinal patterns of intertidal thermal stress. *Science*, 298: 1015–1017.
- Helmuth, B., Mieszkowska, N., Moore, P. & Hawkins, S.J. (2006). Living on the Edge of Two Changing Worlds: Forecasting the Responses of Rocky Intertidal Ecosystems to Climate Change. *Annual Review of Ecology, Evolution, and Systematics*, 37: 373–404.
- Helmuth, B., Carrington, E. & Kingsolver, J.G. (2005). Biophysics, physiological ecology, and climate change: does mechanism matter? *Annual Review of Physiology* 67: 177–201.
- Jones, C.G., Lawton, J.H. & Shachak, M. (1994). Organisms as ecosystem engineers. *Oikos* 69: 373–386.
- Jueterbock, A., Kollias, S., Smolina, I., Fernandes, J.M., Coyer, J.A., Olsen, J.L. & Hoarau, G. (2014). Thermal stress resistance of the brown alga *Fucus serratus* along the North-Atlantic coast: acclimatization potential to climate change. *Marine Genomics*, 13:27-36. doi: 10.1016/j.margen.2013.12.008.
- Jueterbock, A., Franssen, S.U., Bergmann, N., Gu, J., Coyer, J.A., Reusch, T.B.H., Bornberg-Bauer, E. & Olsen, J.L. (2016). Phylogeographic differentiation versus transcriptomic adaptation to warm temperatures in *Zostera marina*, a globally important seagrass. *Molecular Ecology* 25 (21): 5396-5411.

- Jump, A.S. & Penuelas, J. (2005). Running to stand still: adaptation and the response of plants to rapid climate change. *Ecology Letters*, 8: 1010–1020.
- Lago-Leston, A., Mota, C., Kautsky, L. & Pearson, G. (2010). Functional divergence in heat shock response following rapid speciation of *Fucus* spp. in the Baltic Sea. *Marine Biology*, 157: 683–688.
- Li, R. & Brawley, S.H. (2004). Improved survival under heat stress in intertidal embryos (*Fucus* spp.) simultaneously exposed to hypersalinity and the effect of parental thermal history. *Marine Biology* 144: 205.
- Madsen, J.D., Chambers, P.A., James, W.F., Koch, E.W. & Westlake, D.F. (2001). The interaction between water movement, sediment dynamics and submersed macrophytes. *Hydrobiologia* 144: 71–84.
- Marshall, D.J. (2008). Transgenerational plasticity in the sea: context-dependent maternal effects across the life history. *Ecology* 89: 418–427.
- Massa, S.I., Arnaud-Haond, S., Pearson, G.A. & Serrão, E.A. (2009). Temperature tolerance and survival of intertidal populations of the seagrass *Zostera noltii* (Hornemann) in Southern Europe (Ria Formosa, Portugal). *Hydrobiologia*, 619: 195–201.
- McArdle, B.H. & Anderson, M.J. (2001). Fitting multivariate models to community data: a comment on distance-based redundancy analysis. *Ecology* 82 (1): 290–297.
- Mota, C.F., Engelen, A.H., Serrão, E.A. & Pearson, G.A. (2015). Some don't like it hot: microhabitat-dependent thermal and water stresses in a trailing edge population. *Functional Ecology* 29 (5): 640–649.
- Nicastro, K.R., Zardi, G.I., Teixeira, S., Neiva, J., Serrão, E.A. & Pearson, G.A. (2013). Shift happens: trailing edge contraction associated with recent warming trends threatens a distinct genetic lineage in the marine macroalga *Fucus vesiculosus*. *BMC Biology* 11 (1), 6.
- Parmesan, C. (2006). Ecological and Evolutionary Responses to Recent Climate Change. *Annual Review of Ecology, Evolution, and Systematics*, 37, 637–669.
- Pearson, G.A., Lago-Leston, A., Valente, M. & Serrão, E.A. (2006). Simple and rapid RNA extraction from freeze-dried tissue of brown algae and seagrasses. *European Journal of Phycology*, 41: 97–104.
- Pearson, G.A., Lago-Leston, A. & Mota, C. (2009). Frayed at the edges: Selective pressure and adaptive response to abiotic stressors are mismatched in low diversity edge populations. *Journal of Ecology*, 97: 450–462.
- Pearson, G. A., Hoarau, G., Lago-Leston, A., Coyer, J. A., Kube, M., Reinhardt, R., ... & Olsen, J. L. (2010). An expressed sequence tag analysis of the intertidal brown seaweeds *Fucus serratus* (L.) and *F. vesiculosus* (L.) (Heterokontophyta, Phaeophyceae) in response to abiotic stressors. *Marine Biotechnology*, 12 (2), 195–213.
- Phillips, R.C., & Menez, E.G., (1988). Seagrasses. Smithsonian Contributions to the Marine Sciences, no. 34.
- Sagarin, R.D. & Gaines, S.D. (2002). The ‘abundant centre’ distribution: to what extent is it a biogeographical rule? *Ecology Letters*, 5: 137–147.
- Sagarin, R.D. & Somero, G.N. (2006). Complex patterns of expression of heat- shock protein 70 across the southern biogeographical ranges of the intertidal mussel *Mytilus californianus* and snail *Nucella ostrina*. *Journal of Biogeography*, 33: 622–630.

- Sanford, E. & Kelly, M.W. (2011). Local adaptation in marine invertebrates. *Annual Review of Marine Sciences* 3: 509-535
- Smolina, I., Kollias, S., Jueterbock, A., Coyer, J.A. & Hoarau, G. (2016). Variation in thermal stress response in two populations of the brown seaweed, *Fucus distichus*, from the Arctic and subarctic intertidal. *Royal Society open science* 3: 150429.
- Somero, G.N. (2002). Thermal Physiology and Vertical Zonation of Intertidal Animals: Optima, Limits, and Costs of Living. *Integrative and Comparative Biology*, 42: 780–789.
- Southward, A.J., Hawkins, S.J. & Burrows, M.T. (1995). Seventy years' observations of changes in distribution and abundance of zooplankton and intertidal organisms in the western English Channel in relation to rising sea temperature. *Journal of Thermal Biology*, 20: 127–155.
- Terrados, J., & Duarte, C. M. (2000). Experimental evidence of reduced particle resuspension within a seagrass (*Posidonia oceanica* L.) meadow. *J. Exp. Mar. Biol. Ecol.* 243: 45–53.
- Wang, W., Vinocur, B., Shoseyov, O. & Altman, A. (2004). Role of plant heat-shock proteins and molecular chaperones in the abiotic stress response. *Trends Plant Sci.*, 9: 244–252.
- Walther, G.-R., Post, E., Convey, P., Menzel, A., Parmesan, C., Beebee, T.J.C., Fromentin, J.-M., Hoegh-Guldberg, O. & Bairlein, F. (2002). Ecological responses to recent climate change. *Nature* 416: 389-395.
- Willi, Y., Van Buskirk, J. & Hoffmann, A.A. (2006). Limits to the Adaptive Potential of Small Populations. *Annual Review of Ecology, Evolution, and Systematics*, 37: 433–458.
- Williams, S.L. & Dethier, M.N. (2005). High and dry: variation in net photo-synthesis of the intertidal seaweed *Fucus gardneri*. *Ecology*, 86: 2373–2379.

2.6 – Acknowledgements

The study described in this chapter was supported by FCT — Portuguese Science Foundation programs EXCL/AAG-GLO/0661/2012, UID/Multi/04326/2013, and fellowships SFRH/BPD/63/03/2009 to AHE and SFRH/BD/74436/2010 to CFM.

Supporting information

Supporting information to this chapter can be found on the Appendix (digital version)

Table S2.1 – Pairwise tests for Fv/Fm data (EdxTemp).

Fv/Fm values (n=5), normalised to controls at 10°C, were used to build a resemblance matrix of Euclidean distances between samples. Analysis were made with 999 unrestricted permutations of raw data, fixed effects sum to zero for mixed terms and Type III (partial) sums of squares, in the PERMANOVA module of Primer v6 software.

Tables S2.2 – Pairwise tests for the significant factors (Edge or Temperature) in Z. marina Fv/Fm data.

Analyses were made as previously described using the PERMANOVA module of Primer v6 software.

Tables S2.3 – PERMANOVA results for normalised relative expression of seven genes after the 3h HS (n=3).

Analyses were made as previously described using the PERMANOVA module of Primer v6 software.

Tables S2.4 – PERMANOVA results for normalised relative expression of seven genes during Recovery (n=3).

Analyses were made as previously described using the PERMANOVA module of Primer v6 software.

Table S2.5 – Pair-wise tests for gene expression data.

Analyses were made as previously described using the PERMANOVA module of Primer v6 software.

Table S2.6 – Fv/Fm raw data.

Table S2.7 – Relative gene expression data of the technical duplicates normalised to the geometric average of the three reference genes.

Chapter 3

Some don't like it hot: microhabitat-dependent thermal and water stresses in a trailing edge population

Chapter 3 – Some don't like it hot: microhabitat-dependent thermal and water stresses in a trailing edge population

3.0 – Summary

1. The distributional limits of species in response to environmental change are usually studied at large temporal and/or geographical scales. However, organismal scale habitat variation can be overlooked when investigating large scale averages of key factors such as temperature. We examine how microhabitat thermal conditions relate to physiological limits, which may contribute to recent range shifts in an intertidal alga.
2. We defined the onset and maximum temperatures of the heat shock response (HSR) for a southern edge population of *Fucus vesiculosus*, which has subsequently become extinct. The physiological threshold for resilience (assayed using chlorophyll fluorescence) coincided with declining HSR, determined from the temperature-dependent induction of seven heat-shock protein transcripts.
3. In intertidal habitats, temperature affects physiology directly by controlling body temperature and indirectly through evaporative water loss. We investigated the relationship between the thermal environment and *in situ* molecular HSR at microhabitat scales. Over cm to m scales, four distinct microhabitats were defined in algal patches (canopy surface, patch edge, sub-canopy, submerged channels), revealing distinct thermal and water stress environments during low tide emersion.
4. The *in situ* HSR agreed with estimated tissue temperatures in all but one microhabitat. Remarkably, in the most thermally extreme microhabitat (canopy surface) the HSR was essentially absent in desiccated tissue, providing a potential escape from the cellular metabolic costs of thermal stress.

5. Meteorological records, microenvironmental thermal profiles and HSR data indicate that the maximum HSR is approached or exceeded in hydrated tissue during daytime low tides for much of the year. Furthermore, present-day summer seawater temperatures are sufficient to induce HSR during high tide immersion, preventing recovery and resulting in continuous HSR during daytime low tide cycles over the entire summer.
6. HSR in the field matched microhabitat temperatures more closely than local seawater or atmospheric data, suggesting that the impacts of climatic change are best understood at the microhabitat scale, particularly in intertidal areas.

Copyright manuscript published in Functional Ecology

Mota, C. F., Engelen, A. H., Serrão, E. A., Pearson, G. A. (2015), Some don't like it hot: microhabitat-dependent thermal and water stresses in a trailing edge population. *Functional Ecology*, 29: 640–649. doi: 10.1111/1365-2435.12373

Reproduced with permission from John Wiley and Sons

Keywords: algal canopy, climate change, *Fucus vesiculosus*, range edge, heat-shock response (HSR), HSP gene expression, PSII photochemistry, thermal limits.

3.1 - Introduction

Studies investigating the effects of environmental change on distribution limits generally focus on large temporal and geographical scales. However, the conditions that organisms experience often depend strongly on local small scale habitat effects and interactions (Helmuth & Hofmann 2001; Helmuth *et al.* 2006a). Analysis of climatic variation averaged over large scales can therefore fail to account for extensive variation at scales more relevant to the individuals, species or community in question. This is particularly true in studies linking environmental factors with physiological limits.

A good example is the intertidal zone, where organisms are exposed to both marine and terrestrial environments during tidal cycles. Local variation in extreme and fluctuating environmental conditions may overwhelm large scale latitudinal temperature gradients (Helmuth *et al.* 2002a; Helmuth *et al.* 2006a). High amplitude temperature shifts at hourly time scales during low-tide exposure in air or in small pools result in a complex realized thermal environment shaped by local mosaics of abiotic factors, rather than prevailing air or water temperatures (Helmuth & Hofmann 2001; Helmuth 2002b; Seabra *et al.* 2011). In contrast, thermal conditions are comparatively stable during immersion at high tide with relatively little change on daily or even seasonal time scales (but see Pfister, Wootton & Neufeld 2007). Control of cellular water balance is an additional challenge, particularly for poikilohydric intertidal seaweeds that tolerate rather than prevent cellular water loss. Some algae can lose a large proportion (> 90%) of their tissue water over short periods of emersion (Davison & Pearson 1996; Pearson, Lago-Leston & Mota 2009).

Cost effective, miniaturized and autonomous instrumentation for temperature measurements (Helmuth 2002b; Lima *et al.* 2011) now allow the study of temperature effects at small, ecologically relevant spatial and temporal scales. These developments have been matched by the use of molecular tools to monitor responses to thermal stress in natural populations. The Heat Shock Response (HSR) is an ancient and ubiquitous cellular response to the potentially lethal accumulation of unfolded protein at elevated temperatures. The sensing of damaged or denatured proteins triggers an evolutionarily conserved response that involves the synthesis of protein chaperones: the highly conserved heat-shock proteins (HSPs). Assessing thermal regimes and relevant physiological responses at local scales may lead to a better understanding of the role of temperature in shaping species distributions. The HSR in natural populations has been studied for relatively few intertidal species occupying distinct thermal

niches (Dietz & Somero 1992; Roberts, Hofmann & Somero 1997; Tomanek & Somero 1999). The ecologically relevant components of the stress response include both adaptation to the thermal niche, and capacity for acclimation to changing conditions (plasticity).

Concern about the impacts of climate change has renewed interest in the relationship between thermal tolerance limits and species distribution. Such impacts may be higher towards the low latitude range edges, where local habitat effects can become more evident. As edge populations tend to be small and less diverse, local adaptability may be compromised (Pearson *et al.* 2009) and insufficient to prevent extinction under climatic pressure. In fact, work on intertidal gastropods gives some reason to think that intertidal species may exist near the limits of their thermotolerance, with little capacity for further adaptation of the upper bounds of the HSR (Tomanek & Somero 1999; but see Davenport & Davenport 2005). The somewhat counterintuitive conclusion is that many intertidal species inhabiting highly fluctuating thermal environments have limited acclimatory plasticity, and may therefore be at particular risk from climate change (Tomanek 2010).

The trailing edge (southern) distributional boundary for several North Atlantic species is found along SW Iberia. Range contractions and local extinctions in the region have recently been reported for several ecosystem-structuring marine species (Diekmann & Serrão 2012; Assis *et al.* 2013; Cunha, Assis & Serrao 2013; Nicastro *et al.* 2013). Such effects have been particularly striking for the brown alga *Fucus vesiculosus* L. (Nicastro *et al.* 2013), a major model in studies of intertidal stress (Wahl *et al.* 2011), that at its southern limit occurs exclusively inside estuaries and coastal lagoons. Inside a coastal lagoon in southern Portugal, the species occurred on mudflats as patches that expanded during winter and shrank during summer (Pearson & Serrão, pers obs), suggesting seasonally intense environmental stress. Since this study was conducted (in 2008), the formerly extensive patches on intertidal flats have disappeared. Indeed, a dramatic range contraction of 11° latitude over the last 30 years resulted in the local extinction of most southern populations (Nicastro *et al.* 2013).

In this study we investigated microhabitat variation in realized thermal conditions, hydration status, and the molecular heat-shock response in a regressing southern edge population of *F. vesiculosus*, which is now locally extinct (Nicastro *et al.* 2013). Historical climate data are incorporated to develop hypotheses concerning local trends and the biological causes underlying population decline. Conditions measured within each microhabitat diverged considerably from local seawater or atmospheric parameters, and matched more closely

physiological status under laboratory conditions. Our data suggest that processes mediating responses to environmental change may often only be understood by conducting studies at the relevant organismal scales.

3.2 - Material & Methods

Model species and study site

Fucus vesiculosus plays key ecological roles along the European Atlantic, where it has a mid-high intertidal distribution correlated with stress tolerance limits to temperature and desiccation (Dring & Brown 1982; Pearson *et al.* 2009; Zardi *et al.* 2011).

This study was conducted in 2008 on a southern edge population in southern Portugal (Ria Formosa coastal lagoon, 37°00'40"N, 7°59'25"W; Fig. S3.1 in Appendix). There, *F. vesiculosus* formed patches on tidal mudflats across a very narrow vertical range (ca. 1.2 – 2.3 m above ELWS). At the lower vertical limit, individuals occurred also in tidal drainage channels. Sexual reproduction was reduced or absent, with persistence due only to vegetative growth. Although it had been recorded for decades in the Ria Formosa (Ardré 1970 and references therein), in the year following this study patches became locally extinct, and have not recovered. The current southern limit is near Lisbon, except for a remaining site near Cadiz, and unattached vegetative fragments that can still be found entangled in high intertidal *Spartina* in the Ria Formosa (Nicastro *et al.* 2013).

Laboratory HSR and stress resilience experiments

Individuals of *F. vesiculosus* were collected in April and July 2008 and acclimated for 4 weeks in 10 L tanks of aerated and recirculating glass-fiber-filtered natural seawater at 15°C under a photosynthetic photon flux density (PPFD) of 25 – 50 $\mu\text{mol}\cdot\text{m}^{-2}\cdot\text{s}^{-1}$ for either 10 or 14h per day (spring and summer experiments, respectively). Thermal stress resilience assays were carried out by exposing acclimated apical tissue (n = 10 individuals) to heat shock (HS) for 3h at 24, 28, 32 and 36°C ($\pm 0.5^\circ\text{C}$) in thermostatically controlled water baths with filtered recirculating seawater. To more closely simulate low tide field conditions, high PPFD (250 – 300 $\mu\text{mol}\cdot\text{m}^{-2}\cdot\text{s}^{-1}$) was provided by sodium vapour lamps. The final temperature was reached by ramping through sequential 15-min transfers between water baths. Controls were manipulated as for the HS treatments, but were maintained under acclimation temperature and irradiance conditions. After HS, algae were allowed to recover under acclimation conditions for 24h.

Resilience to HS was assayed 24h following stress exposure using chlorophyll fluorescence (FMS2, Hansatech Instruments). The ratio of photochemical quenching (F_v) to total

fluorescence emission from closed PSII reaction centres (F_m) is directly proportional to the quantum efficiency of PSII photochemistry with reductions below maximal values (0.7 – 0.8 in brown algae) providing a rapid and sensitive indicator of physiological stress. The maximum quantum yield of PSII (F_v/F_m) was determined after 5 min dark adaptation in order to estimate photodamage. While short term (min) reductions in F_v/F_m can result from physiological adjustments (e.g., dissipation of excess light energy as heat – non-photochemical quenching), the longer-term (24 h) effects reported here can mainly be attributed to photodamaged PSII reaction centers (Maxwell & Johnson 2000).

Samples for RT-qPCR were taken at the end of the HS exposure, and following 24h recovery, by flash-freezing 5 – 6 apical tips from $n = 3$ individuals in LN₂. Samples were then stored at -80°C prior to lyophilization and RNA extraction.

Thermal limits were characterized from the induction profiles of the seven target heat-shock transcripts, using three parameters: T_{on} (onset of HSR induction, the lowest temperature at which a response is observed), T_{peak} (peak induction, the temperature at which the maximal response is observed) and T_{off} (a temperature too high to sustain the HSR, above which no response is observed).

Air and seawater temperatures

Coastal sea surface temperature (SST) warming data were obtained from <http://www.coastalwarming.org> (Lima & Wethey 2012), based on NOAA data from 1982 – 2011. Seawater temperatures inside the Ria Formosa (ca. 2.5 m below mean low tide) for winter and summer/autumn 2012 were obtained by datalogger (iButtons®) readings at 60 min intervals. Daily air temperatures from Jan 1973 – Sep 2012 were obtained from weather station 85540 (LPFR) at Faro Airport (37°01'N, 07°58'W) and used to compare seasonal temperature profiles and anomalies. Monthly means were used to fit linear models to determine decadal rates of temperature change.

In situ measurements and sampling

We defined four *F. vesiculosus* microhabitats in the Ria Formosa: 1) 'Channel' = lower shore individuals that remain fully hydrated on all but the most extreme spring low tides, 2) 'Top' = top-canopy of high shore patches, exposed to rapid desiccation at low tide, 3) 'Bottom' = individuals lying beneath the canopy surface, and 4) 'Edge' = fronds at the periphery of

patches lying in contact with moist sediment during low tide. Thermal variation in tissue temperature from different microhabitats was estimated using temperature dataloggers (iButtons®). Thermal profiles in *F. vesiculosus* patches / channel were recorded every 1 min at low tide on January 28, March 14, Jun 25 and August 6, 2008, on clear and sunny days with a daytime low tide at 12:00 - 13:00 h. In the channels, loggers (n=3) were placed inside protective brass casing (see Pearson *et al.* 2009) at the mud/water interface adjacent to the algae that remained immersed. For the other microhabitats, loggers (n=3 per habitat) were lightly sealed with silicon grease, wrapped in white teflon tape, and attached with wire clips to the underside of thalli. In August, apical tips (n = 5) were collected in each microhabitat at mid low tide (13:40 h) and at the end of low tide (16:00 h) for tissue water content estimation. Residual surface water was removed by blotting. Each tip was placed in a pre-weighed vial with 2 mL filtered seawater, re-weighed to obtain the initial weight (IW) of the tissue when sampled. This, together with the hydrated (FW) and dry weights (DW; after drying at 60°C for 24 h) allows the calculation of the tissue water content (TWC) at the time of collection from:
$$\text{TWC (\%)} = [(IW - DW)/(FW - DW)] \times 100$$

Samples for analysis of the HSR were taken at 1) the onset of emersion, 2) mid low tide and 3) immediately prior to re-immersion. At each time, 12 – 15 apical tips (ca. 3 cm) per microhabitat were selected from 3 patches separated by ≥ 5 m, immediately flash-frozen in LN₂ in the field, and stored at -80°C.

RNA extraction and qPCR

Total RNA was extracted from lyophilized tissue from 30 laboratory HS samples (May experiment; 3 replicates x 5 temperatures x 2 times) and from 72 field samples (3 replicates x 4 microhabitats x 3 tide times x 2 months) following Pearson *et al.* (2006), DNase-treated and further purified with RNeasy Mini Kit (QIAGEN). Total RNA was reverse-transcribed with SuperScript III RT (Invitrogen) and oligo-dT, with an extended synthesis of 1h at 50°C followed by 50 min at 55°C, in two independent (2 µg) reactions for field material, or a single (4 µg) reaction for laboratory HS samples. Additional information on target HSP transcripts and reference genes is given in Table S1. qPCR reactions were performed in triplicate with PerfeCta Fastmix for iQ (Quanta biosciences) on an iCycler iQ Detection System (Bio-Rad) and analysed using iQ5 software (Bio-Rad). Normalized expression values (geometric mean of the three reference genes) were analysed using the PERMANOVA module in Primer 5.

3.3 - Results

Laboratory HSR and physiological resilience

Physiological data (F_v/F_m) from Spring and Summer HS experiments were pooled after the analyses indicated no effect of sampling time (PERMANOVA, $P > 0.914$; see Table S2). After recovery from temperatures between 24 and 32°C, F_v/F_m was only slightly (but significantly) lower than in controls at 15°C (Fig. 1a). In contrast, the effect of 3 h exposure at 36°C was much greater, indicating that HS resilience was significantly impaired between 32°C and 36°C (Table S2).

a) F_v/F_m following 24 h recovery from a 3 h heat-shock (HS) at 24, 28, 32 and 36 °C. Controls were at 15 °C, $n = 20$, \pm SE.

b) Gene expression for seven Hsp transcripts following 3 h HS at the same temperatures as in a).

c) Gene expression for the same 7 transcripts after 24 h recovery in seawater at 15 °C. Values for b) and c) are normalized (to controls at 15 °C) relative expression values of 3 individuals, \pm SE. Different letters within each gene indicate significantly different means. (See Tables S2 and S3 for PERMANOVA and post-hoc tests).

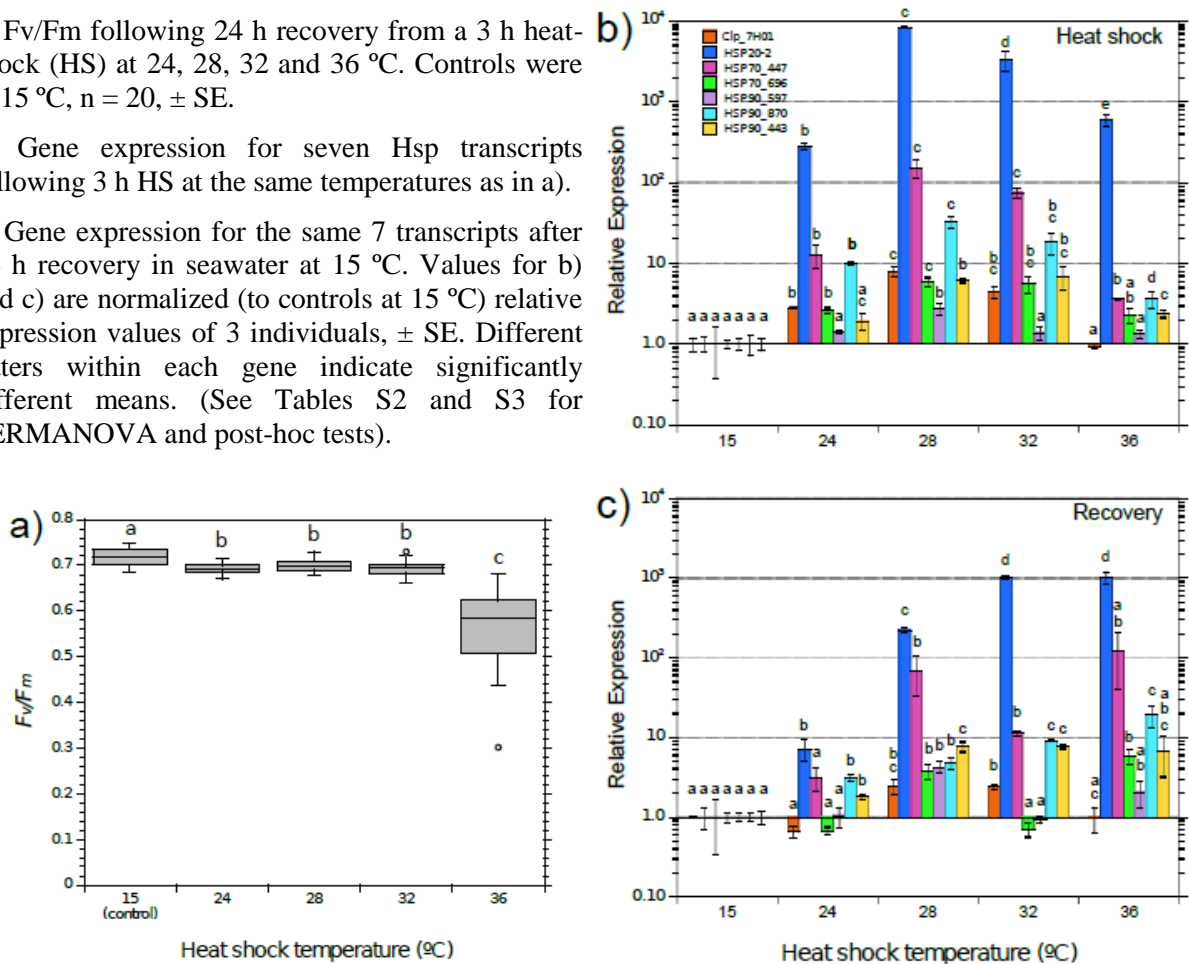


Figure 3.1 - *F. vesiculosus* response after 3 h of heat-shock at 24, 28, 32 and 36 °C and following 24 h recovery.

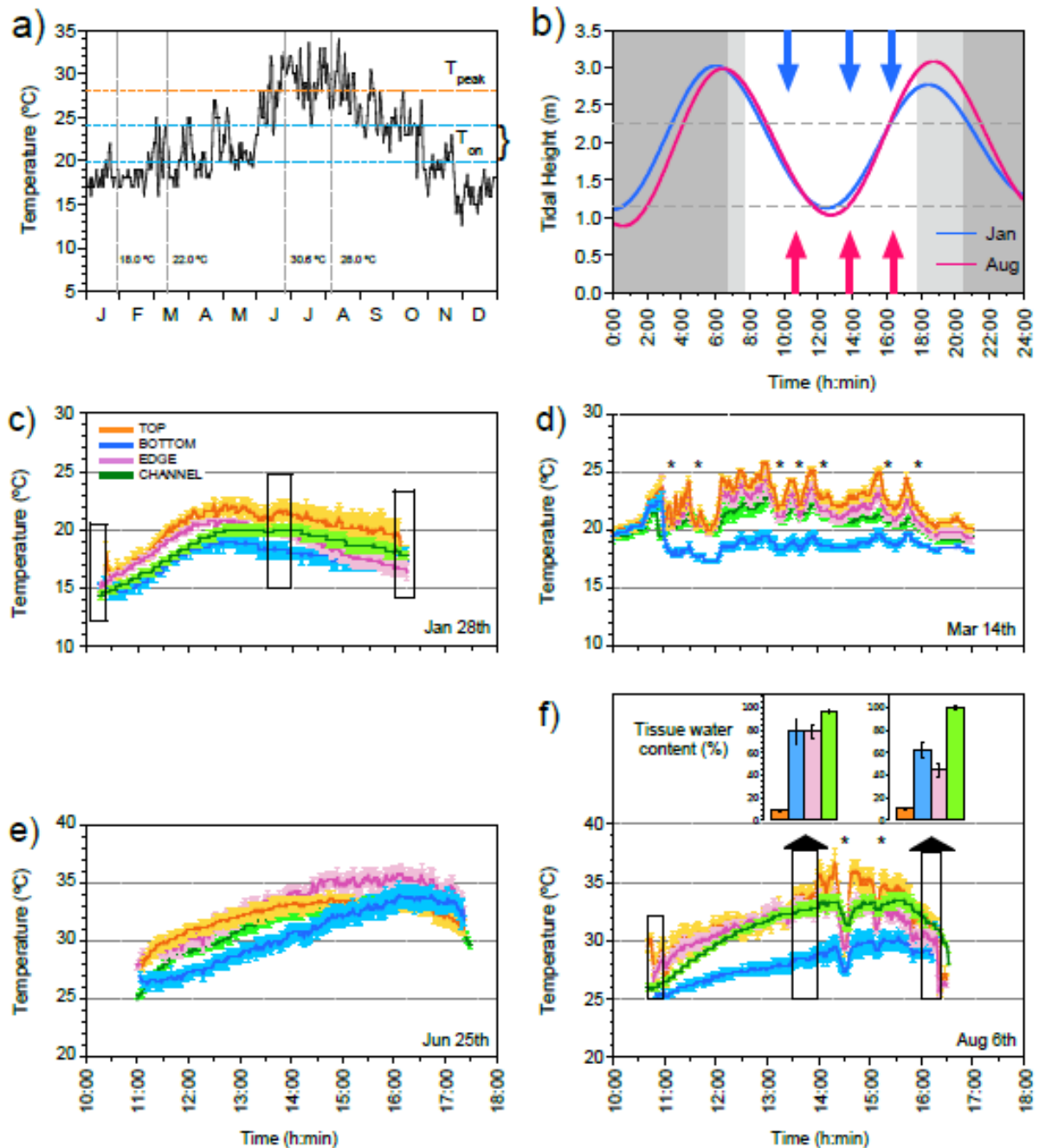


Figure 3.2 - Site maximum air temperatures, tidal cycle and microhabitat temperatures.

a) Daily maximum air temperatures (TM) (Faro Airport, 2008). Horizontal broken lines indicate onset of HSR (T_{on}), and peak HSR (T_{peak}). TM for the thermal profiling days are indicated by vertical broken lines. b) Tidal cycles when sampling temperature profiles and for qPCR: coloured arrows show sampling as algae emerged, at mid low tide, and as they immersed. Dashed lines indicate the vertical distribution of *F. vesiculosus* in the Ria Formosa. Shading indicates sunset to sunrise periods. c - f) Microhabitat temperatures (Jan, Mar, Jun, Aug 2008, and tissue water contents (inset bar charts; Aug only). Temperature loggers ($n = 3$, every 1 min) were attached to thalli at the canopy top (orange), bottom (blue) and edge (purple) and in a channel (green), covering the vertical range. Asterisks = light cloud cover. Sampling times for HSR are the dashed boxes (Jan, Aug).

Short-term (3 h) exposure of *Fucus vesiculosus* to HS between 24 and 36°C induced a HSR in all seven genes (Fig. 1b). Maximum induction across genes ranged between ca. 3-fold (HSP90_597) to > 8000-fold (HSP20-2). The small HSP family chaperone HSP20-2 had the greatest dynamic range, as shown previously (Pearson et al. 2009; Lago-Leston et al. 2010; Pearson et al. 2010). Peak expression levels were observed at 28°C for all transcripts, remaining equally high or declining slightly at 32°C. Expression declined significantly for all genes at the highest temperature tested (36°C), with no significant induction for three transcripts (see Table S3). After 24 h recovery from 24°C all but three transcripts (HSP20-2, HSP90_870 and HSP90_443) had returned to control levels (Fig. 1c). However, expression was still elevated after recovery from exposure to higher temperatures (28 – 36°C). After exposure to 36°C, overall expression was higher after 24 h recovery than immediately post-stress (Fig. 1b, c). A reduced capacity to mount a HSR at 36°C, and maintenance of high expression levels in the recovery phase correlate with reduced physiological resilience at this temperature (Fig. 1a-c).

Microhabitat temperature profiles

Maximum air temperatures on sampling dates varied from 18.0 – 22.0°C (January and March), to 28.0 - 30.6°C (August and June) (Fig. 2a). Profiles in the 4 microhabitats were taken on days with similar midday low tides, when algae were emersed between 10:00 – 11:00 h (Fig. 2b). At the onset of low tide emersion, water temperatures in the channel varied from 14°C in January, 19°C in March, to ca. 25°C in June-August (Fig. 2c-f).

In January (Fig. 2c), water was at ca. 14°C and fronds peaked ca. 4°C above maximum air temperature at the canopy surface (Top; 22.2°C), followed by the Edge (20.8°C), Channel (20°C) and the marginally cooler sub-canopy (Bottom; 19°C). Cloudy conditions in March resulted in temporal variation of up to 5°C in the Top, while the Bottom (18 – 19°C) remained below maximum air temperature (22°C; Fig. 2d).

Tissue temperatures in June were above 25°C at the onset of emersion, reaching > 35°C at the Edge of the canopy by mid-afternoon (Fig. 2e). Sub-canopy Bottom temperatures increased less, but were still > 30°C for ca. 3 h (Fig. 2e). As in June, August temperatures were > 10°C higher than in January (Fig. 2f). The most extreme microhabitat was the Top, where TM reached 36.7°C; temperatures of ≥ 35°C between 14:00 – 15:30 were interrupted only by passing light cloud cover (asterisks, Fig. 2f). Under the canopy was ca. 5°C lower than the

Top (TM = 31.2°C versus 36.7°C on a cm scale), and also increased at a lower rate; reaching 30°C later and cooling within an hour. In contrast, both the Top and Edge remained at >30°C for ca. 4.5 h. Similarly, Channel water reached > 30°C for 4 h (Fig. 2f). Algae at the canopy surface (Top) were severely desiccated by mid low tide (TWC = 8.5 ± 0.8%, Fig. 2f), while at the other microhabitats they had some refuge from desiccation – Channel algae were fully immersed, Edge algae were in contact with the wet sediment or immersed in small depressions, and Bottom algae were protected from evaporative water loss thermally and by shading. At the end of low tide, Edge and Bottom algae still retained 44.8 ± 6.8% and 62.1 ± 6.9% TWC, respectively (Fig. 2f, inset bar plots).

HS gene expression profiles in natural stands of *F. vesiculosus*

In January and August the expression of Hsp transcripts in field samples under known temperatures at low tide (Fig. 2), can be compared with laboratory baseline HSR and physiological resilience (Fig. 1). The data plotted for each transcript (see Fig. 3 and Tables S4 and S5) are normalized to the average initial values for January across all microhabitats, thus allowing comparison of spatial and temporal variation. Transcriptional responses in January were small in all microhabitats, concordant with a temperature range of 14.6 – 21.4°C (Fig. 3a-d). Although the highest temperatures were observed at the Top, no significant HSR occurred there. However, a mild HSR was clearly evident in the Channel microhabitat, with a small but significant induction of 5 transcripts at mid low tide (Fig. 3d). The over-expression of HSP20-2 transcripts in August compared with January (ca. 100 – fold) was striking in all microhabitats at the onset of low tide (Fig. 3). These results suggest that significant HS expression had either already been induced in seawater (ca. 26°C) prior to the first sampling period, or that transcript levels remained elevated due to previous stress cycles.

Field and laboratory HSRs agree well for algae under similar hydration status and temperature: c.f. 3 h laboratory HSR at 32°C (Fig. 1b) versus Channel HSR at mid low tide in August (ca. 2.5 h between 28 – 33°C; Figs. 2f and 3h). The Log-linear relationship between field expression values for HSP20_2 (the transcript with the highest dynamic range) and temperature was highly significant across samples for January and August (Fig. 4). Furthermore, estimates of Ton for the HSP20_2 HSR transcript vary little when combined January and August data, or solely August data are considered (ca. 21 – 23°C), showing little evidence for seasonal acclimation (plasticity).

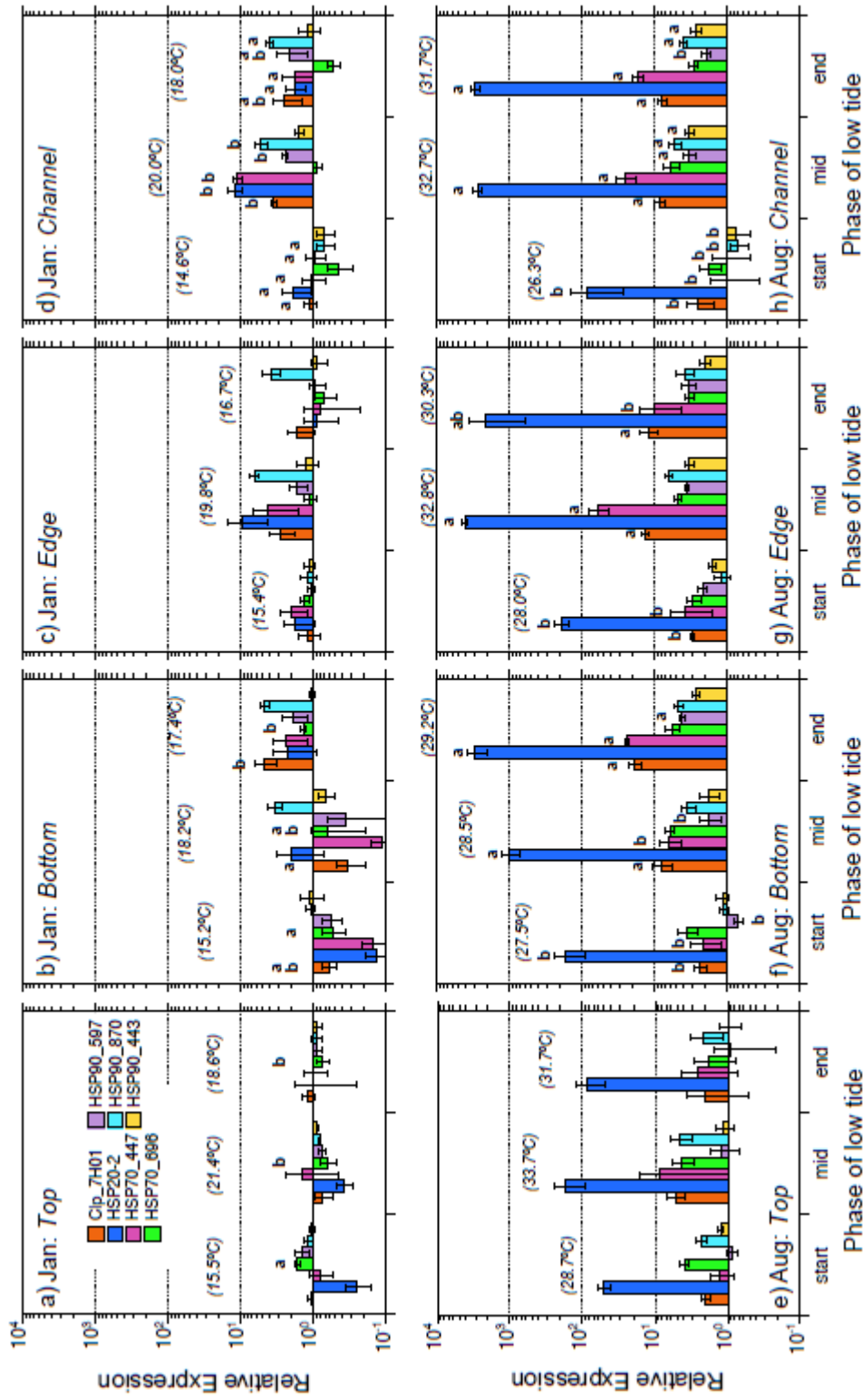


Figure 3.3 - Gene expression for 7 Hsp transcripts in the field microhabitats in January (a – d) and August (e – h) 2008. *F. vesiculosus* samples were taken at the onset of low tide (= start), mid low tide (= mid), and prior to re-immersion (= end). Values are relative expression assayed by RT-qPCR, normalized to the mean of initial values of the transcript over all microhabitats in January (n = 3 individuals, ± SE). Values with the same letter within a gene and month are not significantly different. Italics show the temperature at the time of sampling in each microhabitat and phase of the low tide. (see Tables S4 and S5 for PERMANOVA and post-hoc tests).

There was a clear mismatch between temperature and HS gene expression in the Top microhabitat linked with desiccation (Fig. 3a, e). No inducible HSR occurred at the canopy surface either in August (36°C) or January (22°C), while seawater at 20°C already elicited a mild HSR in hydrated algae (Fig. 3d). The canopy surface rapidly desiccated to < 10% TWC in the first hours of emersion, resulting in transcriptional arrest.

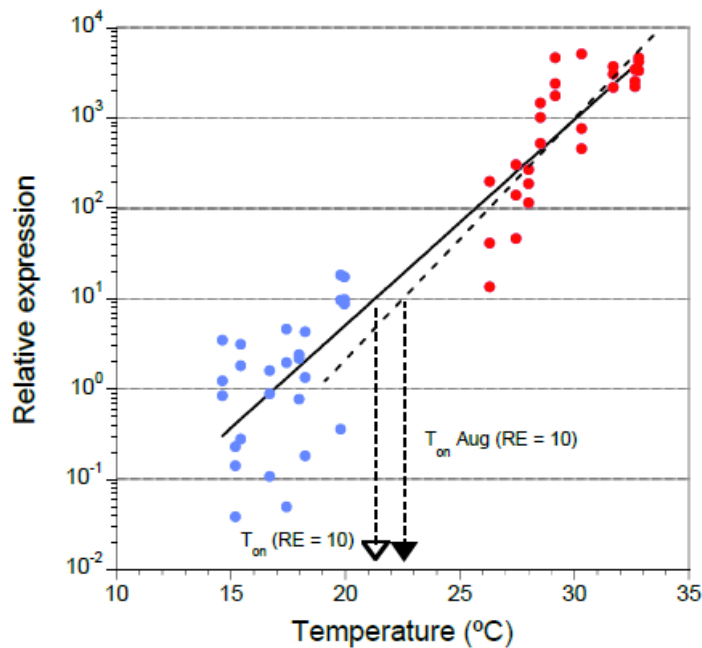


Figure 3.4 - Relationship between temperature and HSP20_2 expression for January and August field samples. Relative expression (RE) of sHsp (HSP20_2) in field-collected samples of *F. vesiculosus* from January (blue) and August (red) in relation to tissue temperature. Values are for biological replicates taken from all microhabitats except the canopy surface (i.e., edge, bottom and channel), sampled at the start, mid and end of low tide (as shown in Fig. 2b); N = 54 (January + August) or 27 (August only). A linear regression fitted to $\text{Log}_{10}(\text{RE})$ gives $\text{RE} = -3.8398 + 0.22719 (\text{T}^{\circ}\text{C})$ $R^2 = 0.88393$ (solid black line). For August data only, the regression gives $\text{RE} = -4.9961 + 0.2659(\text{T}^{\circ}\text{C})$ $R^2 = 0.6728$ (broken black line). At $\text{RE} = 10$ the estimates for HSR T_{on} are 21.3 °C, and 22.5 °C, respectively (broken open and filled arrows).

Current temperature regimes and regional warming trends

Maximum daily air and hourly seawater temperatures in the Ria Formosa in 2012 provide a picture of an extreme thermal environment for *F. vesiculosus* (Fig. 5). Maximum air temperature began to exceed field-estimated T_{on} for the HSR in fully hydrated algae (ca. 20°C; Fig. 3d) in March and mostly exceeded the 10 – fold induction of a sHsp transcript at 21 – 23°C (Fig. 4) between May – Sep. Seawater temperatures exceed these values for the entire summer period (except during spring tides tidal flushing). So *F. vesiculosus* would have only intermittent refuge from HS on spring tides, and would be exposed to HS each

daytime low tide. The frequency of such events is clustered, since daytime low tides between 11:00 – 15:00 h (when solar/ thermal exposure is highest), occur during five or six consecutive days, twice monthly.

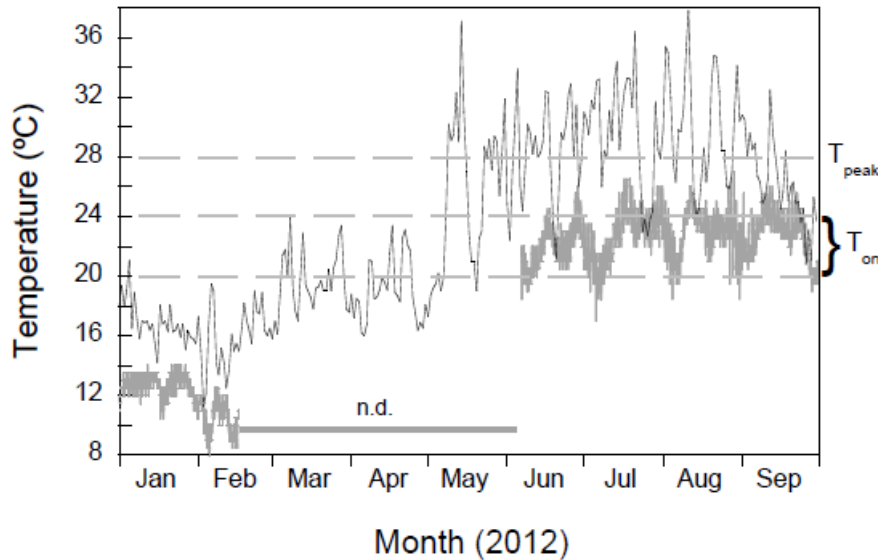


Figure 3.5 - Air and seawater temperatures in the Ria Formosa in 2012. Maximum daily air temperatures for 2012 from Faro Airport weather station (black line) and SW temperatures within the Ria Formosa (ca. 2.5 m below MLT, see Fig. S3.1; grey line). 2012 SW temperatures were measured hourly by datalogger. For reference the HSR T_{on} range and T_{peak} value estimated from laboratory and field data are shown as horizontal broken lines.

Southern Portuguese coastal waters have experienced significant warming over the last 4 decades; SST adjacent to Faro (36°52'50"N, 7°52'50"W) indicate mean warming rates of 0.29°C/decade (Lima & Wethey 2012; Nicastro et al. 2013). Warming is mainly seen from Apr - Jun, and Oct – Jan (Table 1), resulting in earlier warming (based on changes exceeding 75% of SSTs) of ca. 10 Julian days/y, and with between 11 - 15 more days/y warmer than 95% of SSTs.

Monthly minimum air temperatures for Faro are increasing for all but the winter months, at around 1°C/decade, with lower rates for mean and maximum temperature, both significant in spring (Table 1). Decadal means for 1973 – 2011 show a clear increasing trend that is particularly marked in the spring and early summer, while the trend in maximum air temperatures is less dramatic (see Fig. S3.2). Analysis of daily temperature anomalies in 1973 – 2011 show a similar steadily mean increase, with the largest shifts in the spring and early summer (see Fig. S3.3.).

Table 3.1 – Rates of change in sea surface temperature (SST) and mean minimum (Tm), average (T) and maximum (TM) air temperatures in the Faro region. Based on data from 1982 - 2010 for seawater (Lima & Wethey, 2012) and 1973 - 2011 for air temperatures.

* Station 11_8152: 36°52'50"N, 07°52'05"W

Season	Month	SST*		Tm			T			TM		
		P-value	Rate (°C /decade)	R ²	P-value	Rate (°C /decade)	R ²	P-value	Rate (°C /decade)	R ²	P-value	Rate (°C /decade)
Winter	Jan	<0.05	0.21	0.098	n.s.	0.42	0.079	n.s.	0.23	0.007	n.s.	0.05
	Feb	n.s.	0.20	0.070	n.s.	0.41	0.074	n.s.	0.27	0.029	n.s.	0.15
Spring	Mar	n.s.	0.10	0.447	<0.0001	0.99	0.373	<0.0001	0.58	0.036	n.s.	0.18
	Apr	<0.05	0.31	0.515	<0.0001	1.12	0.409	<0.0001	0.73	0.169	0.009	0.44
	May	<0.05	0.37	0.616	<0.0001	1.07	0.369	<0.0001	0.69	0.109	0.04	0.35
Summer	Jun	<0.05	0.61	0.496	<0.0001	0.88	0.303	0.0003	0.68	0.185	0.006	0.57
	Jul	n.s.	0.33	0.386	<0.0001	0.71	0.129	0.025	0.34	0.060	n.s.	0.24
	Aug	n.s.	0.38	0.435	<0.0001	0.77	0.135	0.021	0.33	0.000	n.s.	0.01
Autumn	Sep	n.s.	0.09	0.234	0.002	0.51	0.033	n.s.	0.16	0.063	n.s.	-0.25
	Oct	<0.05	0.49	0.335	0.0001	0.80	0.275	0.001	0.63	0.050	n.s.	0.22
	Nov	<0.05	0.33	0.033	n.s.	0.24	0.057	n.s.	0.25	0.000	n.s.	0.01
Winter	Dec	<0.05	0.23	0.011	n.s.	0.14	0.039	n.s.	0.19	0.000	n.s.	0.01

3.4 - Discussion

This paper presents the most comprehensive characterization yet of the heat-shock response (HSR) in an ecosystem-structuring alga. The data were recorded from a southern edge population immediately prior to local extinction, with microenvironmental thermal profiles, together with molecular and physiological data on HSR, revealing the common occurrence of non-permissive temperatures in natural algal patches.

We first established the temperature-dependence of the HSR for the expression of seven chaperones, encompassing the range of environmentally relevant temperatures up to levels that severely affect physiological resilience. Second, *in situ* thermal profiles and HSR indicated that local (microhabitat) scale tissue temperatures at or above T_{peak} and seawater temperatures around T_{on} , resulted in extreme thermal loads throughout the entire summer period, likely resulting in a semi-permanent, or chronic HSR. Third, we present the first molecular evidence that desiccation arrests or prevents the HSR. As a consequence, the canopy surface in natural populations did not display the same temperature-dependent HSR kinetics as that shown in hydrated tissue, despite reaching the highest temperatures. While other causes have not been excluded, local and regional warming trends over the last 40 years are consistent with steadily increasing thermal stress loads that may have contributed to population decline and range contraction at the trailing southern edge (Nicastro *et al.* 2013). A recent study combining biogeographic patterns of genetic diversity with species distributional modelling identified both increasing sea surface and air temperatures as explanatory factors (Assis *et al.* 2014).

The HSR of *Fucus vesiculosus*

The main features of the *F. vesiculosus* HSR were established in laboratory experiments with a suite of seven HSP transcripts. The onset temperature (T_{on}) was below 24°C (the lowest temperature tested), and T_{peak} occurred at 28°C, with induction and peak expression in close agreement for all the transcripts. Importantly, the decline in capacity to mount a HSR at 36°C coincided with a loss of resilience in PSII photochemistry, implying fitness costs associated with enhanced rates of protein turnover and repair. Similar induction patterns were reported in intertidal brown algae (although responses differ in subtidal populations) for a single Hsp70 gene (Henkel, Kawai & Hofmann 2009) and in the lower shore *Fucus serratus*, for three Hsp genes (Jueterbock *et al.* 2013). At temperatures that exceed T_{peak} and impair

photosynthetic physiology (36°C), HSP expression was greater after recovery than immediately post-stress. Extensive repair of misfolded and aggregated proteins therefore appears to be required at least 24h after a return to growth temperatures, implying non-trivial metabolic costs and impacts on energy allocation for normal metabolism and growth.

Does microhabitat variation moderate thermal stress?

We hypothesized that microhabitat variation provides distinct local environmental conditions, which should result in variable stress loads during emersion. In this case, it is interesting to note that (with the exception of channels) these microhabitats arise solely from the patch structure created by *F. vesiculosus*, rather than from intrinsic habitat heterogeneity (e.g., shading due to aspect or crevices on rocky intertidal shores). More specifically, we hypothesized that the top and edges of patches would be more thermally stressful than shaded lower canopy or channels. In fact the situation was quite complex. The bottom, or sub-canopy, was consistently the most thermally benign microhabitat, with the lowest warming rate and generally the lowest maximum temperature attained (but see Fig. 2e). Algal canopies are generally considered to provide relatively cool and moist conditions favourable for growth (Brawley & Johnson 1991; Davison, Johnson & Brawley 1993), and this was reflected in delayed and/or reduced HSR. However, even here a severe HSR was observed in summer. The similarity in thermal conditions and HSR in patch edges and channels was striking, and although channels warmed at a slightly lower rate, our data show that they did not provide a significant escape from thermal stress.

Contrary to our predictions, we found that the hottest and driest microhabitat, the top of the canopy, may actually be the most benign for a poikilohydric alga like *F. vesiculosus*. The occurrence of rapid and severe desiccation prevents any transcriptional response to thermal stress, and may have a protective role, by keeping fronds in a metabolically inactive state. Desiccation is a well-known survival strategy not only for resting stages such as seeds and spores, but for a variety of adult taxa as well, in which organisms can enter a remarkable ametabolic state known as anhydrobiosis. In most organisms, the desiccated state increases thermotolerance (Alpert & Oliver 2002), and this is a confirmed but little-explored feature of some intertidal macroalgae (Hunt & Denny 2008). We tentatively suggest that poikilohydry may be an alternative strategy that allows individuals to escape the energetic costs of mounting a HSR during peak stress periods. If so, it would be a particularly important adaptation to life near the southern range edge. Additional work is required to elucidate the

potential benefits of this strategy in the long term, to determine the metabolic costs, not only of desiccation but also of the subsequent rehydration/ recovery process, and compare them to the costs associated with a HSR in the hydrated state.

Thermal conditions at the southern edge; a chronic heat stress environment

Contrasting winter and summer thermal conditions were reflected in large differences in HSP induction. Optimal warming conditions in January (full sun, air temperature of 18°C) induced a small but significant HSR in submersed algae warmed to 20°C, but recovery to initial conditions had occurred by the end of low tide. The fact that we could detect a minor HSR close to 20°C in the field does, however support what we saw in laboratory trials, in which a clear HSR was already evident after exposure to 24°C, and suggests a T_{on} nearer to 20°C than 24°C. The current average winter maximum air temperature remains below 18°C in the Ria Formosa, indicating that thermal stress during winter months is unlikely to have significant effects on metabolism and growth. In contrast, during equivalent low tide periods in summer, levels and frequency of heat shock exposure were extreme, based on the observed parameters of the *F. vesiculosus* HSR. Tissue temperatures were consistently above maximum air temperatures, and therefore likely to surpass the T_{peak} throughout summer when algae are emersed during daytime low tides, resulting in a widespread and prolonged HSR in hydrated algae. Even under the moderate August sampling conditions (maximum air temperature 28.0°C), tissue temperatures in all microhabitats (31 - 36°C) exceeded T_{peak} during the low tide sampled. Repeated exposure to such temperatures and induction of HSR over five or six consecutive days during daytime low tides would impose large metabolic costs. High mortality in response to repeated heat shock exposures has been documented in intertidal mussels (Jones, Mieszkowska & Wethey 2009). Multiple sequential exposures to high temperatures likely decrease thermal tolerance thresholds (Jones *et al.* 2009; Sorte, Jones & Miller 2011), since individuals are still repairing accumulated damage from previous exposures.

The HSR has been characterized in very few intertidal species. Reported T_{on} was higher in an intertidal snail (27°C) than the 20 – 24°C we determined here for *F. vesiculosus* (Tomanek & Somero 1999), but in a similar range or even lower for low intertidal to subtidal kelp species (Henkel & Hofmann 2008; Henkel *et al.* 2009). An important question in seasonally varying thermal environments is the degree of plasticity shown by the HSR. Somewhat counterintuitively however, it appears that the thermal variability of intertidal habitats may

constrain the evolution of significant plasticity. Intertidal organisms generally live near to their thermal limits, frequently inducing a HSR in nature as part of their life history strategy, and in contrast to subtidal organisms that rarely experience temperatures near to their observed T_{on} (Tomanek 2010). While we did not directly address this question, the apparently small seasonal variation in T_{on} we observed in sHSP induction in the field (Fig. 4) supports this idea.

An additional and chronic stress for southern populations is predicted by seawater temperatures during immersion that are non-permissive for HS recovery. In the shallow Ria Formosa, seawater temperatures of 20 – 26°C prevail during summer, resulting in a semi-constant T_{on} for the HSR. This is the likely cause of the elevated sHSP expression observed in August compared with January at the onset of low tide (Fig. 3). South of Lat 41°38'N (i.e., Northern Portugal), *F. vesiculosus* occurs exclusively in estuaries and embayments where decadal scale rising air temperatures also increase warming of local semi-enclosed water masses. In contrast, in northern Portugal (the southern edge of open coast rocky intertidal populations, and more typical habitat for the species) seawater temperatures during immersion do not exceed the estimated T_{on} range of 20 – 24°C (Pearson *et al.* 2009). A detailed understanding of the interaction of seawater and air temperatures on the timing and extent of the HSR, together with direct measures of fitness-related traits, could be powerful in developing predictive niche models for population persistence throughout the (declining) southern range of the species (Assis *et al.* 2014).

Several recent studies have documented the impacts of climate change on intertidal invertebrates and algae (reviewed in Helmuth *et al.* 2006b; Hawkins *et al.* 2009), revealing widespread northern range expansions and some southern range contractions since the 1970s/80s, coinciding with the steady increase in regional coastal SST. While other factors cannot be excluded, regional sea surface warming trends over recent decades correlate with the local extinction of the Ria Formosa population, as well as other southern edge populations of *F. vesiculosus* (Nicastro *et al.* 2013). Combining microenvironmental measurements with characterization of the HSR shows that these edge populations exist(ed) very near to their thermal limits, and together provide a strong argument that thermal stress plays a significant role in population persistence near the southern (trailing) edge.

3.5 - References

- Alpert, P. & Oliver, M.J. (2002). Drying Without Dying. Desiccation and survival in plants: drying without dying (eds M. Black & H.W. Pritchard), pp. 3 - 43. CABI Publishing.
- Ardré, F. (1970). Contribution à l'étude des algues marines du Portugal. I. La flore. *Portugaliae Acta Biologica*, Série B, Sistemática, Ecologia, Biogeografia e Paleontologia, pp 137-555.
- Assis, J., Coelho, N., Alberto, F., Valero, M., Raimondi, P., Reed, D. & Serrão, E.A. (2013). High and distinct range-edge genetic diversity despite local bottlenecks. *PLoS ONE*, 8, e68646.
- Assis, J., Serrão, E.A., Claro, B., Perrin, C. & Pearson, G.A. (2014). Climate-driven range shifts explain the distribution of extant gene pools and predict future loss of unique lineages in a marine brown alga. *Molecular Ecology* 23, 2797–2810.
- Brawley, S.H. & Johnson, L.E. (1991). Survival of furoid embryos in the intertidal zone depends upon developmental stage and microhabitat. *Journal of Phycology*, 27, 179-186.
- Cunha, A.H., Assis, J.F. & Serrão, E.A. (2013). Seagrasses in Portugal: A most endangered marine habitat. *Aquatic Botany*, 104, 193-203.
- Davenport, J. & Davenport, J.L. (2005). Effects of shore height, wave exposure and geographical distance on thermal niche width of intertidal fauna. *Marine Ecology Progress Series*, 292, 41-50.
- Davison, I.R., Johnson, L.E. & Brawley, S.H. (1993). Sublethal Stress in the Intertidal Zone - Tidal Emersion Inhibits Photosynthesis and Retards Development in Embryos of the Brown Alga *Pelvetia fastigiata*. *Oecologia*, 96, 483-492.
- Davison, I.R. & Pearson, G.A. (1996) Stress tolerance in intertidal seaweeds. *Journal of Phycology*, 32, 197-211.
- Diekmann, O.E. & Serrão, E.A. (2012). Range-edge genetic diversity: locally poor extant southern patches maintain a regionally diverse hotspot in the seagrass *Zostera marina*. *Molecular Ecology*, 21, 1647-1657.
- Dietz, T.J. & Somero, G.N. (1992). The threshold induction temperature of the 90-kDa heat shock protein is subject to acclimatization in eurythermal goby fishes (genus *Gillichthys*). *Proceedings of the National Academy of Sciences of the United States of America*, 89, 3389-3393.
- Dring, M.J. & Brown, F.A. (1982). Photosynthesis of inter-tidal brown-algae during and after periods of emersion - a renewed search for physiological causes of zonation. *Marine Ecology Progress Series*, 8, 301-308.
- Hawkins, S.J., Sugden, H.E., Mieszkowska, N., Moore, P.J., Poloczanska, E., Leaper, R., Herbert, R.J.H., Genner, M.J., Moschella, P.S., Thompson, R.C., Jenkins, S.R., Southward, A.J. & Burrows, M.T. (2009). Consequences of climate-driven biodiversity changes for ecosystem functioning of North European rocky shores. *Marine Ecology Progress Series*, 396, 245-259.
- Helmuth, B. (2002b). How do we measure the environment? Linking intertidal thermal physiology and ecology through biophysics. *Integrative and Comparative Biology*, 42, 837-845.

- Helmuth, B., Broitman, B.R., Blanchette, C.A., Gilman, S., Halpin, P., Harley, C.D.G., O'Donnell, M.J., Hofmann, G.E., Menge, B. & Strickland, D. (2006a). Mosaic patterns of thermal stress in the rocky intertidal zone: Implications for climate change. *Ecological Monographs*, **76**, 461-479.
- Helmuth, B., Harley, C.D.G., Halpin, P.M., O'Donnell, M., Hofmann, G.E. & Blanchette, C.A. (2002a). Climate change and latitudinal patterns of intertidal thermal stress. *Science*, **298**, 1015-1017.
- Helmuth, B., Mieszkowska, N., Moore, P. & Hawkins, S.J. (2006b). Living on the edge of two changing worlds: Forecasting the responses of rocky intertidal ecosystems to climate change. *Annual Review of Ecology Evolution and Systematics*, **37**, 373-404.
- Helmuth, B.S.T. & Hofmann, G.E. (2001). Microhabitats, thermal heterogeneity, and patterns of physiological stress in the rocky intertidal zone. *Biological Bulletin*, **201**, 374-384.
- Henkel, S.K. & Hofmann, G.E. (2008). Differing patterns of hsp70 gene expression in invasive and native kelp species: evidence for acclimation-induced variation. *Journal of Applied Phycology*, **20**, 915-924.
- Henkel, S.K., Kawai, H. & Hofmann, G.E. (2009). Interspecific and interhabitat variation in hsp70 gene expression in native and invasive kelp populations. *Marine Ecology-Progress Series*, **386**, 1-13.
- Hunt, L.J.H. & Denny, M.W. (2008). Desiccation protection and disruption: a trade-off for an intertidal marine alga. *Journal of Phycology*, **44**, 1164-1170.
- Jones, S.J., Mieszkowska, N. & Wetthey, D.S. (2009). Linking thermal tolerances and biogeography: *Mytilus edulis* (L.) at its southern limit on the east coast of the United States. *The Biological bulletin*, **217**, 73-85.
- Jueterbock, A., Tyberghein, L., Verbruggen, H., Coyer, J.A., Olsen, J.L. & Hoarau, G. (2013). Climate change impact on seaweed meadow distribution in the North Atlantic rocky intertidal. *Ecology and Evolution*, **3**, 1356-1373.
- Lago-Leston, A., Mota, C., Kautsky, L. & Pearson, G.A. (2010) Functional divergence in heat shock response following rapid speciation of *Fucus* spp. in the Baltic Sea. *Marine Biology*, **157**, 683-688.
- Lima, F., Burnett, N., Helmuth, B., Kish, N., Aveni-Deforge, K. & Wetthey, D.S. (2011). Monitoring the intertidal environment with biomimetic devices. *Biomimetic Based Applications* (ed. M. Cavrak). InTech.
- Lima, F.P. & Wetthey, D.S. (2012). Three decades of high-resolution coastal sea surface temperatures reveal more than warming. *Nature communications*, **3**, 704.
- Maxwell, K. & Johnson, G.N. (2000). Chlorophyll fluorescence - a practical guide. *Journal of Experimental Botany*, **51**, 659-668.
- Nicastro, K.R., Zardi, G.I., Teixeira, S., Neiva, J., Serrao, E.A. & Pearson, G.A. (2013). Shift happens: trailing edge contraction associated with recent warming trends threatens a distinct genetic lineage in the marine macroalga *Fucus vesiculosus*. *BMC biology*, **11**, 6.
- Pearson, G., Lago-Leston, A., Valente, M. & Serrao, E. (2006). Simple and rapid RNA extraction from freeze-dried tissue of brown algae and seagrasses. *European Journal of Phycology*, **41**, 97-104.

- Pearson, G.A., Hoarau, G., Lago-Leston, A., Coyer, J.A., Kube, M., Reinhardt, R., Henckel, K., Serrao, E.T.A., Corre, E. & Olsen, J.L. (2010). An expressed sequence tag analysis of the intertidal brown seaweeds *Fucus serratus* (L.) and *F. vesiculosus* (L.) (Heterokontophyta, Phaeophyceae) in response to abiotic stressors. *Marine Biotechnology*, **12**, 195-213.
- Pearson, G.A., Lago-Leston, A. & Mota, C. (2009). Frayed at the edges: selective pressure and adaptive response to abiotic stressors are mismatched in low diversity edge populations. *Journal of Ecology*, **97**, 450-462.
- Pfister, C.A., Wootton, J.T. & Neufeld C. (2007). The relative roles of coastal and oceanic processes in determining physical and chemical characteristics of an intensively sampled nearshore system. *Limnology & Oceanography*, **52**, 1767-1775.
- Roberts, D.A., Hofmann, G.E. & Somero, G.N. (1997). Heat-shock protein expression in *Mytilus californianus*: Acclimatization (seasonal and tidal-height comparisons) and acclimation effects. *Biological Bulletin*, **192**, 309-320.
- Seabra, R., Wetthey, D.S., Santos, A.M. & Lima, F.P. (2011). Side matters: Microhabitat influence on intertidal heat stress over a large geographical scale. *Journal of Experimental Marine Biology and Ecology*, **400**, 200-208.
- Sorte, C.J.B., Jones, S.J. & Miller, L.P. (2011). Geographic variation in temperature tolerance as an indicator of potential population responses to climate change. *Journal of Experimental Marine Biology and Ecology*, **400**, 209-217.
- Tomanek, L. (2010). Variation in the heat shock response and its implication for predicting the effect of global climate change on species' biogeographical distribution ranges and metabolic costs. *Journal of Experimental Biology*, **213**, 971-979.
- Tomanek, L. & Somero, G.N. (1999). Evolutionary and acclimation-induced variation in the heat-shock responses of congeneric marine snails (genus *Tegula*) from different thermal habitats: Implications for limits of thermotolerance and biogeography. *Journal of Experimental Biology*, **202**, 2925-2936.
- Wahl, M., Jormalainen, V., Eriksson, B.K., Coyer, J.A., Molis, M., Schubert, H., Dethier, M., Karez, R., Kruse, I., Lenz, M., Pearson, G., Rohde, S., Wikstrom, S.A. & Olsen, J.L. (2011). Stress ecology in *Fucus*: abiotic, biotic and genetic interactions. *Advances in Marine Biology*, Vol 59, **59**, 37-105.
- Zardi, G.I., Nicastro, K.R., Canovas, F., Costa, J.F., Serrao, E.A. & Pearson, G.A. (2011). Adaptive traits are maintained on steep selective gradients despite gene flow and hybridization in the intertidal zone. *Plos One*, **6**.

3.6 – Acknowledgements

We thank João Reis for seawater temperature data from the Ria Formosa (2012). This manuscript was greatly improved by comments from Dr. Brian Helmuth, an anonymous reviewer and the Editors of Functional Ecology. This study was supported by FCT - Portuguese Science Foundation (projects POCTI/MAR/61105/2004, EXCL/AAG-GLO/0661/2012 and PhD fellowship SFRH/BD/74436/2010 to CFM).

Supporting information

Supporting information to this chapter can be found on the Appendix (digital version)

Figure S3.1. Map of Portugal showing Ria Formosa. The sampling (yellow arrow) and SW temperature measurements (white arrow) sites are indicated.

Figure S3.2. Decadal temperature trends in Ria Formosa. Monthly averages for mean and maximum air temperatures for 1973 – 2011.

Figure S3.3. Average daily mean temperature anomalies in Ria Formosa 1973 - 2011.

Table S3.1. Primers for RT-qPCR and PCR reaction efficiencies for laboratory and field-collected samples.

Table S3.2. PERMANOVA and pairwise post hoc comparisons of F_v/F_m from laboratory HS experiments.

Table S3.3. PERMANOVA and pairwise post hoc comparisons of HSR after 3 h HS and subsequent recovery.

Table S3.4. PERMANOVA and pairwise post hoc comparisons of January HSR in four microhabitats.

Table S3.5. PERMANOVA and pairwise post hoc comparisons of August HSR in four microhabitats.

Chapter 4

Optimizing protein extraction and separation to study desiccation-tolerance in *Fucus* macroalgae

Chapter 4 – Optimizing protein extraction and separation to study desiccation-tolerance in *Fucus* macroalgae

4.0 - Abstract

Shifting between marine and terrestrial habitats, *Fucus vesiculosus* is a brown alga that desiccates rapidly when exposed to air, yet forms dense canopies along European intertidal areas. Desiccation, together with temperature and high light, often limits the distribution of intertidal organisms. To identify mechanisms responsible for desiccation tolerance, we searched for proteins differentially expressed during the recovery period following intense desiccation at low tide, when repair and protection mechanisms should be active.

First we developed an optimized method for protein extraction from *Fucus vesiculosus*, an organism with many polysaccharides and phenolics, compounds known to interfere with the extraction of proteins from other macroalgae and terrestrial plants. We tested four methods previously described for algal or plant tissues. Two methods including a phenol extraction and multiple precipitation steps, both developed for brown algae, were effective with *Fucus* vegetative tissue, producing well resolved protein spots in 2-DE. Simpler methods could reduce extraction time and avoid potential protein losses during the various cleaning steps, but these methods failed to eliminate contaminants present in *Fucus* tissues that cause high viscosity and aggregation of proteins. A simpler protocol for plant tissues with successive methanol and acetone precipitations, using a commercial kit, and a method developed for other macroalgae, using RNA extraction columns, resulted in very viscous extracts unsuitable for protein separation.

To detect differential protein expression associated with recovery from desiccation, purified protein extracts were separated in 2-DE gels and the resulting spot patterns analysed. Even after increasing spot separation, few spot volume changes were detected and all failed multiple testing correction. This lack of significant expression differences between control

and recovery treatments may result from the constitutive expression of desiccation tolerance. Alternatively these differences may be undetected due to the large individual variation in protein expression levels or other methodological limitations. Further studies are thus required to confirm if these results reflect the constitutive expression of desiccation protection in this intertidal alga.

4.1 – Introduction

Brown macroalgae in general (and fucoids in particular) are among those organisms that can give molecular biologists difficulties. Elaborate extraction protocols are often required by these tissues with low amounts of proteins and nucleic acids and many potentially interfering secondary metabolites. Extensive extractions and washing steps are then required to obtain purified DNA (Varela-Alvarez *et al.* 2006, Phillips *et al.* 2001, Hoarau *et al.* 2007), RNA (Pearson *et al.* 2006, Masters *et al.* 1992) or proteins (Nagai *et al.* 2008, Contreras *et al.* 2008) that can be successfully used in downstream analysis.

Intertidal brown algae from the genus *Fucus* are abundant in European rocky shores, where they endure a stressful environment exposed to periodic desiccation. Among other stress factors these algae are often exposed to high light, UV radiation, extreme temperatures, wave action and grazing (Wahl *et al.* 2011). *Fucus* algae produce abundant secondary metabolites, thought to protect the algal fronds from some stressors. Among them a diversity of alginates and sulphated fucans (polysaccharides) and phlorotannins (phenolics) have been found in cell walls and algal extracts that may have protective roles, e. g. phlorotannins in protection against UV radiation (Schoenwaelder *et al.* 2003) or as grazing deterrents (Pavia & Toth 2000). The term “tannins” defines high molecular weight phenolic compounds that can form strong complexes with proteins and other macromolecules (Horvath 1981). There are different chemical classes of tannins in land plants, different from those found in brown algae (phlorotannins). Phlorotannins are a group of complex polymers of phloroglucinol unique to macroalgae, often abundant in special storage vesicles called physodes and are also integral structural components of the cell wall in brown algae (Schoenwalder & Clayton 1998, Schoenwaelder 2008). Tissue composition (diversity and abundance of these polymeric structures) is species-specific but also varies widely with season, location on the shore, and other genetic and environmental factors. Some of these compounds (mostly polysaccharides and polyphenolics) have been shown to possess useful bioactive properties (antioxidant, anticoagulant, anti-inflammatory and antitumoral) and current research shows promising applications in the prevention of human pathologies like cancer, arthritis, neurodegenerative diseases, diabetes and hypertension or in biomaterials for bone tissue regeneration (Li *et al.* 2008, Li *et al.* 2011, Barbosa *et al.* 2014, Venkatesan *et al.* 2014).

Despite a large body of literature concerning protein extraction methods, and many protocols for detailed analysis of particular protein modifications and large studies of whole proteomes

and sub-proteomes, many organisms and tissues are still recalcitrant to standard methods of extraction. Many plants and algae fall into this category, given their large amount and diversity of secondary metabolites. These compounds not only decrease the relative amount of protein present, but often are co-extracted forming insoluble precipitates. They can also interfere with quantification or inhibit subsequent analysis. We describe our experience with protein extraction from vegetative apical tips of field-collected *Fucus* spp., using four protein extraction methods described for plants or algae containing large amounts of viscous polysaccharides and polyphenols, particularly other brown macroalgae. We report the selection and optimization of an effective method capable of producing high-quality protein extracts suitable for 2-DE analysis of differential protein expression.

Fucus vesiculosus is an intertidal brown algae that desiccates quickly when exposed to air at low tide, yet is capable of surviving the loss of over 90% of its water to resume normal metabolic activity shortly upon reimmersion (Davison & Pearson 1996; Pearson *et al.* 2009). Previous research on the desiccation tolerance of furoid algae has reported species differences in tolerance, showing *F. vesiculosus* to be more tolerant than *F. serratus*, but less than *F. spiralis* (Dring & Brown 1982). Desiccation tolerance in these species is consistent with their typical vertical zonation and geographical distribution (Dring & Brown 1982, Davison & Pearson 1996). Studies on growth, survival, photosynthesis and respiration rates or other photosynthetic parameters, have shown metabolic arrest in severely dehydrated tissues, and a fast recovery of photosynthesis upon rehydration. On a molecular level, previous analysis of gene expression during desiccation and recovery failed to identify significant differences at the mRNA level (Pearson *et al.* 2010). Despite their long history as ecological models, due to their conspicuous zonation patterns on Atlantic shores, few studies attempted to analyse desiccation tolerance at the molecular level in fucales or other brown algae, probably due to the lack of appropriate extraction methods and genomic resources. The recent availability of effective protein extraction protocols, as well as the completion of the first brown algal genomes (Cock *et al.* 2010, *Ectocarpus siliculosus*; Ye *et al.* 2015, *Saccharina japonica*) finally allow the use of molecular biology tools, opening the modern “omics” world to the brown algae group (Dittami *et al.* 2009; 2011; Pearson *et al.* 2009; Lago-Leston *et al.* 2010; Konotchick *et al.* 2013; Heinrich *et al.* 2015).

Using the optimized protocol for protein extraction (modified from Contreras *et al.* 2008), we can obtain reproducible 2-DE proteomic profiles from both field-collected and lab-desiccated

fucoïd tissues. Specific proteins, whose concentration changes in response to desiccation and subsequent rehydration, can be identified by comparing the 2-DE patterns from desiccated and non-desiccated tissues. Following image analysis, spots changing significantly between these conditions (control and recovery from desiccation) are expected to represent differentially expressed proteins involved in the protection and repair of damage caused by desiccation or in the metabolic reactivation after desiccation-induced arrest. The identification of such differentially expressed proteins could indicate the pathways and processes contributing to the desiccation-tolerance of this organism. We aim to compare protein patterns among *Fucus vesiculosus* tissues, during the early phase of recovery from severe desiccation to corresponding controls kept fully hydrated under submerged conditions, under natural levels of light and temperature to identify the molecular processes underlying desiccation-tolerance.

4.2 – Material and methods

In situ desiccation and sampling

In Viana do Castelo, northern Portugal, three large intertidal individuals of *Fucus vesiculosus* and three of *F. serratus* were selected, with abundant undamaged, non-reproductive (vegetative), apical tips free of visible epiphytes. On June 8, 2012, around 11:00 am, two similar frond fragments were collected from each of these hydrated plants, as the tide receded. Half were placed in a lower shore pool, where they remained submerged and fully hydrated (Control). The remaining fronds (n = 3 per species) were placed on an upper shore rock face and allowed to dry for 2.5 h under natural field conditions (Desiccation). At the end of the desiccation period, 3 vegetative tips per plant were collected into pre-weighted vials containing 2 ml of seawater, to determine tissue water content (TWC) of control and desiccated tips. The fronds were then submerged in the same lower shore pool to rehydrate for 1 hour (Recovery from desiccation), after which samples were collected for proteomic analysis (Recovery and Control). Approximately 20 vegetative tips per plant were briefly rinsed 3 times in ddH₂O and 3 times in 50 mM Tris-HCl pH 8.8 to remove excess salt, blotted dry with clean paper towels, then flash-frozen in liquid nitrogen on the shore. Collection, washing and freezing of all samples took about 1 h, so final samples (R3) were allowed to recover for almost two hours. Upon return to the laboratory, in Faro, vials were weighted to determine the weight of each tip at the time of collection (cW), and the tips were then gently blotted to remove surface water and weighted to determine fully hydrated weight (hW). Tips were then dried at 65°C for two days to determine dry weight (DW), and TWC determined as:

$$\text{TWC (\%)} = (\text{cW} - \text{DW}) / (\text{hW} - \text{DW}) \times 100.$$

Protein extraction methods for *Fucus* spp.

The following protein extraction methods were described in the literature as suitable for plants or macroalgae. Some modifications were made to the original protocols that have proven effective for *Fucus* tissue in other protocols. The same protease inhibitor cocktail (reference #P9599; Sigma-Aldrich) was used in all protocols. Modifications to the extraction buffer of protocol A (Contreras *et al.* 2008) were made on advice of authors of the original report (personal communication). To obtain adequate amounts of tissue for the extractions,

tissue fragments were briefly removed from liquid nitrogen and quickly weighed to avoid thawing. Tissues were then stored at -80°C until protein extraction. For each method four independent (technical) replicates were used in each trial.

Method A – Phenol extraction for brown algae

This method was adapted from Method 5 described in “Two-Dimensional Gel Electrophoresis Analysis of Brown Algal Protein Extracts” (Contreras *et al.* 2008).

Frozen tissue was thoroughly pulverized in liquid nitrogen using a cooled mortar and pestle. All extraction steps were performed on ice or at 4°C except if otherwise indicated. The frozen powder was carefully resuspended in extraction buffer (2% w/v PVP-40, 0.7 M sucrose, 0.5% w/v CHAPS, 0.75 M KCl, 0.5 M Tris-HCl pH 7.5, 250 mM EDTA and freshly added 2% v/v beta-mercaptoethanol and protease inhibitor cocktail) and homogenized at 5°C for 20-40 min on an orbital shaker. Two volumes of phenol (Tris-HCl-saturated-phenol, pH 8.0) were added and the mixture was homogenized again for 20 min at 5°C, centrifuged at 10,000 x g for 20 min and the upper phenol phase was transferred to a new tube, avoiding the interface. Proteins were precipitated by adding five volumes of 0.1 M ammonium acetate dissolved in (cold) methanol and incubating at -20°C until a large “cloud” of precipitate was visible (about 2 h). After discarding the supernatant following 15 min centrifugation at 10,000 x g, the resulting protein pellet was washed twice in ice-cold 0.1 M ammonium acetate in methanol (with a 20 min incubation at -20°C and a 12 min centrifugation at 12,000 x g), once with ice-cold 10% TCA in acetone (30 min at -20°C, 10,000 x g for 15 min) and four times in ice-cold 80% acetone containing 20 mM DTT (20 min at -20°C, 12,000 x g for 12 min). The final pellet was air-dried at room temperature for 5-10 min, quickly dissolved in 0.5 ml of 2DE rehydration solution (6 M urea, 2 M thiourea, 4% w/v CHAPS, 60 mM fresh DTT, protease inhibitor cocktail) and stored at -20°C. For convenience, the pellet was sometimes incubated overnight instead of 20 minutes during the final acetone washes, without noticeable effects on the extraction yield.

Method B – Ethanol/phenol method

This method, adapted from (Nagai *et al.* 2008), was developed for another brown macroalgae (*Ecklonia kurome*, Laminariales) that also presents high levels of viscous polysaccharides and phlorotannins. It is similar to method A, with a phenol extraction and subsequent methanol

and acetone washes, but uses an extraction buffer containing SDS and includes preliminary ethanol washes to remove pigments and sugars.

All extraction steps were performed on ice or at 4°C except if otherwise indicated. Frozen tissue was thoroughly pulverized in liquid nitrogen using a cooled mortar and pestle before extensive homogenization in ice-cold 100% ethanol by vortexing and vigorous shaking for 15 min on an orbital incubator. The homogenates were centrifuged at 10,000 x g for 20 min, the supernatant discarded and the pellets washed twice in cold 100% ethanol (15 min at -20°C and 15,000 x g for 15 min) and then once in 80% ice-cold acetone containing 20 mM DTT (30 min at -20°C and 15,000 x g for 15 min). The pellet was air-dried briefly and immediately resuspended (vortex) in 0.8 mL of SDS extraction buffer (2 % w/v PVP-40, 30 % w/v sucrose, 100 mM Tris-HCl pH 8.0, 2% w/v SDS, freshly added 30 mM DTT and protease inhibitor cocktail). Then one volume of phenol (Tris-HCl-saturated-phenol, pH 8.0) was added, the mixture was homogenized at 5°C for 15-30 min (vortex and orbital shaker) and centrifuged at 15,000 x g for 5 min. The clear phenol phase was transferred to a new tube, the aqueous phase was re-extracted with one volume of phenol and the proteins were precipitated from both phenol extracts with five volumes of ice-cold 0.1 M ammonium acetate dissolved in methanol overnight at -20°C. After a 15 min centrifugation at 10,000 x g, the pellet was washed twice in 0.1 M ammonium acetate in methanol and twice in 80% ice-cold acetone with 20 mM DTT (always 20 min at -20°C and 12,000 x g for 12 min). The powder was briefly air-dried and dissolved in 2DE rehydration solution (same as in method A).

Method C – Protein extraction using RNeasy columns (QIAGEN)

This method was adapted from Parages *et al.* (2012) and uses reagents and columns from an RNA extraction kit (RNeasy Plant kit, QIAGEN). This method reportedly maintains the phosphorylation state of proteins, allowing detection of phosphorylated proteins by Western blot. It allowed detection of a phosphorylated kinase from *Cystoseira* spp. (a related brown macroalgae). It was developed specifically to allow detection of the phosphorylation state of macroalgal protein kinases because other suitable extraction methods use trichloroacetic acid and phenol for protein precipitation, what may reportedly increase loss of labile phosphate groups (Parages *et al.* 2012).

Frozen tissue was thoroughly pulverized in liquid nitrogen using a cooled mortar and pestle and homogenized in RLT buffer (QIAGEN) with β -mercaptoethanol by repeated vortexing

and shaking for 20 min at 5°C. These homogenates were centrifuged at 15,000 x g for 20 min at 4°C and the supernatant was transferred to a QIAshredder column (QIAGEN) that was centrifuged for 2 min at full speed (15,000 x g) at RT. The flow-through was reloaded onto the same QIAshredder column and centrifuged again. The resulting flow-through was centrifuged again for 2 min at full speed and the supernatant pipetted to a new microcentrifuge tube. At room temperature, 0.5 volume of ethanol (100%) was added and the solution was mixed, vortexed and loaded onto an RNeasy Mini spin column (QIAGEN). The column was centrifuged for 30 s at 8,000 x g and 0.2 volume of 10% SDS was added to the flow-through and mixed. No SDS was added to half of the samples tested. Five volumes of ice-cold 0.1 M ammonium acetate in methanol were added before overnight incubation of the resulting mixture at -20°C. Finally the proteins were pelleted by centrifuging at 15,000 x g for 30 min at 4°C, the supernatant discarded and the air-dried pellet resuspended in the same 2DE rehydration solution.

Method D – Plant fractionated protein extraction kit

This method uses a commercial kit, the “Plant fractionated protein extraction kit” (reference #PE0240, Sigma-Aldrich), recommended for any type of plant tissue, to obtain separate hydrophilic and hydrophobic protein fractions. Reagents #1 and #4 (R#1 and R#4) were prepared according to the kit instructions, with the same protease inhibitor cocktail as the other methods.

All extraction steps were performed on ice or at 4°C except if otherwise indicated. Frozen tissue was pulverized in liquid nitrogen as in previous methods, homogenized in ice-cold methanol with protease inhibitor cocktail, incubated at -20°C for 15 min and centrifuged at 15,000 x g for 6 min at 4°C. The resulting pellet was washed twice in ice-cold methanol, briefly dried and washed twice with ice-cold acetone (-20°C for 15 min and 15,000 x g for 6 min). On the second extraction trial, three additional methanol washes and four acetone washes were performed. The pellets were air-dried, weighed and resuspended at room temperature in R#1, vortexing to completely break up the pellet. After mixing for 15 min at room temperature, the solution was centrifuged at 16,000 x g for 6 min and the supernatant (hydrophilic proteins on R#1) transferred to a new tube and stored at -20°C. The pellet was washed twice with R#1, by periodic vortexing at room temperature for 10 min and centrifugation at 16,000 x g for 5 min, then resuspended in R#4 at room temperature for 15

min (as before). This mixture was centrifuged at 16,000 x g for 30 min and the supernatant (hydrophobic proteins on R#4) transferred to a new tube and stored at -20°C.

Protein quantification

Protein concentrations were determined by Bradford assay using the Quick Start™ Bradford Protein Assay (Bio-Rad), on a microplate reader (Synergy 4), using Bovine Serum Albumin standards (0-100 ug/ml in water). Absorbance at 595 nm was measured on replicate wells with 20ul of sample (diluted 50x and 100x in water), 40ul of Bradford reagent and 140ul water. Because different re-suspension buffers were used, the absorbance of corresponding “blanks” (buffer diluted 50 x or 100 x) was subtracted from sample absorbance values.

SDS-PAGE

One-dimensional SDS-PAGE analysis was carried out under standard conditions. Laemmli buffer (8 µl) was mixed with undiluted sample (10 µl), boiled for 5 min, spun down and the supernatant loaded into pre-cast polyacrilamide gels (NuPage 4-12 %, BioRad).

2-DE

Protein samples were diluted in 2DE rehydration solution with ampholytes (Bio-Lyte 3-10 buffer) and 0,005 % Bromophenol Blue, to obtain the desired amount of protein (200 µg in 200 µl). IEF separation (first dimension) was performed on an Ettan IPGphor (GE Healthcare) after overnight passive rehydration of the ReadyStrip IPG Strips (11 cm, pH 4-7, BioRad). The IEF protocol used was: gradient to 150 V in 1:30 h, gradient to 500 V in 1 h, gradient to 6000 V in 2 h and constant voltage at 6000 V for 3h. The focused strips were stored at -20°C. Strips were equilibrated for 20 min in EqB1 (50 mM Tris-HCl, pH 8.8; 6 M urea; 30 % glycerol; 2 % SDS; 1 % DTT) and for 20 min in EqB2 (50 mM Tris-HCl, pH 8.8; 6 M urea; 30 % glycerol; 2 % SDS; 4.5 % iodoacetamide) before being loaded on the 12 % SDS-PAGE gels. All six small gels (Criterion 12 % Bis-Tris, 13.3 x 8.7 cm, BioRad) were run simultaneously in a Criterion Dodeca cell with MOPS buffer pH 7.7 (50 mM MOPS; 50 mM TrisBase; 0.1 % SDS; 1 mM EDTA). The gels were rinsed to remove excess SDS and fixed in 50 % ethanol; 2 % phosphoric acid for 2 h, washed 3 x with d H2O for 30 min and equilibrated 1 h in 34 % methanol; 17 % aluminium sulphate; 2 % phosphoric acid, before adding colloidal Coomassie (G-250) to stain the gels overnight. Gels were destained in water before scanning.

Separation on large gels was performed similarly, using 500 µg of protein in 450 µl, on 24 cm Immobiline DryStrips (pH 4-7, GE Healthcare). The IEF protocol was: 1 h gradient to 500 V, hold at 500 V for 1 h, gradient to 1000V for 1 h, gradient to 8000 V in 3 h, and hold at 8000 V for 5 h40 min, on an Ettan IPGphor 3 (GE Healthcare). Large gels were run on Ettan DALTsix, with TGS 1 x (192 mM glycine; 25 mM Tris-base; 0.1 % SDS) in the lower tank and TGS 2 x in the upper tank. Gels were rinsed and stained (45 % MeOH; 9.1 % acetic acid; 0.025% Coomassie Blue R-250) for 24 h, then destained (5% MeOH; 7.5% acetic acid) as needed to remove background colour.

Image Analysis

Coomassie Blue stained gels were scanned on a GS-800 calibrated densitometer (BioRad) and exported as (12-bit) TIFF files to Progenesis SameSpots software (NonLinear Dynamics) for image analysis. Gel images (3 biological replicates x 2 conditions) were aligned with some manual editing, and spot boundaries were defined across all gels. Spot volumes were normalized after removing low intensity spots, i.e. spots with an area, or normalised volume, below a defined threshold. The experimental design compared paired Control and Recovery samples (two treatments x three individuals), producing a list of putative differentially expressed spots between the treatments, their fold-change, *p*-values (ANOVA), *q*-values (multiple testing corrected *p*-value) and power of the analysis (see SameSpots software). To control False Discovery Rate (FDR) at 0.05, correction for multiple testing was also performed using the Benjamini & Hochberg approach (Benjamini & Hochberg, 1995).

4.3 – Results

Protein extraction methods for *Fucus* spp.

Previous desalting of the algal samples is important to improve resolution of 2-DE gels (Contreras *et al.* 2008), since excess salts interferes with IEF, so all methods were tested using the same set of desalted samples.

Method A (phenol extraction) after optimization produces generally good quality extracts suitable for 2-DE separation (Fig. 4.1). Protein yields of 3 mg of protein per gram of tissue (fresh weight) could be obtained with this method from field collected samples, but yields were somewhat variable (Tab. 4.1). Variable yields can result from composition (protein content) heterogeneity between samples but also from variable losses during the multiple steps of the extraction. Overall, after some practice, satisfactory yields can be consistently obtained from good quality tissue, particularly if the final washing steps are performed in small (2 ml) tubes. In the trials approximately 1 g of tissue (wet weight) was used with 5 ml of extraction buffer, but later 0.1 g of tissue was used on small scale extractions with 0.5 ml of buffer, with similar yields of 1-2 mg protein per g of tissue (data not shown). Extraction of large amounts of tissue (0.5-1g) requires larger tubes (50ml Teflon tubes), because of the volume required to precipitate proteins from the phenol phase(s). Small protein pellets spread over a large surface can suffer relatively greater losses during each supernatant removal. To minimize protein loss, washes were preferentially performed in 2 ml tubes. All experimental samples were successfully extracted using method A and produced well resolved spots in 2-DE.

Method B (ethanol/phenol extraction) initially produced somewhat lower yields than method A, but downscaling the extraction (500 mg to 100 mg of tissue) and using small (2 ml) tubes resulted in higher protein yields (Tab. 4.1). Higher yields may be due to the formation of thicker pellets in smaller tubes, reducing possible losses of protein pellet at each washing step, but may also result from additional practice. Method B also produced good resolution in both 1-D (Fig. 4.1) and 2-DE gels (data not shown), as expected for a method quite similar to method A. The band patterns obtained were also indistinguishable from those obtained with method A, with good representation of high MW proteins and well defined bands of all sizes, except for very low MW (under 15 kDa). It is likely that very small proteins (or very soluble ones) will be preferentially lost during the multiple washing steps required by both protocols.

Table 4.1 – Protein yields obtained with different extraction protocols from *Fucus* tissues. The extraction methods are represented by the letters A, B, C and D (see text) and 1 and 2 represent two trials (n=4). Differences between trials are summarized in the table.

method	A.1	A.2	B.1	B.2	C.1	C.2	D.1	D.2
species ^a	Fves	Fser	Fser + Fves	Fves	Fves	Fves	Fves	Fves
yield (mg/g) ^b	1.5 - 3	1 - 2	0.2 – 0.6	0.7 - 2	n.d. ^c (0.1)	n.d. ^c (0.1)	3 – 6 ^{cd} 6 – 8 ^{ce}	0.4– 3 ^{cd} 3 – 13 ^{ce}
tissue ^f	1g	1g	0.5g	0.1g	0.3g	0.3g	0.1g	0.1g
notes ^g				small tubes	+ SDS	no SDS		+ washes (+PVPP)

a) species extracted, Fves – *F. vesiculosus*, Fser – *F. serratus*; b) yield in mg of protein per gram of tissue (wet weight), range of four replicates; c) yield could not be accurately determined due to high viscosity of the extracts; d) hydrophilic fractions, in R#1; e) hydrophobic fractions, in R#4; f) initial amount of tissue (scale of the extraction); g) changes made to the protocol between trials: in trial B.2 the extraction was downscaled to use 2 ml tubes, in trial C.2 SDS was not added to the flow-through of the RNeasy column and in trial D.2 additional methanol and acetone washes were made and PVPP was added to two of the replicate samples during the initial grinding in liqN2 (see text for details).

Method C (extraction using RNeasy Plant kit) did not produce satisfactory results. After repeated homogenization in QIAshredder columns, the (green) flow-through seemed somewhat viscous when ethanol was added. After passage through the RNeasy column, that should retain RNA, polysaccharides and polyphenols (Parages *et al.* 2012), the solution turned extremely viscous upon addition of SDS (to 2%). Addition of five volumes of ice-cold 0.1 M ammonium acetate in methanol decreased viscosity, and the (yellowish) solution presented the characteristic “clouds” of protein precipitation. The final pellet was yellow and large, but dissolved in 300 µl of 2DE rehydration solution without great difficulty, producing a yellow viscous solution with some foaming, that did not always freeze at -20°C. Given the high viscosity observed, SDS addition was omitted in the second trial, but no differences were apparent in the samples. The resulting solution was too viscous to allow accurate pipetting and quantification, but concentrations obtained approached 0.3 mg/ml, which suggests a low yield of 0.1 mg per gram of tissue (Tab. 4.1). Samples run on SDS-PAGE presented a large blur near the wells, indicative of large aggregates, with few bands visible at low MW, albeit not well resolved (Fig. 4.1). Since the gel indicated that most proteins were trapped in high MW complexes no further improvements were attempted for this method.

Method D (using “Plant fractionated protein extraction kit”) was not effective with our brown algal tissue and after the acetone washes some of the pellets still presented a greenish colour. These precipitation steps did not seem very effective in removing the pigments. The initial trial (D.1) included three methanol and two acetone precipitations, and the resulting acetone pellets were yellowish or green (weighting 50-100 mg). Since the protocol recommends additional washes for tissues with high phenolics and tannin content, until the pellets became colourless, on the second trial (D.2) a total of four methanol and four acetone precipitations were made, but the final pellets were still green or yellow/green and more variable in size (30-160 mg). It is doubtful that additional washes would be beneficial because these seemed to have small effects on the colouration of the pellets.

The hydrophilic protein fraction (supernatant in R#1) was dark yellow and viscous, and the resulting pellet was hard to re-suspend during the washes in R#1. The hydrophobic protein fraction (supernatant in R#4) was also yellow and very viscous (some gel-like samples), despite additional amounts of R#4 used (300 - 500 μ l per sample) to improve solubilisation. Adding R#4 did not significantly decrease the sample viscosity, and accurate quantification was not possible. In the hydrophilic fractions (R#1) no protein bands were visible in the gel, only a smear at high MW. Some poorly defined bands were visible in the hydrophobic fractions (R#4) that seem to correspond to major and low MW bands seen with phenol-based methods (A and B), while most proteins were retained at or near the wells, as in the hydrophilic fractions (Fig. 4.1). As with method C, the resulting protein concentrations (not shown) and yields (Tab. 4.1) are only indicative, since sample viscosity and putative contaminants likely impacted the protein quantification results. An attempt was made to decrease viscosity by adding some PVPP (40 mg) to the frozen tissue (150 mg) during grinding, as PVPP would potentially remove some of the phenolic compounds (possibly phlorotannins) present and prevent them from precipitating the proteins, but no noteworthy differences were seen in viscosity, colour, yield or gel pattern (see Fig. 4.1-B. lanes 5 and 6).

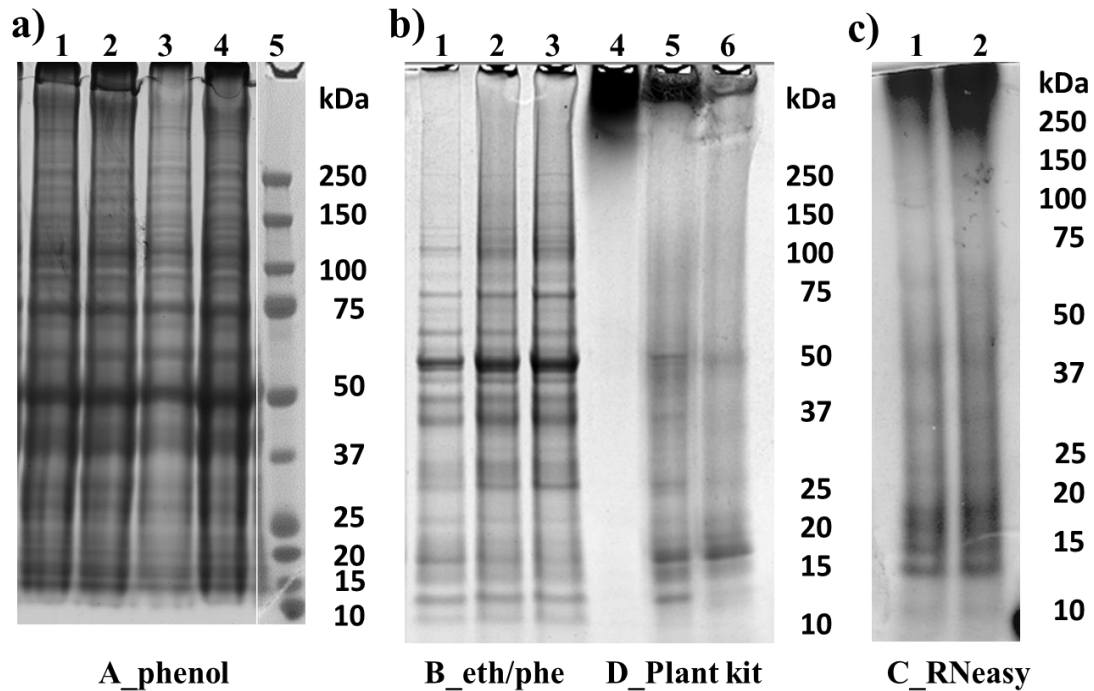


Figure 4.1 – SDS-PAGE profiles of *Fucus vesiculosus* extracted with the four protocols. a) Phenol extraction (Method A) of four different samples, of control (lane 1) and rehydration (lanes 2, 3 and 4) treatments; Molecular Weight Marker (lane 5). b) Ethanol/ phenol extraction (Method B) of one sample of the rehydration treatment (lanes 1, 2 and 3); Extraction with a Plant kit (Method D) that separates a hydrophilic fraction (lane 4) and a hydrophobic fraction (lane 5) of a control sample; hydrophobic fraction (lane 6) of the same control sample ground with PVPP. c) Extraction using RNeasy Plant kit (Method C) of a control sample, with (lane 1) or without (lane 2) addition of SDS to the flow-through of the RNeasy column.

TWC after field desiccation

Control apical tips, kept fully hydrated in a tide pool, were estimated to retain 95% TWC (range 85% - 107%), while those placed over a rock to desiccate averaged 1% TWC (-9% to 18%) at the end of the desiccation period (Tab. 4.2). These large intervals and the negative values may reflect weighing errors or water loss from some vials due to evaporation during sampling and transport. Controls were fully hydrated and submerged and desiccated samples were all below the threshold (30-40% TWC) where strong inhibitory effects are detected (e.g., Dring & Brown 1982; Pearson 2000; Pearson *et al.* 2009) and close to 5% TWC, a level corresponding to tissue that has completely lost unbound water from the cells.

Table 4.2 – Average Tissue Water Content (TWC) of the desiccated algae (n = 3 tips per plant). C – controls; R – recovery from desiccation; *n=2, one vial excluded.

frond	C1	C2	C3	R1	R2	R3
TWC	98%	95%	91%	-2%	7%	11%*

2-DE separation and image analysis

Bidimensional separation (of 200 µg protein) using 11 cm IPG strips produced reproducible patterns with well resolved spots, although somewhat clustered in the region around 50 kDa (Fig.4.2). Automatic alignment using the software Same Spots performed generally well, but adding some manual vectors in some areas of the gels improved alignment. On small gels, the use of MOPS buffer with 12% Bis-Tris gels improved the separation of mid-sized proteins (around 50 kDa), allowing the analysis of a large number of spots (1523, after automatically excluding small/ faint detections). At a $p < 0.05$ threshold, 59 spots differed between control and recovery samples, half of these (31 spots) changing over 1.5-fold, of which 19 were more expressed in control and 12 in recovery samples (Tab. 4.3). After correcting for multiple tests however, none were retained as differentially expressed (Benjamini-Hochberg correction at 0.05). The SameSpots FDR procedure also indicated a larger than 40% change of false discoveries ($q=0.4051$) and the power of the analysis was overall low (only 5 spots had power > 0.98).



Figure 4.2 – Representative Coomassie-stained small gel. *F. vesiculosus* sample C3 (no desiccation) separated in 11 cm, pH4-7 IPG strips and 12% Bis-Tris gels run in MOPS buffer.

To improve the ability to detect significant changes in protein expression between the treatments, 2-DE using larger gels and 24-cm IPG strips was performed. Larger gels can improve separation of proteins with similar pI and MW to allow improved alignment, spot detection and spot volume determination, thus increasing the ability to detect true biological differences.



Figure 4.3 – Representative Coomassie-stained large gel. *F. vesiculosus* sample C3 (no desiccation) separated in 24 cm, pH 3-7 IPG strips and 12% hand-cast gels run in TGS buffer.

Separation using 24 cm IPG strips on large gels also yielded reproducible, well resolved patterns, allowing good quality automatic alignment, improved with some manual vectors (Fig.4.3). SameSpots software detected 5320 spots, although many were artifactual. After excluding small/ faint spots and some problem areas, 2481 spots were analysed, of which 64 potentially changed between control and recovery treatments (ANOVA $p < 0.05$, but all $q > 0.29$), albeit with small differences (only 17 of these spots had over 1.5-fold difference between treatments), (Tab. 4.4). None was confirmed as a true discovery after Benjamini-Hochberg multiple testing correction (at 0.05) and only 19 of these spots had power > 0.98 .

Some gels showed dye particles or irregular destaining, or suffered breakage during manipulation (see Fig.4.3). All these issues affected gel images and probably impacted alignment quality, spot volume determination and analysis power.

Table 4.3 – Small gel protein spots potentially changing expression during recovery from natural desiccation. These 31 spots (from 11 cm gels) presented significant (ANOVA $p < 0.05$, fold change > 1.4) differences in mean between treatment groups (Control vs Recovery) following image analysis using the SameSpots software. FDR - Benjamini-Hochberg False Discovery Rate testing.

spot #	Anova (p)	Fold	q Value	Power	Highest Mean	FDR test
1169	0.0024056	1.8	0.4051	0.99819	Control	FALSE
368	0.0029169	1.8	0.4051	0.99636	Control	FALSE
447	0.0056006	1.5	0.4051	0.97614	Control	FALSE
333	0.0143153	1.9	0.4051	0.86624	Recovery	FALSE
574	0.0171257	1.6	0.4051	0.83106	Control	FALSE
569	0.0182068	1.7	0.4051	0.81806	Recovery	FALSE
2005	0.0208332	1.8	0.4051	0.78785	Control	FALSE
2008	0.0220247	2.4	0.4051	0.77478	Recovery	FALSE
1966	0.0231219	1.8	0.4051	0.76309	Control	FALSE
2228	0.0231607	1.9	0.4051	0.76268	Control	FALSE
363	0.0239242	1.5	0.4051	0.75475	Recovery	FALSE
2127	0.0257286	2.6	0.4051	0.73661	Control	FALSE
461	0.0262458	2.1	0.4051	0.73156	Control	FALSE
404	0.0278569	1.9	0.4051	0.71627	Recovery	FALSE
2479	0.0296387	2.1	0.4051	0.70008	Recovery	FALSE
2419	0.0304848	1.7	0.4051	0.69264	Control	FALSE
372	0.0315962	1.5	0.4051	0.68311	Control	FALSE
2231	0.0318588	2	0.4051	0.6809	Recovery	FALSE
730	0.0321063	1.7	0.4051	0.67883	Control	FALSE
2171	0.0331225	1.6	0.4051	0.67045	Recovery	FALSE
1163	0.0342116	1.9	0.4051	0.6617	Control	FALSE
205	0.0345738	2	0.4051	0.65884	Control	FALSE
1232	0.0362128	2.1	0.4051	0.64622	Control	FALSE
1917	0.039366	1.6	0.4051	0.62327	Recovery	FALSE
887	0.0396044	1.8	0.4051	0.62161	Control	FALSE
41	0.0403937	1.8	0.4051	0.61615	Recovery	FALSE
326	0.0430327	2	0.4051	0.59861	Control	FALSE
1066	0.0436981	2.6	0.4051	0.59435	Recovery	FALSE
1503	0.0454104	2.2	0.4051	0.58366	Recovery	FALSE
1444	0.0457342	1.6	0.4051	0.58168	Control	FALSE
1044	0.0462101	1.5	0.4051	0.5788	Control	FALSE

Table 4.4 – Large gel protein spots potentially changing expression during recovery from natural desiccation. These spots (from 24 cm gels) presented significant differences (ANOVA $p < 0.05$, fold change > 1.4) in mean between treatments groups (Control vs Recovery) following image analysis using the SameSpots software. FDR - Benjamini-Hochberg False Discovery Rate testing.

spot #	Anova (p)	Fold	q Value	Power	Highest Mean	FDR test
5101	0.000377	1.8	0.29061	1	Control	FALSE
3883	0.001694	2.1	0.38922	1	Recovery	FALSE
2357	0.004311	2.4	0.38922	1	Control	FALSE
1881	0.00696	1.6	0.38922	0.980958	Control	FALSE
2709	0.010696	1.8	0.38922	0.955244	Recovery	FALSE
416	0.010879	1.6	0.38922	0.95985	Recovery	FALSE
3567	0.019931	4	0.38922	0.729147	Control	FALSE
1040	0.029682	1.7	0.38922	0.646652	Control	FALSE
788	0.0299	1.5	0.38922	0.868266	Control	FALSE
1802	0.030444	2.1	0.38922	0.817501	Recovery	FALSE
1283	0.03106	1.8	0.38922	0.616146	Control	FALSE
717	0.034153	1.5	0.38922	0.998668	Recovery	FALSE
2364	0.035286	1.7	0.38922	1	Control	FALSE
1757	0.038801	1.6	0.38922	0.475018	Control	FALSE
5323	0.041633	1.8	0.38922	0.47123	Recovery	FALSE
3552	0.046028	1.7	0.38922	0.629803	Control	FALSE
667	0.04791	1.5	0.38922	0.512478	Recovery	FALSE

4.4 - Discussion

Protein extraction methods for *Fucus vesiculosus*

Brown macroalgae, and particularly intertidal Fucales, are known to contain high amounts of secondary metabolites that interfere with protein and nucleic acid extractions, requiring specially formulated protocols. To select an optimized protocol for examination of the frond proteome of *Fucus* species we browsed the literature for methods suitable for other brown algae, or plants with similar issues (high levels of polyphenolics and viscous polysaccharides). We tested two methods developed for other brown macroalgae, both including a phenol extraction and extensive washes and two simpler kit-based methods, one using homogenisation and separation columns from an RNA extraction kit to assist in the extraction of phosphoproteins from several macroalgal species and a protocol designed to extract two protein fractions of differing solubility from many plant species. Neither of the kit-based methods was effective with *Fucus* tissue, probably by failing to remove polysaccharides and phenolics, resulting in a viscous yellow solution where proteins were trapped in high MW complexes. The RNeasy columns and buffer used apparently failed to avoid protein complexation. Although SDS addition seemed to increase viscosity of the extracts, excluding SDS caused no detectable improvements. The plant extraction kit also failed to extract soluble proteins, particularly using the buffer intended to solubilise the “hydrophilic fraction”, but even the “hydrophobic” proteins were largely in large MW insoluble complexes. As *Fucus* tissues often have abundant phlorotannins, failure to remove these phenolic compounds in the initial steps may have allowed them form strong insoluble complexes with proteins and other macromolecules (Horvath 1981). PVPP (or soluble PVP) is often used to remove phenolics, but adding PVPP during the initial grinding of *Fucus* tissue did not improve results with the plant extraction kit. The original ethanol/ phenol method does not include PVPP or PVP (Nagai *et al.* 2008), so it is likely that the solvents used are effective in preventing tannin action until phenol extraction and selective precipitations separate the proteins, but that was not tested since we initially chose to add 2% PVP to the SDS buffer. Both phenol-based methods had comparable yields and produced similar protein profiles on SDS-PAGE. Yield improved after optimization of starting tissue amounts and using smaller tubes, which improved reproducibility, as thinner pellets were more likely to breakup and suffer losses during the multiple steps of supernatant removal.

Since method A avoided the initial ethanol and acetone washes and resulted in good quality extracts it was selected for further analysis of differential protein expression by 2-DE. Using the selected method we were able to produce reproducible 2-DE protein patterns with a large number of well resolved spots (ca. 1500 using 11 cm gels and ca. 2500 using 24 cm gels detected with SameSpots).

In conclusion, suitable methods for protein extraction from difficult tissues or species, for which no specific protocols are available, can be obtained by searching the literature for protocols used in related species and in tissues of similar composition, particularly concerning levels of compounds known to interfere with extraction methods. Several methods should be tested to identify the most effective in terms of protein yield and quality. Some optimization is likely to be required and can be guided by comparing alternative strategies from relevant methods. When available, direct communication with the researchers that produced the original protocols can provide valuable advice and greatly reduce the time and cost required to obtain high-quality protein extracts from tissues with high levels of interfering substances.

Protein separation, image analysis and detection of differentially expressed spots

Bidimensional separation of the proteome from apical vegetative tissue of intertidal *Fucus vesiculosus* produced complex and reproducible patterns with a large number of well-resolved spots. Comparing 2-DE profiles of samples taken after 1 hour of recovery from intense desiccation with hydrated controls should allow identification of protein spots that changed in expression during recovery. However few differences were detected between the treatments, with mean differences generally low and not statistically significant ($q > 0.05$).

Since initially many spots were clustered in a small gel area, despite the use of a 4-7 pH interval for IEF separation and MOPS buffer for SDS-PAGE, 24 cm strips were tested to physically improve separation between spots, hoping it would lead to better definition of spot borders, areas and volumes, resulting in higher power and detection of significant differences in protein expression. However, separation using larger gels also failed to detect significant changes in protein expression between the treatments and presented minor improvements in power. Despite high reproducibility, small differences between the three biological replicates used may prevent detection of significant treatment effects. Identification of all the proteins present on these candidate spots (with ANOVA $p > 0.05$) might reveal true desiccation-related

molecules, as some will likely represent true biological changes in expression undetected under more stringent multiple testing due to a low number of replicates and small detected changes in expression (in small gels, only 78 of 1523 spots presented mean changes over two-fold). Given the complex patterns obtained, the large number of spots and differences in protein profiles between small and large gels, it is not possible to currently ascertain (by image analysis) if some of these putative differentially expressed proteins were detected in both analysis (of the small and the large gels). Independent selection of the same protein on both screens might be a sign of a true discovery, not detected simply because of the low power of the analysis. At this stage it is advisable to improve the analysis by increasing the number of replicates (biological or technical), decreasing the technical variability and improving image quality. Two-dimensional difference in gel electrophoresis (2D-DIGE) allows the simultaneous separation of three different samples (two treatments and a common standard) in the same gel, by labelling the proteins with three fluorescent dyes having non-overlapping spectra. Using 2D-DIGE could improve the detection of expression changes, by increasing sensitivity of detection, allowing more replicate samples to be run simultaneously, improving alignment with the use of an internal standard common to all gels and improving image quality by using a fluorescence scanner and eliminating gel staining steps. Further studies should therefore include additional replicates, preferably biological replicates given the large biological variability expected in these species.

In conclusion, we selected and optimized a suitable method to extract proteins from vegetative tissues of intertidal macroalgae from the genus *Fucus*. This method prevents complexation of proteins by phlorotannins and other cellular compounds in insoluble high molecular weight aggregates. The resulting good-quality protein extracts contain a large number of proteins that can be separated by 2-DE, allowing determination of differentially expressed proteins by image analysis. However, identification of differentially expressed proteins between algae rehydrated for 1 hour after intense desiccation and non-desiccated controls was not possible with the current experimental setup. The potentially differentially expressed protein spots identified retained a high number of false positives (probabilities of being a false positive of ca. 40% according to SameSpots q-value, except one with 30%). The low power to detect significant differences is likely related to the large biological variation in protein expression levels and the small number of replicates. To improve the identification of differentially expressed proteins future studies should therefore include additional biological replicates and minimize technical problems that interfere with image analysis.

4.5 - References

- Barbosa, M., Valentão, P. & Andrade, P. B. (2014). Bioactive Compounds from Macroalgae in the New Millennium: Implications for Neurodegenerative Diseases. *Marine Drugs*, 12 (9), 4934–4972.
- Beer, S. & Kautsky, L. (1992). The recovery of net photosynthesis during rehydration of three *Fucus* species from the Swedish west coast following exposure to air. *Botanica Marina*, 35, 487-491.
- Benjamini, Y. & Hochberg, Y. (1995). “Controlling the False Discovery Rate: A Practical and Powerful Approach to Multiple Testing,” *Journal of the Royal Statistical Society, Series B (Methodological)*, 57 (1): 289-300.
- Contreras, L., Ritter, A., Dennett, G., Boehmwald, F., Guitton, N., Pineau, C., Moenne, A., Potin, P. & Correa, J.A. (2008). Two-Dimensional Gel Electrophoresis Analysis of Brown Algal Protein Extracts. *Journal of Phycology*, 44: 1315-1321
- Cock J.M., Sterck L., Rouzé P., Scornet D., Allen A.E., Amoutzias G., *et al.* (2010). The *Ectocarpus* genome and the independent evolution of multicellularity in brown algae. *Nature*, 465: 617-621.
- Davison, I.R. & Pearson, G.A. (1996). Stress tolerance in intertidal seaweeds. *Journal of Phycology*, 32, 197-211.
- Dittami, S.M., Gravot, A., Renault, D., Goulitquer, S., Eggert, A., *et al.* (2011). Integrative analysis of metabolite and transcript abundance during the short-term response to saline and oxidative stress in the brown alga *Ectocarpus siliculosus*. *Plant. Cell Environ.* 34, 629–642.
- Dittami, S. M., Scornet, D., Petit, J.-L., Ségurens, B., Da Silva, C., *et al.* (2009). Global expression analysis of the brown alga *Ectocarpus siliculosus* (Phaeophyceae) reveals large-scale reprogramming of the transcriptome in response to abiotic stress. *Genome Biology*, 10: R66 10.1186/gb-2009-10-6-r66
- Dring, M.J. & Brown, F.A. (1982). Photosynthesis of intertidal brown algae during and after periods of emersion: A renewed search for physiological causes of zonation. *Marine Ecology Progress Series*, 8, 301-308.
- Heinrich, S., Valentin, K., Frickenhaus, S. & Wiencke, C. (2015), Temperature and light interactively modulate gene expression in *Saccharina latissima* (Phaeophyceae). *Journal of Phycology*, 51: 93–108. doi:10.1111/jpy.12255
- Hoarau, G., Coyer, J. A., Stam, W. T., & Olsen, J. L. (2007). A fast and inexpensive DNA extraction/ purification protocol for brown macroalgae. *Molecular Ecology Notes*, 7(2), 191-193.
- Horvath, P. J. (1981). The nutritional and ecological significance of acer-tannins and related polyphenols. MSc thesis, Cornell University, Ithaca, New York, USA.
- Konotchick, T., Dupont, C. L., Valas, R. E., Badger, J. H., & Allen, A. E. (2013). Transcriptomic analysis of metabolic function in the giant kelp, *Macrocystis pyrifera*, across depth and season. *The New Phytologist*, 198 (2), 398–407.
- Lago-Leston, A., Mota, C., Kautsky, L., & Pearson, G. A. (2010). Functional divergence in heat shock response following rapid speciation of *Fucus* spp. in the Baltic Sea. *Marine Biology*, 157, 683–688.

- Li, B., Lu, F., Wei, X. & Zhao, R. (2008). Fucoidan: Structure and Bioactivity. *Molecules* 13, 1671-1695.
- Li Y., Wijesekara, I., Li, Y., & Kim S. (2011). Phlorotannins as bioactive agents from brown algae. *Process Biochemistry*, 46 (12), 2219-2224.
- Masters, A. K., Shirras, A. D., & Hetherington, A. M. (1992). Maternal mRNA and early development in *Fucus serratus*. *The Plant Journal*, 2(4), 619-622.
- Nagai, K., Yotsukura, N., Ikegami, H., Kimura, H. & Morimoto, K. (2008). Protein extraction for 2-DE from the lamina of *Ecklonia kurome* (laminariales): Recalcitrant tissue containing high levels of viscous polysaccharides. *Electrophoresis* 29: 672-681
- Parages, M.L., Capasso, J.M., Meco, V. & Jimenez, C. (2012). A novel method for phosphoprotein extraction from macroalgae. *Botanica Marina* 55: 261-267.
- Pavia, H. & Toth, G. B. (2000). Inducible chemical resistance to herbivory in the brown seaweed *ascophyllum nodosum*. *Ecology*, 81: 3212–3225.
- Pearson, G.A. & Davison, I.R. (1993). Freezing rate and duration determine the physiological response of intertidal fucoids to freezing. *Marine Biology*, 115, 353-362
- Pearson, G., Kautsky, L., and Serrão, E. A. (2000). Recent evolution in Baltic *Fucus vesiculosus*: reduced tolerance to emersion stresses compared to intertidal (North Sea) populations. *Marine Ecology Progress Series*, 202, 67–79.
- Pearson, G., Lago-Leston, A., Valente, M., & Serrão, E. (2006). Simple and rapid RNA extraction from freeze-dried tissue of brown algae and seagrasses. *European Journal of Phycology*, 41(1), 97-104.
- Pearson, G. A., Lago-Leston, A., & Mota, C. (2009). Frayed at the edges: selective pressure and adaptive response to abiotic stressors are mismatched in low diversity edge populations. *Journal of Ecology*, 97, 450–462.
- Phillips, N., Smith, C. M., & Morden, C. W. (2001). An effective DNA extraction protocol for brown algae. *Phycological research*, 49 (2), 97-102.
- Schoenwaelder, M. E., & Clayton, M. N. (1998). Secretion of phenolic substances into the zygote wall and cell plate in embryos of *Hormosira* and *Acrocarpia* (Fucales, Phaeophyceae). *Journal of Phycology*, 34(6), 969-980.
- Schoenwaelder M.E.A., Wiencke C., Clayton M.N. and Glombitza K.W. 2003. The effect of elevated UV radiation on *Fucus* spp. (Fucales, Phaeophyceae) zygote and embryo development. *Plant Biology* 5: 366-377
- Schonbeck, M.W. & Norton, T.A. (1978). Factors controlling the upper limits of fucoid algae on the shore. *Journal of Experimental Marine Biology and Ecology*, 31, 303-313.
- Varela-Álvarez, E., Andreakis, N., Lago-Lestón, A., Pearson, G.A., Serrao, E.A.,... & Marba, N. (2006). Genomic DNA isolation from green and brown algae (Caulerpales and Fucales) for microsatellite library construction. *Journal of Phycology* 42:741–745.
- Venkatesan, J., Bhatnagar, I. & Kim, S. (2014). Chitosan-Alginate Biocomposite Containing Fucoidan for Bone Tissue Engineering, *Marine Drugs*, 12 (1), 300-316.
- Wahl, M., Jormalainen, V., Eriksson, B.K., Coyer, J.A., Molis, M., ... & Olsen, J.L. (2011). Stress Ecology in *Fucus*: Abiotic, Biotic and Genetic Interactions. *Advances in Marine Biology*, Vol 59, 59, 37-105.

Ye N., Zhang X., Miao M., Fan X., Zheng Y., Xu D., *et al.* (2015). *Saccharina* genomes provide novel insight into kelp biology. *Nature Commun* 6: 6986.

4.6 – Acknowledgements

I would like to thank the help of Sofia Cavaco, and all the Functional Biochemistry and Proteomics group at CCMAR, particularly Dr. Dina Simes, for assistance and use of their equipment for all the 2-DE small gels and one dimensional SDS-PAGE.

I would also like to thank the help of Denise Schrama and Dr. Pedro Rodrigues from Aquagroup at CCMAR, for assistance and use of their equipment for all the 2-DE large gels.

This study was supported by FCT - Portuguese Science Foundation (project UID/Multi/04326/2013 and PhD fellowship SFRH/BD/74436/2010).

Supporting information

Supporting information to this chapter can be found on the Appendix (digital version)

Table S4.1 – Protein changes between desiccated and non-desiccated tissues (recovery from shore desiccation). Same Spots output for pairwise design (n=3) analysis of small Coomassie-stained gels and result of False Discovery testing at 0.05 confidence level.

Table S4.2 - Protein changes between desiccated and non-desiccated tissues (recovery from shore desiccation). Same Spots output for pairwise design (n=3) analysis of large Coomassie-stained gels and result of False Discovery testing at 0.05 confidence level.

Chapter 5

Desiccation *in situ*: the importance of seaweed canopies in modulating temperature and desiccation stress

Chapter 5 – Desiccation *in situ*: the importance of seaweed canopies in modulating temperature and desiccation stress

5.1 – Introduction

Desiccation is a major stressor for intertidal algae and a number of studies have highlighted differences in desiccation-tolerance among intertidal species and their relation to species zonation, showing that more desiccation-tolerant species are found at higher shore levels, where they face longer emersion times and a greater risk of desiccation (e.g. Zaneveld 1937; Schonbeck & Norton 1978; Dring & Brown 1982; Brawley & Johnson 1991; Davison & Pearson 1996; Hunt & Denny 2008).

In nature, many factors (e.g. temperature and high-light stress) often co-occur with intertidal desiccation and genetic variation within individuals can also lead to different individual responses to the same stress. Moreover, intertidal macroalgae have elaborate 3D structures (shapes) that modulate the stress intensity over different portions of the fronds causing heterogeneous levels of desiccation. Submerged *Fucus vesiculosus* fronds can float near the water surface thanks to air filled bladders, increasing light exposure of longer fronds. However, the fronds (lacking the support systems of land plants) are laid down as the tide recedes, forming extense emersed canopies where there is a dense algal cover (see cover photo of intertidal *Fucus* canopies in front of the SBR, Roscoff, France). In these canopies the algal branches cross and overlap abundantly and branches from the same individual can be fully shaded under many moist fronds while others experience full sunlight and wind exposure at the top of the canopy. While the ability to control confounding factors favours the use of laboratory experiments in controlled-culture conditions, translating those results into the understanding of ecological processes requires simultaneous research of the ecological environment *in situ*. This issue can arise in the determination of thermal limits in laboratory experiments, when the aim is to predict the suitable thermal habitat of that species. A good example is shown in Mota et al. 2014, where the molecular response to heat stress was

examined under controlled laboratory conditions and *in situ*, to determine thermal limits for the brown intertidal macroalga *Fucus vesiculosus*. It was apparent that tissue temperatures of isolated apical tips in laboratory experiments were not representative those experienced in natural conditions, under the same ambient temperatures. In the intertidal zone the structure of the emersed algal canopies constructs distinct microhabitats, where tissues of *F. vesiculosus* presented microhabitat-specific thermal and desiccation profiles that correlated with the molecular heat stress responses examined (Mota *et al.* 2014, chapter 3). A most interesting effect interacting with intertidal thermal stress is that of desiccation; no molecular response was detected in severely desiccated tissue despite exposure to high temperatures, due to metabolic arrest induced by fast desiccation (Mota *et al.* 2014, chapter 3). This fast desiccation can have a protecting effect, avoiding the high energy costs of a heat-shock response and raising the thermal lethal limits (Hunt & Denny 2008; Mota *et al.* 2014).

In order to obtain ecologically relevant results, we must therefore characterize the conditions effectively experienced *in situ* by the organisms, which in the case of intertidal algae that typically grow clustered forming dense canopies means the need to examine the microhabitats present. A first approach towards this goal is to characterize natural desiccation conditions for *Fucus* species that may indicate the realistic suitable conditions to understand physiological stress in such habitats. Given the large natural variability in the intensity of stress exposure in intertidal settings and the complex structure of macroalgal canopies, a large number of parameters and micro sites could potentially be examined, undoubtedly revealing a large microhabitat heterogeneity. The most contrasting microhabitats that can easily be defined for patchy intertidal seaweeds are the Top and the Bottom of the canopy. The same individual algal genotype is present in tissue from a microhabitat that promotes fast and intense desiccation (Top) and other parts of the tissue experience a slow rate of water loss (Bottom), often keeping the tissue hydrated throughout the low tide emersion period. The frequency of the exposure to emersion stress is a poorly understood factor that is likely to have major consequences for organismal survival in the intertidal zone. A key process determining resilience of intertidal organisms to emersion stress is their capacity to recover from stress, more important than resisting the stress (e.g. Pearson *et al.* 2009; Jueterbock *et al.* 2014; Jueterbock *et al.* 2016; chapter 2). Maximal desiccation stress is expected to occur during midday low tides that do not occur in isolation but tend to last for many consecutive days, exposing intertidal organisms to maximum solar intensity and often the highest temperatures. Therefore, sequential days of exposure to conditions favoring intense emersion

stress (low tides occurring during the middle of the day) may not allow sufficient recovery thereby aggravating potential detrimental effects of single exposures (Davison & Pearson 1996; Jones *et al.* 2009).

We aimed to determine if sequential emersion exposures produced a cumulative impact in intertidal *F. serratus* and *F. vesiculosus*, if that impact could be related to the desiccation levels experienced and how canopy microhabitats influenced the impact of ambient environmental conditions. We related tissue temperatures and desiccation across two contrasting canopy microhabitats (Top and Bottom) to the maximum quantum yield of PSII photochemistry (F_v/F_m) after recovery, to determine how canopy microhabitats modulate emersion stress. We measured the same tissues during consecutive days of midday low tides to assess cumulative impacts of the stress exposures during periods of potentially higher emersion stress. We also compared the responses of two species, *F. serratus* and *F. vesiculosus*, from the same shore heights to determine possible species differences.

Another aim of this study was to understand the temporal variability in physiological stress conditions experienced by intertidal seaweeds at microhabitat scales during sequential periods of emersion exposure. We repeatedly examined the microhabitat location of tagged apical tips during an extended period of multiple emersions, to determine whether most tips inhabited a temporally stable environment (favoring the same microhabitat across several weeks). We also asked whether species differences between *F. serratus* and *F. vesiculosus* could be detected in microhabitat preference and stability, likely related to their distinct branch morphologies. The results revealed that although the pattern of microhabitat location during emersion was unpredictable for many branch tips, others were preferentially located in a given microhabitat (canopy top) over the long-term.

5.2 – Material and methods

Study site and microhabitat selection

Field studies were conducted on the low-slope intertidal in front of the Roscoff Marine Station (Station Biologique de Roscoff), in Brittany, France, where several furoid species are abundant. Here, *F. vesiculosus* and *F. serratus* can form dense canopies, often growing on mixed stands with other furoids, where they find suitable hard substrate (large rocks, debris or constructions). Individuals can also be found attached to small rocks or pebbles, transported along the shore by wave action. The study sites were selected in the mid-high intertidal, with mixed furoid canopies attached to areas of hard substrate (old pipeline walls), where fronds were emersed for approximately 6 hours during the sampling periods. The canopy microhabitats examined here are not permanent, they are formed when the fronds are laid down at each receding tide and during emersion the status of fronds can occasionally be changed by wind bursts or other physical disturbances. It is worth noting that most large individuals have (at any given moment) both Top and Bottom apical tips, while smaller, young algae (juveniles) are often sheltered under the adult canopy (Brawley & Johnson 1991; Lamote *et al* 2007; Lamote & Johnson 2008).

Since our chosen proteomic approach cannot handle a large number of samples, an attempt was made to select two representative conditions exposed to contrasting desiccation intensity. We focused on comparing two microhabitats within individual *Fucus* fronds: the Top and the Bottom of the canopy. This design allows comparing samples with the same genomic background (from the same individual), in contrasting microhabitats. Two microhabitats were defined within the emersed algal canopies at low tide, Top and Bottom, encompassing those frond portions laying at the top of the canopy, fully exposed to direct sunlight and wind, and those found at the bottom of the canopy, sheltered by the overlaying tissues.

Temporal stability of the Top microhabitat

From both *F. vesiculosus* and *F. serratus*, ten large individuals per species were haphazardly selected from mid-high shore mixed stands. In each individual, six apical tips were selected across the frond and tagged with light plastic ribbon about 4 cm from the apex. Between April and June, usually daily, these individuals were examined during daytime low tide emersion to determine the position of the preselected tips. The position of each tagged apical

tip was recorded as “Top” whenever it was found exposed at the top of the canopy. In early May one lost individual was replaced, and data from the lost individual was discarded. In June most of the tags were repositioned about 4 cm from the apex and where growing tips had branched one of the tips was randomly selected and tagged. A few tags (ten) were lost and replaced at some stage in the experiment, and since only the exposed (Top) tips were examined daily this might underestimate the frequency of residence in the Top microhabitat. To prevent this, data for such lost tip was discarded since its last recorded observation in any microhabitat (previous days were recorded as missing data). Only five of the total 120 tips could have been lost over five days before being replaced, and none over 10 days.

Emersion stress in Top and Bottom microhabitats

To examine the effect of microhabitats on desiccation, temperature and physiological stress and the effect of cumulative exposure to desiccation, we selected peak stress periods, when algae were emersed for several sequential days during the warmest part of the day (midday low tides). Large individuals from *F. vesiculosus* and *F. serratus* were selected from mid-high shore mixed stands and two apical tips were placed either in Top or in Bottom microhabitat for 5-7 subsequent midday low tides (approximately six hours of emersion starting between 9.00-14.00h). Top and Bottom measurements were conducted over three separate sampling periods, on the same area. During the first sampling period (10-16 May) only *F. vesiculosus* was examined and only four tips per microhabitat were sampled for TWC and tissue temperatures. Also some (T3, B3, T2, B2, B3') of the tagged tips were lost and had to be replaced throughout the sampling period. On the second sampling (24-31 May) only *F. serratus* was examined (n=6) but TWC and tissue temperatures were also determined for *F. vesiculosus* microhabitats from 26 to 31 of May. On the last period (23-28 June) both species were sampled (n=6, per species and microhabitat, except n=5 for *F. serratus* on 23rd June).

TWC, temperature and *Fv/Fm* determinations

Each sampling period, two large apical tips from each individual from *F. serratus* or *F. vesiculosus* were selected in mixed fucoid beds. These algae tips were tagged as either “Top” or “Bottom” and manually placed in these microhabitats, for the duration of midday low tide emersion, during sequential days (see Fig. 5.1).

Daily, immediately upon emersion at low tide, the tagged tips were placed in the selected microhabitat (Top or Bottom of the *Fucus* canopy) and chlorophyll fluorescence (*Fv/Fm*) was

measured to determine physiological stress from previous exposures. Physiological resilience was assayed in tissues dark-adapted for 5-15 minutes using chlorophyll fluorescence (Diving-PAM, Walz), measuring the maximum quantum yield of PSII (F_v/F_m) with a saturation pulse to evaluate long-term damage to PSII reaction centers (Maxwell & Johnson 2000). It is assumed that during these sampling periods the nocturnal low tide emersion will not cause significant stress to these algae.

May 9, 9.23h – hydrated tissues

May 9, 12.50h – desiccated



Figure 5.1 – Experimental setup for microhabitat characterization. The large plastic clip tags the tip used for daily F_v/F_m determination and a nearby tip, selected as a “proxy” for tissue temperature and water content measurements, shows a red wire clip used to attach the temperature datalogger (“Top” arrows). The corresponding tips in the Bottom habitat are not visible at the start of the measurements, since they are under the remaining canopy, but after some time the exposed (Top) tips desiccated and shrunk, partially exposing some of the Bottom tissues (“Bottom” arrow pointing to a green clip on the Bottom “proxy” tip).

For tissue water content (TWC) estimation, that requires destructive sampling, each day a set of “proxy” apical tips from the same fronds, adjacent and similar to the tagged tips (used during sequential days for F_v/F_m measurements). These “proxy” tips were placed in the corresponding microhabitats at the beginning of the low tide, collected and placed into a pre-weighed vial with seawater at the end of low tide to determine the level of desiccation stress. The vials were closed, transported back to the laboratory and weighted to obtain the weight of the tissue at the time of collection (cW). After 1-2 days the fully rehydrated tips were blotted to remove surface water and weighted to determine the hydrated weight (hW), placed to dry

at 60°C and re-weighted after 1 and 2 days to determine the dry weight (DW). TWC was calculated using the formula: $TWC (\%) = (cW - DW) / (hW - DW) \times 100$.

Thermal characterization of the microhabitats was made using temperature dataloggers (Thermochron iButton DS1922L-F5) and tissue temperatures were recorded every five minutes during low tide exposures. The dataloggers were lightly sealed with silicon grease, wrapped in parafilm, and attached with wire clips to the underside of the “proxy” apical tips used for TWC estimation, shortly after low tide emersion, where they remained until tip collection. It was decided to measure tissue temperatures on the “proxy” tips because the loggers interfere with placing of the clips for the PAM measurements and repetitive placing of the dataloggers could damage the tips and influence physiological measurements. Additional temperature dataloggers (8) were attached to the rocky substrate to measure site temperature every 30 minutes, inside protective brass casing or silicone-filled shells.

Proteomic analysis

Samples for proteomic analysis were collected after each sampling period (5-7 days), on May 31 and June 28. The tagged tips (Top and Bottom) were collected, briefly rinsed twice with ddH₂O and twice with 50 mM Tris-HCl, pH8, blotted dry and flash-frozen in liquid nitrogen in the field. Protein extraction and DIGE were performed as described in Chapter 6, to identify proteins differentially expressed across the two contrasting microhabitats (Top x Bottom) in *F. serratus* (n = 5) and in *F. vesiculosus* (n = 6), after cumulative emersion stress exposure.

5.3 - Results

Temporal stability of the Top microhabitat

Usually the position of the fronds resulted from the receding water movement at low tide and remained stable until reimmersion, but wind and trampling occasionally moved some fronds. Also on some days the resident fronds were covered by a large amount of drift algae fragments, resulting in fewer exposed (Top) resident tips. The microhabitat was assessed once each emersion period. The resulting data produced between 282-360 observations per individual frond (6 independent tips, 40-60 observations per tip, except one with just 22).

For *F. vesiculosus*, the total number of “Top” observations (1670) was half the total possible observations and varied between 39% and 71% across individuals but for each tip the proportion of the time at the Top microhabitat varied as much as 2% to 91% (Tab. 5.1). Thus, although the average might indicate a 50% chance for a particular tip to be found in the Top of the canopy at any given time, values for independent tips illustrate the wide variation expected given the complex structure of the algal fronds and canopies. Most apical tips (52 out of 60 tips, 50 after FDR correction) presented microhabitat preferences not consistent with a random distribution (binomial $p < 0.05$, see appendix).

Table 5.1 – Percentage of observations on the Top microhabitat per tip and per individual of *Fucus vesiculosus*. Top % = recorded “Top” observations / total observations.

Top %	Tip1	Tip2	Tip3	Tip4	Tip5	Tip6	indiv.
ves I.2	35%	82%	32%	75%	33%	48%	51%
ves I.3	32%	12%	13%	63%	55%	57%	39%
ves I.4	37%	27%	20%	53%	78%	67%	47%
ves I.5	43%	64%	63%	53%	82%	82%	66%
ves I.6	55%	40%	60%	91%	89%	87%	71%
ves II.1	63%	32%	5%	76%	20%	83%	47%
ves II.2	34%	73%	39%	36%	80%	64%	54%
ves II.3	2%	68%	39%	12%	90%	64%	46%
ves II.4	71%	10%	41%	49%	39%	14%	39%
ves II.5	66%	28%	28%	38%	31%	79%	45%

F. serratus tips were found less frequently in the “Top” microhabitat (under 32% of the total 3149 observations), only between 13% and 47% across individuals (Tab. 5.2). Assuming a mean presence on the Top microhabitat of 31.5%, 41 (40 after FDR correction) out of the 60 tips deviated significantly from this frequency (binomial, $p < 0.05$, see appendix). Histograms of “Top” frequencies also seem to suggest heterogeneity between sites and individuals,

showing an apparent skewed or bimodal distribution (Fig. 5.2), but the number of tips sampled is too low to draw any conclusion.

The *F. serratus* fronds examined were thicker and more densely branched than the *F. vesiculosus* fronds (Tab. 5.3). The lower number of “Top” observations for *F. serratus*, (31% versus 50%) may be related to algae localisation in the canopy and to the shape of its fronds, usually flatter, more branched and compact, where tips tended not to outgrow their neighbours or spread out at the edge of the canopy, while *F. vesiculosus* tips were sometimes seen more exposed, with longer and thinner fronds spreading outside the algal canopy.

Table 5.2 – Percentage of observations on the Top microhabitat per tip and per individual of *Fucus serratus*. Top % = recorded “Top” observations / total observations.

Top %	Tip1	Tip2	Tip3	Tip4	Tip5	Tip6	indiv.
ser I.1	45%	11%	2%	6%	13%	2%	13%
ser I.2	49%	17%	13%	9%	26%	36%	25%
ser I.3	13%	26%	53%	38%	28%	36%	32%
ser I.4	72%	43%	2%	38%	11%	11%	29%
ser I.5	66%	17%	38%	40%	51%	45%	43%
ser II.1	33%	13%	31%	20%	61%	59%	36%
ser II.2	11%	36%	38%	27%	26%	69%	35%
ser II.3	15%	2%	12%	30%	37%	27%	21%
ser II.4	20%	28%	18%	23%	58%	57%	34%
ser II.5	15%	54%	15%	46%	90%	61%	47%

Table 5.3 – Size and branching of the *Fucus serratus* and *F.vesiculosus* individuals. Length is from holdfast to longest tip, perimeter measured at the widest point and number of branching points counted.

(June)	<i>F.serratus</i> length	<i>F.serratus</i> perimeter	<i>F.serratus</i> branching	<i>F.vesiculosus</i> length	<i>F.vesiculosus</i> perimeter	<i>F.vesiculosus</i> branching
Average	45 cm	23 cm	90	47 cm	21 cm	54
Range	36 - 63	16 - 36	28 - 335	34 - 60	16 - 25	27 - 133

Despite the temporal variability globally observed in canopy microhabitats, some tips experienced a fairly stable environment. Six of the *F. serratus* tips were almost never exposed (<10% days in the Top) while one was almost never sheltered (90% of the observed period in the Top microhabitat). In *F.vesiculosus* results were more balanced: three tips mostly sheltered (<10% Top) and three usually exposed (ca. 90% Top). It is likely that some growing apical tips do preferentially locate in a specific microhabitat for prolonged periods. Such preferences, dependent on canopy and frond structure, might play an ecological role by

shielding a portion of the algae during heat waves, thus avoiding lethal damage of the whole organism during major stress periods (Hunt et al, 2008) that can last several days.

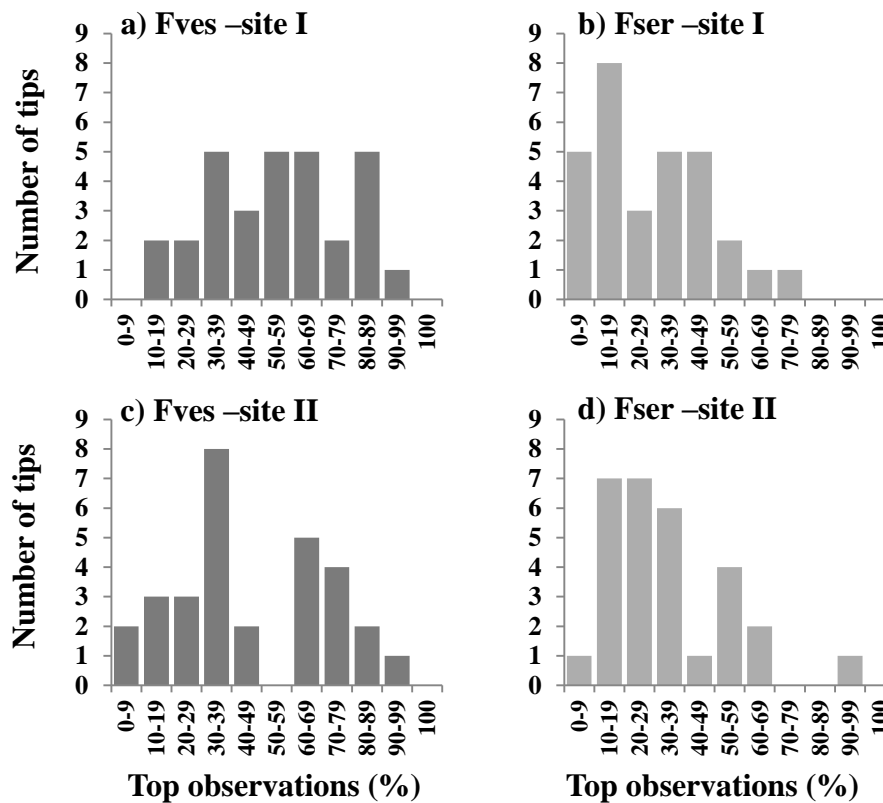


Figure 5.2 – Frequency at the Top microhabitat for *Fucus serratus* and *F. vesiculosus*. Histograms representing the number of tips (Y-axis) in each frequency class (X-axis, percentage of observations on the Top microhabitat), (n=60 tips).

Differences between Top x Bottom canopy microhabitats: TWC (desiccation)

Despite our attempts to control microhabitat position, unavoidable changes were occasionally observed in experimental tips. Although this was minimized on the experimental tips by the large plastic clips or the temperature dataloggers, wind bursts would sometimes move tips, occasionally exposing experimental tips that had been placed in a sheltered microhabitat (Bottom). This effect is reflected in the large variation of TWC of Bottom tips, since the loss of canopy cover over some tips leads to much higher desiccation (low TWC, see Fig. 5.3). These tips were placed in the Bottom of the canopy soon after emersion, but movement (and desiccation-induced shrinkage) of overlaying branches left them exposed to a distinct microenvironment. The Top microhabitat usually experienced intense desiccation under all weather conditions present (cloudy or sunny, diverse temperatures and wind intensities), except during the 14th and 16th May, when it rained throughout emersion (data not shown).

Because we used “proxies” to measure TWC, it’s important to notice that physiological measurements (recovery F_v/F_m) don’t necessarily match individual TWCs, but represent the same (general) microenvironment. As can be seen in Figs 5.3, 5.8 and 5.9, the desiccation experienced in the exposed canopy (Top) by the end of the low tide was always intense however in the sheltered Bottom microhabitat most tips remained hydrated after several hours of emersion. Desiccation levels were very similar in both species (*Fucus serratus* and *F. vesiculosus*). Contrary to Top tissues, Bottom tips experienced larger variation in TWC, both among days and among replicates (Figs 5.3, 5.8 and 5.9). This may partly relate to sporadic wind disturbance of the Bottom microhabitat, but also reflects the end-point nature of TWC measurement. Top tissues probably lost virtually all its “free” water much earlier, attaining a stable state with similar water contents. Weather conditions (like wind and temperature) impact the rate of desiccation on both microhabitats, but after over six hours all the exposed (Top) tips are very dry while large TWC differences remain in sheltered (Bottom) tissues.

Differences between Top and Bottom canopy microhabitats: tissue temperature

Tissue temperatures also differed between Top and Bottom microhabitats, particularly in sunny days, as can be seen on data from the 26th of May (see Fig 5.4). In this moderately warm day (dataloggers measured T_{air} 18-22°C, T_{rock} 10-20°C), large temperature differences were recorded between Top and Bottom microhabitats (over 10°C over a few centimetres in some individuals), despite local heterogeneity. These microhabitat differences were not exclusive of a few sunny days, albeit more pronounced under warm conditions. Figure 5.5 represents all recorded tissue temperatures, for individual tips over the successive low tide exposures, showing that the Top is consistently the warmest microhabitat, presenting the highest values and overall higher temperatures. This figure also illustrates the similarity between sampled tissues of both species, since within each microhabitat (Top or Bottom) variation on thermal properties of the canopy is similar within and between species. This temperature data reflects the situation during the studied period (May and June), where despite variable weather conditions and local heterogeneity consistent tissue temperature differences can be detected between both microhabitats ($p=0.0001$), but not between species ($p=0.7615$, see Fig. 5.6 and table S5.1).

Differences between Top and Bottom canopy microhabitats: F_v/F_m (recovery)

To evaluate long-term photodamage to PSII resulting from cumulative stress exposure over the previous days, F_v/F_m measurements were made as soon as possible after emersion intercalating both microhabitats (T1, then B1, T2; B2...) to minimize any effect of on-going desiccation. As we do not have direct measures of the temperature and desiccation state of the tips used to evaluate photodamage and despite our best efforts the “proxies” sometimes presented noticeable differences in desiccation status (personal observation), data cannot be compared for each individual. Data pooled across all six sites from each microhabitat is less sensitive to individual disturbances and can be contrasted to thermal and desiccation status from the (destructively sampled) “proxy” tips.

In general, the most stressful microhabitat (Top of the canopy) presents lower F_v/F_m values than Bottom tissues, indicative of greater PSII damage from previous day(s) exposure, but there is considerable variability between individual tips in both microhabitats (Fig.s 5.7, 5.8 and 5.9). Some tips in the Bottom microhabitat were also exposed to stressful conditions and present signs of photodamage ($F_v/F_m < 0.7$). Unlike TWC, recovery F_v/F_m values are not so divergent between microhabitats, which is not surprising as most tips are expected to recover from natural desiccation under the observed mild weather conditions.

Across the three sampling periods (Fig.s 5.7, 5.8 and 5.9), F_v/F_m on the first day (before microhabitat manipulation) was always above 0.7 (except for three tips in May) and similar in both microhabitats (larger difference in medians in May, $p < 0.040$), indicating no relevant previous photodamage. On subsequent days F_v/F_m values generally decreased and variability within days increased, particularly on Top sites, but with large daily changes and no clear decreasing trend could be detected due to cumulative effects of sequential stress exposures (except maybe in the end of May in the Top microhabitat).

Correlations between temperature, desiccation and recovery F_v/F_m

Overall, across months and in both species, clear differences can be seen between Top and Bottom microhabitats (see Fig. 5.10 for June data), but not between species. Bottom tips were generally protected from intense desiccation (TWC < 60%), photodamage ($F_v/F_m > 0.7$) and high temperatures (tissue > 24°C). Despite the intense desiccation and higher temperatures experienced in the Top microhabitat, where tissues present more photodamage, it is difficult to relate particular stress conditions to decreases in F_v/F_m . For example, on May, 14th rain

prevented desiccation and tissue temperatures were low (median 13°C, range 9-16.5°C on Top, median 12°C, range 9-14°C on Bottom), but the next day F_v/F_m decreased, for the lowest values that week (median 0.744, range 0.465-0.735). A decrease in F_v/F_m in result of simulated rainfall during emersion has been previously described in *F. spiralis*, probably related to the detrimental effect of osmotic shock (Schagerl & Möstl 2011). On the Bottom microhabitat, from 24 to 31 May, desiccation dropped below 50% TWC only the 27th, May, but F_v/F_m was not noticeably impacted (median 0.739; range 0.576-0.807, lowest median 0.726 on the 29th), (Figures 5.7 and 5.3).

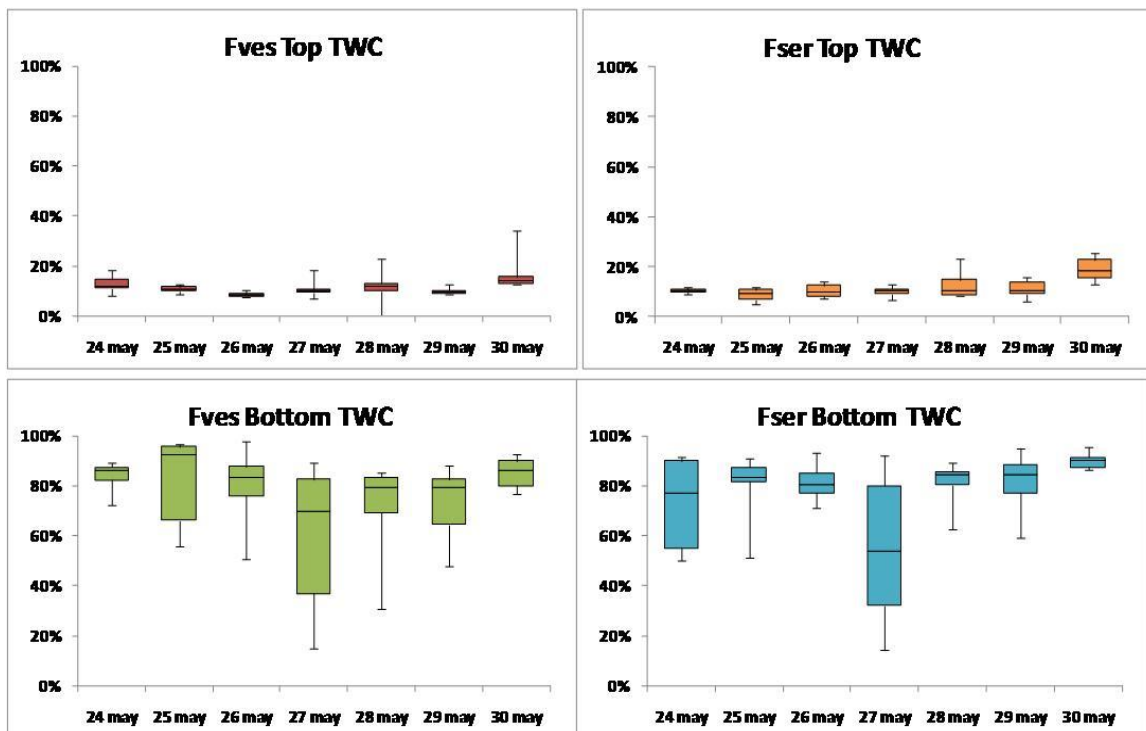


Figure 5.3 – Tissue Water Content of the *Fucus serratus* and *F.vesiculosus* tips (n = 6) at the end of the low tide emersion between 24 and 30 May, 2013. Note the large variation of TWC occasionally seen on the Bottom microhabitat. See Materials and methods for details. Boxplots show Maximum - 3rd quartile – median - 1st quartile - minimum values.

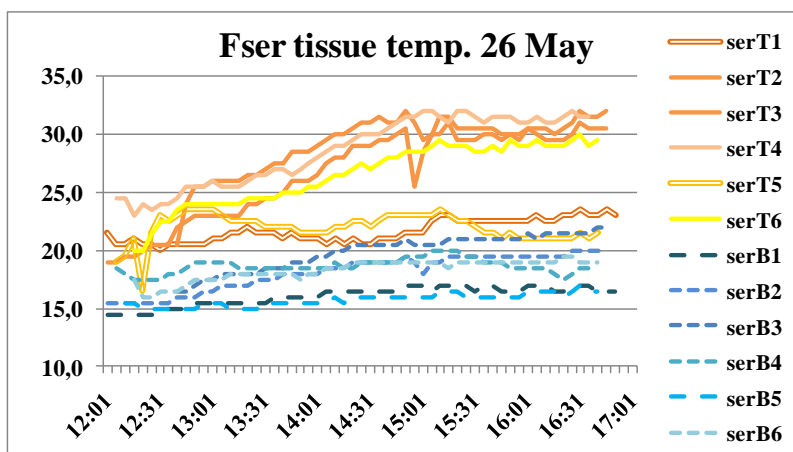


Figure 5.4 – Recorded tissue temperatures on six Top (solid yellow/orange lines) and six Bottom (dashed blue lines) *Fucus serratus* apical tips recorded during daytime low tide emersion (12:00 – 17:00h data) on May 26th, 2013. Note the lower temperatures on sites 1 and 5, but always a cooler Bottom microhabitat. See Materials and methods for details.

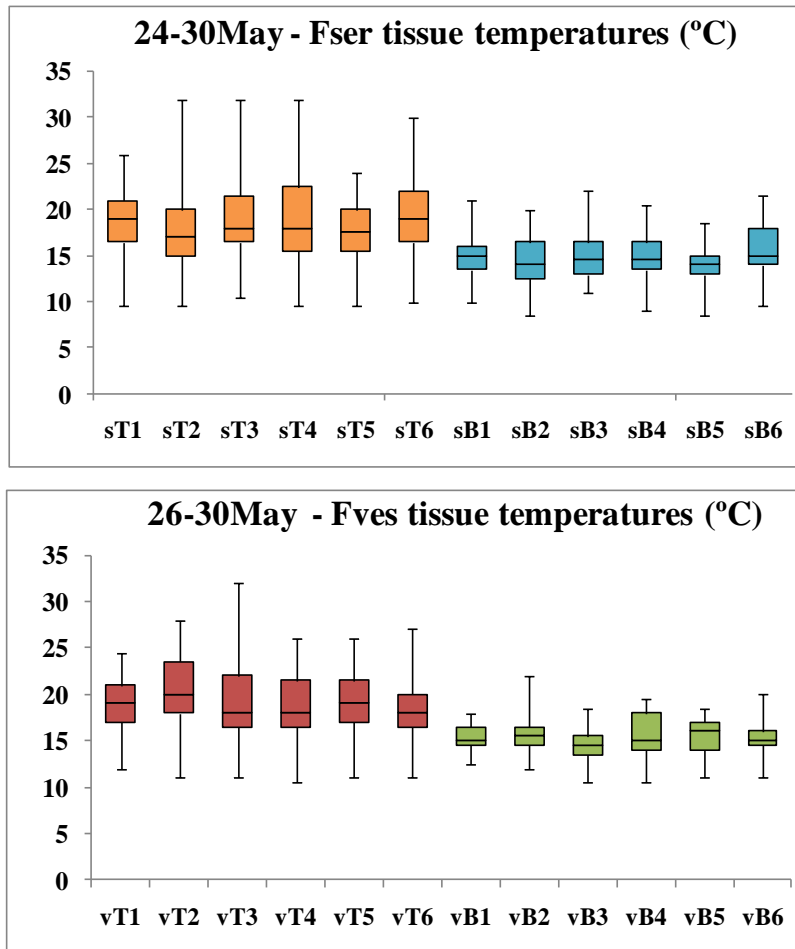


Figure 5.5 – Tissue temperatures on Top and Bottom microhabitats. Temperatures recorded every 5 min, only during daytime emersion, over six Top and six Bottom microhabitats for each species. Note the higher temperatures in Top habitats and the similarities between species, despite missing data (two days missing for Fves). See Materials and methods for details. Boxplots show Maximum - 3rd quartile - median - 1st quartile - minimum values.

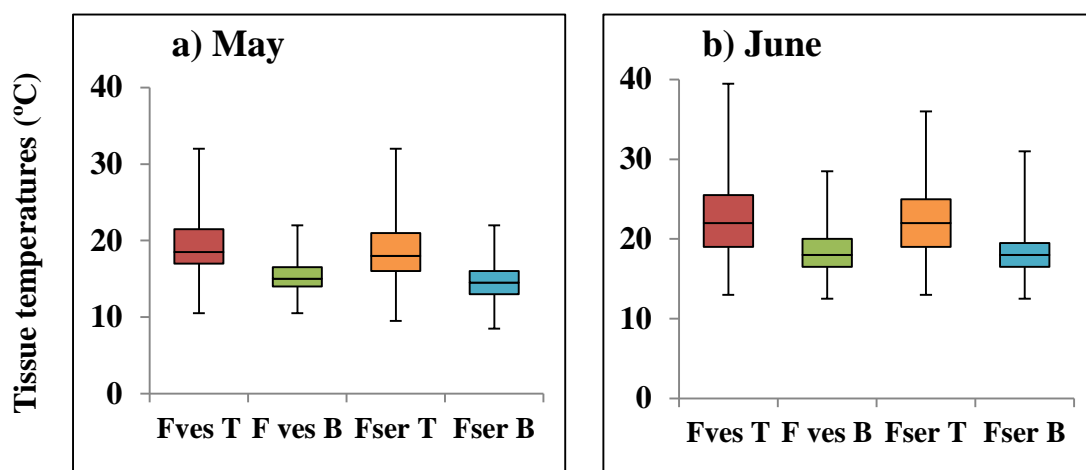


Figure 5.6 – Tissue temperatures of *Fucus serratus* (ser) and *F.vesiculosus* (ves) canopy microhabitats (T = Top, B = Bottom). Temperatures recorded on six individuals during daytime emersion from 23 - 27 June and from 24/ 26 - 30 May, 2013 (n=5 for Fser T in June). See Materials and methods for details. Boxplots show Maximum - 3rd quartile - median - 1st quartile - minimum values.

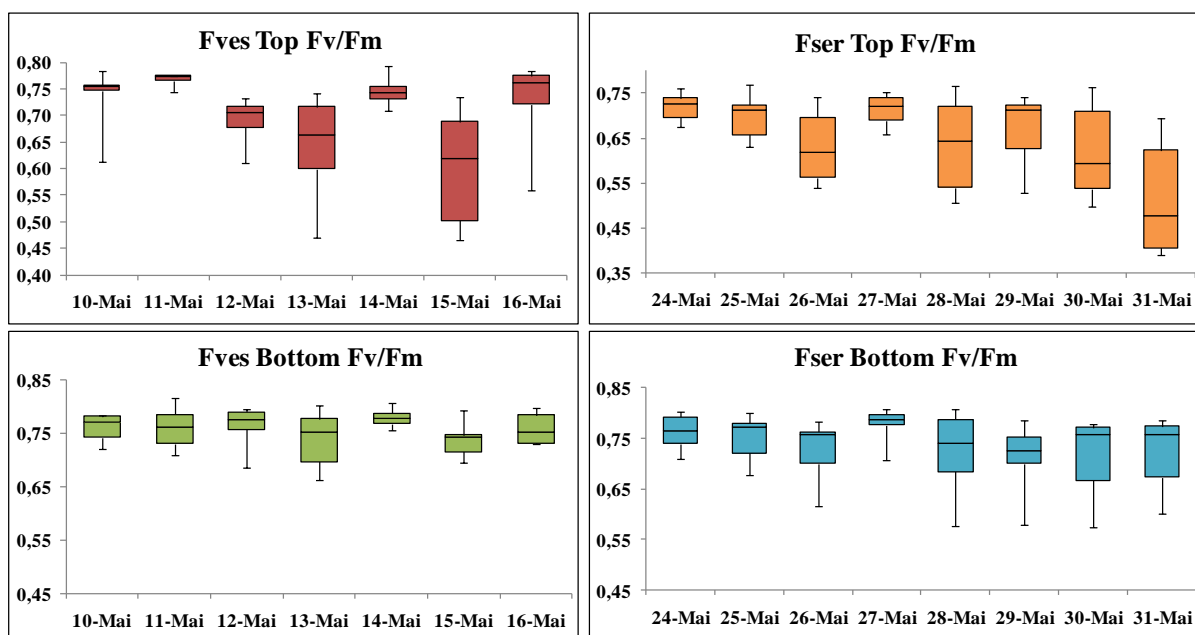


Figure 5.7 – Recovery Fv/Fm on Top (T) and Bottom (B) microhabitats in May, 2013. PSII yield (Fv/Fm) after sequential desiccation exposures in *Fucus serratus* (Fser, 24-31 May) and *F. vesiculosus* (Fves, 10-16 May), (n=6). See Materials and methods for details. Boxplots show Maximum - 3rd quartile – median - 1st quartile - minimum values.

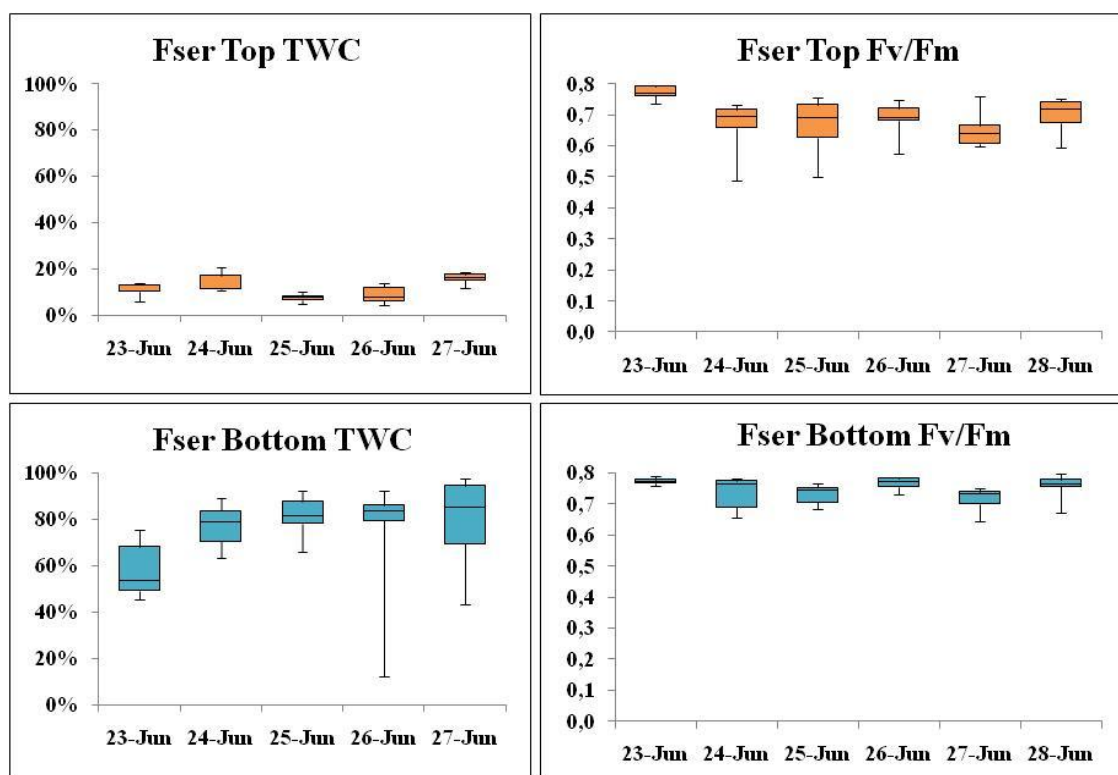


Figure 5.8 – Recovery Fv/Fm and TWC on Top (T) and Bottom (B) microhabitats in June, 2013. TWC measured daily at the end of the emersion period (n=6). Fv/Fm after sequential desiccation exposures, in *Fucus serratus* (Fser), measured daily to reflect accumulated damage from previous days (n=6, n=5 on 23Jun). See Materials and methods for details. Boxplots show Maximum - 3rd quartile – median - 1st quartile - minimum values.

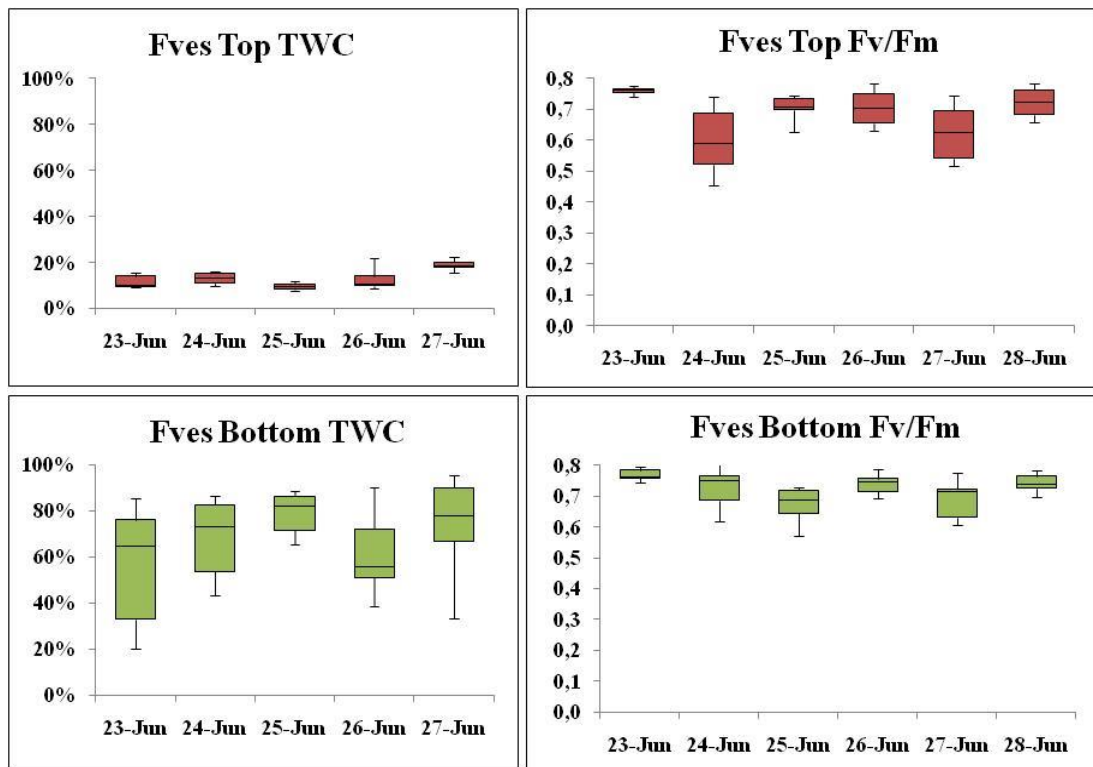


Figure 5.9 – Recovery Fv/Fm and TWC on Top (T) and Bottom (B) microhabitats in June, 2013. TWC measured daily at the end of the emersion period ($n=6$). Fv/Fm after sequential desiccation exposures, in *F. vesiculosus* (Fves), measured daily to reflect accumulated damage from previous days ($n=6$). See Materials and methods for details. Boxplots show Maximum - 3rd quartile – median - 1st quartile - minimum values.

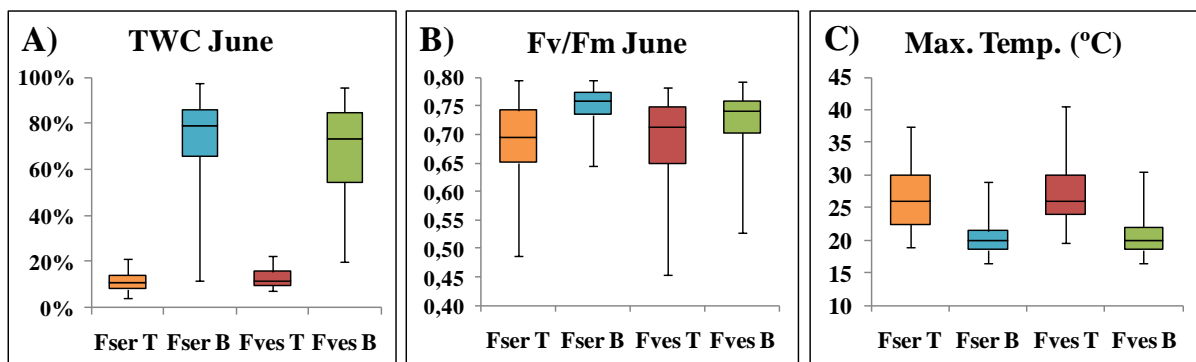


Figure 5.10 – Microhabitat differences in desiccation, recovery Fv/Fm and (peak) tissue temperature between Top (T) and Bottom (B) microhabitats. A) TWC measured daily at the end of the emersion period ($n=30$). B) PSII yield (Fv/Fm) after sequential desiccation exposures, measured daily shortly after emersion ($n=36$). C) Maximal (daily) tissue temperature during low tide emersion ($n=30$). Measurements were performed on six apical tips per microhabitat from 23 to 28 June, on *Fucus serratus* (Fser) and *F. vesiculosus* (Fves). See Materials and methods for details. Boxplots show Maximum - 3rd quartile – median - 1st quartile - minimum values.

There was a weak ($r^2=0.3581$) correlation between TWV and recovery Fv/Fm in Bottom tissues (Fig. 5.11) but only in June *F. vesiculosus* ($r^2=0.0063$ in *Fucus serratus*). TWC in Bottom tissues of *Fucus serratus* was always above 40% with tissue temperatures below

25°C (except one value) with recovery F_v/F_m close to or above 0.7. Under such mild conditions (and low impact on recovery F_v/F_m) it may be difficult to detect desiccation effects. In *F. vesiculosus* the correlation seems dependent on moderately desiccated tissues (under 70% TWC) that do not fully recover from the stress (F_v/F_m under 0.7). This correlation may be affected by the use of “proxy” tips for TWC and temperature measurements that sometimes experience different conditions from the tissues sampled for recovery F_v/F_m . Averaging conditions by microhabitat might improve the correlation, but results in few data points (not shown). The maximal tissue temperature measured in each tip was selected to correlate the data because it may represent thermal stress better than the average temperature during the sampling period.

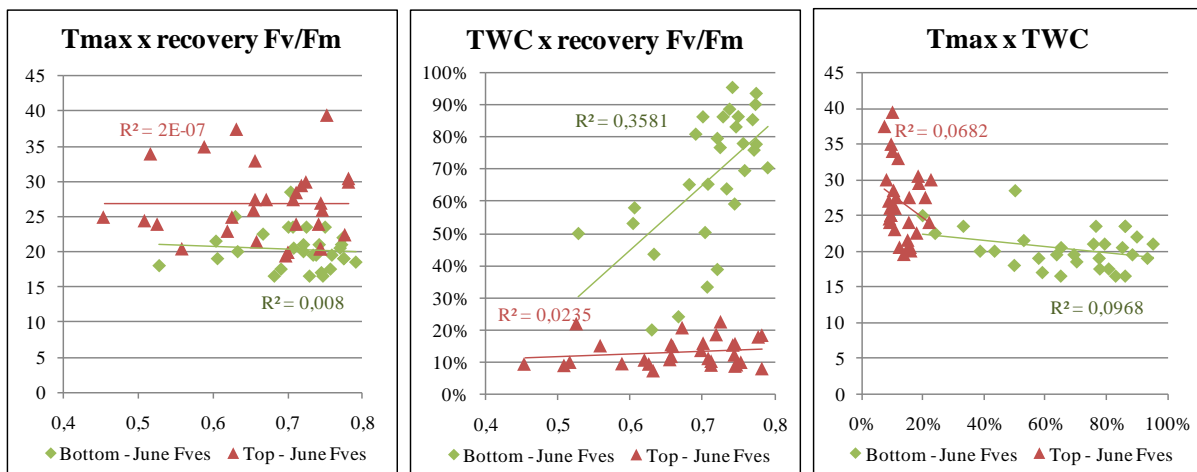


Figure 5.11 – Correlation between microhabitat parameters: maximum tissue temperature (T_{max}), desiccation (TWC) and PSII yield after recovery (F_v/F_m). T_{max} was the highest temperature recorded on apical tissue during low tide emersion (dataloggers), TWC was determined at the end of the emersion period and recovery F_v/F_m was measured the day after the temperature and desiccation stress, shortly after emersion. Measurements were made on *F. vesiculosus* between 23-28 June on six apical tips per microhabitat. See Materials and methods for details.

During the sampling periods temperatures were usually mild (substrate and air temperatures mostly below 20°C, barely rising above 25°C) yet tissue temperatures occasionally rose above 30°C (T_{Max} 39.5°C). With water temperatures below 15°C thermal stress was restricted to a few periods during emersion and effective recovery was possible during immersion. Moderate Bottom thermal stress (T_{Max} usually below 25°C) and the weak TWC vs. F_v/F_m correlation detected (Fig. 5.11) indicate a potential impact of desiccation on tissues that dry slowly. Slower drying may also account for lower recovery F_v/F_m of some Top tips, as fast Top desiccation (see Chapter 3) should have small effects on photosynthetic performance

after 24h. Without additional data on desiccation rates, or suitable desiccation stress markers, we can't clearly identify the physiological impacts of desiccation exposure on these tissues.

Protein expression changes between Top and Bottom microhabitats

The tissue samples from both species (*F. serratus* and *F. vesiculosus*) collected in June after sequential *Fv/Fm* measurements were examined using 2DE-DIGE to detect changes in protein profiles between the two microhabitats (Top and Bottom). Separate DIGE experiments were performed for each species, but in both experiments separation in the first dimension was not complete, using the voltages that were previously optimized for the unlabelled protein samples. The excess dye (not linked to proteins) did not migrate out of the strip during the first dimension, affecting protein separation. The resulting gels all presented a similar reduction in separation area, but the remaining spots were fairly well resolved and subsequent image analysis was limited to the area containing resolved spots (Fig. 5.12). In *F. serratus* 996 total spots were examined across five gels (pairwise comparison of Top and Bottom tissues from each individual), resulting in 79 changing spots (ANOVA $p < 0.05$), most with very small fold changes (only six spots have $p < 0.05$ and fold change > 1.4 , Tab. 5.5). In *F. vesiculosus*, a pairwise comparison of Top and Bottom tissues from each of six individuals (six gels) resulted in 68 changing spots ($p < 0.05$ out of 761 total spots), six with fold change > 1.4 (Tab. 5.6). In both species, all candidate spots ($p < 0.05$) were considered false discoveries according to Benjamini-Hochberg correction for multiple testing.

Table 5.5 – Candidate differentially expressed protein spots between Top and Bottom microhabitats, in *F. serratus* (n=5). Only six spots are presented (those with $p < 0.05$ and fold change > 1.4), out of 996 total spots, 79 having $p < 0.05$. Values from SameSpots analysis software, except FDR test (Benjamini-Hochberg correction for multiple testing at 0.05).

spot Fser#	Anova (p)	Fold	q-value	Power	Highest Mean	FDR alpha	FDR result
781	1.57E-03	1.5	0.270	1.000	Top	2.51E-04	False
1035	3.01E-03	2.8	0.323	0.969	Top	4.02E-04	False
1166	4.15E-03	1.7	0.358	0.930	Top	4.52E-04	False
414	5.22E-03	2.2	0.358	0.923	Bottom	6.02E-04	False
1178	4.05E-02	1.5	0.394	0.539	Top	3.21E-03	False
875	4.15E-02	1.6	0.394	0.378	Top	3.26E-03	False

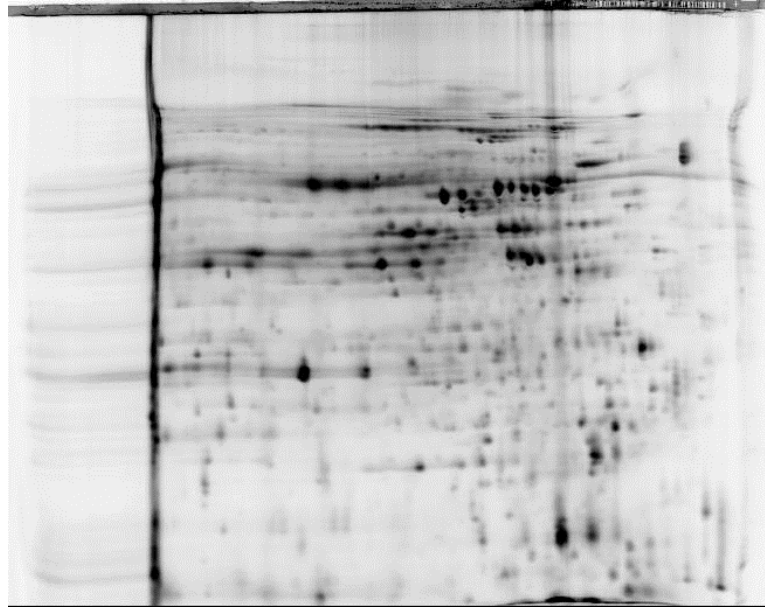


Figure 5.11 – Representative gel image of a Bottom sample from *F. serratus* labelled with Cy5dye (FserB2_Cy5). Note the dye line on the left, reducing protein separation on the first dimension.

Table 5.6 – Candidate differentially expressed protein spots between Top and Bottom microhabitats, for *F. vesiculosus* (n=6). Only six spots are presented (those with $p < 0.05$ and fold change > 1.4), out of 761 total spots, 68 having $p < 0.05$. Values from SameSpots analysis software, except FDR test (Benjamini-Hochberg correction for multiple testing at 0.05).

spot Fves#	Anova (p)	Fold	q-value	Power	Highest Mean	FDR alpha	FDR result
417	3.67E-03	1.6	0.344	1.000	Bottom	3.28E-04	False
492	4.21E-03	1.5	0.344	0.998	Top	3.93E-04	False
410	1.30E-02	1.9	0.344	0.872	Bottom	1.05E-03	False
254	2.58E-02	2.4	0.344	1.000	Bottom	1.83E-03	False
265	3.96E-02	4.9	0.344	0.996	Bottom	3.15E-03	False
377	4.67E-02	1.5	0.344	0.730	Bottom	4.06E-03	False

5.4 - Discussion

This study revealed the impact of natural exposure to consecutive cycles of desiccation stress on natural canopies of two species of intertidal algae, *Fucus serratus* and *F. vesiculosus*. Algal canopies modulate their environment forming distinct microhabitats during emersion. This data shows the large variability experienced by different portions of the same individual during sequential days of exposure to potentially intense field desiccation. We found that these temporary microhabitats, the Top and the Bottom of the algae canopy, differed in tissue temperatures, desiccation intensity and long-term damage to photosynthesis resulting from emersion during midday low tides. We detected no species differences in tissue temperatures, desiccation or recovery F_v/F_m in the mixed *Fucus* beds examined, but the morphology of *F. serratus* apparently reduces the proportion of exposed tissue at the Top of the canopy. Overall mild temperatures and frequent wind may have reduced thermal and desiccation stress, limiting our ability to detect cumulative effects of desiccation and species differences.

These peculiar canopy microhabitats are “rebuilt” every new low tide emersion, as the algal fronds can potentially be laid down in in any microhabitat. We determined the temporal variability of these canopy microhabitats, in two species with distinct frond morphologies, *F. serratus* and *F. vesiculosus*. Individual tips presented different preferences, with a small number of apical tips clearly favoring one environment for an extended period while others shifted freely between microhabitats, possibly due to their shape, size and position on the frond structure. The likelihood of standing in the Top microhabitat was 50% for *F. vesiculosus* and 31% for *F. serratus* tips examined. The more compact structure of *F. serratus* (flatter, more branched, denser fronds) may cause higher packing and sheltering of these fronds, reducing the fraction of exposed (Top) tissue. This sheltering strategy may allow sustained growth of the less-tolerant *F. serratus* species in these higher shore mixed beds. A complex canopy structure may also provide some protection from heat waves or other stress events, as fronds residing in a more protected microhabitat during the whole stress period may have improved survival (Brawley & Johnson 1991; Hunt & Denny 2008; Mota et al 2015), reducing stress-induced mortality.

Considerable differences in thermal and desiccation stress were detected, as expected, between the more exposed microhabitat (Top of the canopy) and the more sheltered (Bottom), but not between equivalent microhabitats created by the fronds of the two species (*F. serratus* and *F. vesiculosus*). During our study period (May and June) apical tissue

exposed in the Top microhabitat was always severely desiccated (TWC <20%) by the end of the low tide, except when it rained during emersion. Top tissues also presented the highest temperatures and the largest increases during low tide, although tissue temperature fluctuations in time and space were considerable and dependent on many variables (air temperature, wind, rain, solar exposure). Tissues sheltered in the Bottom of the canopies usually remained relatively hydrated and cooler throughout emersion, often retaining over 80% of their water and seldom increasing their tissue temperature more than 5°C. Nonetheless, these microhabitats are not permanent, and occasionally a tip laying under the canopy (Bottom) can be exposed if a disturbance (like strong winds) displaces some of the fronds above it. The intense desiccation of the exposed tissues (Top) also promotes shrinkage that may also partially expose the underlying tissues. Such events contribute to temperature and desiccation variability at the Bottom. The exposure in microhabitats with higher temperature and desiccation had minor physiological impacts on *F. serratus* and *F. vesiculosus* revealed in long-term photodamage (decreases in recovery F_v/F_m). The PSII damage detected (expected to be reflected in changes in protein expression across Top and Bottom tissues) was moderate, particularly at the Bottom microhabitat. This small effect may result from mild environmental conditions, where wind induced fast desiccation that protects Top tissues, while dense canopies and moderate temperatures avoid impacts in Bottom tips. Given the large variations in temperature and desiccation that occurred (often between days, occasionally within replicates) it was not possible to relate the observed photodamage events to a particular stress condition. Despite the recognized differences in stress tolerance between the two species (*F. serratus* and *F. vesiculosus*), no differences in sensitivity to PSII damage were detected between species with the mild conditions prevalent in this setup.

Comparing the protein profiles in both microhabitats, no significant differences in protein expression were detected between the exposed Top of the canopy and the sheltered Bottom, in either species (*F. serratus* and *F. vesiculosus*), after sequential desiccation in the field. The absence of protein expression changes between Top and Bottom microhabitats may indicate the constitutive nature of desiccation tolerance mechanisms. Alternatively, it could be that the lack of differences results from low statistical power to detect small protein changes, given the large biological and environmental variation within microhabitats, coupled to limited spot separation on the gels.

5.5 – References

- Benjamini, Y. & Hochberg, Y. (1995). “Controlling the false discovery rate: a practical and powerful approach to multiple testing,” *Journal of the Royal Statistical Society, Series B* (Methodological), **57** (1): 289-300.
- Brawley, S.H. & Johnson, L.E. (1991). Survival of furoid embryos in the intertidal zone depends upon developmental stage and microhabitat. *Journal of Phycology*, **27**, 179-186.
- Davison, I.R. & Pearson, G.A. (1996). Stress tolerance in intertidal seaweeds. *Journal of Phycology*, **32**, 197-211.
- Dring, M.J. & Brown, F.A. (1982). Photosynthesis of intertidal brown algae during and after periods of emersion: a renewed search for physiological causes of zonation. *Marine Ecology Progress Series* **12**, 301–308.
- Hunt, L.J.H. & Denny, M.W. (2008). Desiccation protection and disruption: a trade-off for an intertidal marine alga. *Journal of Phycology*, **44**, 1164-1170.
- Jones, S.J., Mieszkowska, N. & Wethey, D.S. (2009). Linking thermal tolerances and biogeography: *Mytilus edulis* (L.) at its southern limit on the east coast of the United States. *The Biological bulletin*, **217**, 73-85.
- Jueterbock, A., Kollias, S., Smolina, I., Fernandes, J.M., Coyer, J.A., Olsen, J.L. & Hoarau, G. (2014). Thermal stress resistance of the brown alga *Fucus serratus* along the North-Atlantic coast: acclimatization potential to climate change. *Marine Genomics*, **13**:27-36.
- Jueterbock, A., Franssen, S.U., Bergmann, N., Gu, J., Coyer, J.A., ... & Olsen, J.L. (2016). Phylogeographic differentiation versus transcriptomic adaptation to warm temperatures in *Zostera marina*, a globally important seagrass. *Molecular Ecology* **25** (21): 5396-5411.
- Lamote, M., Johnson, L. E., & Lemoine, Y. (2007). Interspecific differences in the response of juvenile stages to physical stress: fluorometric responses of furoid embryos to variation in meteorological conditions. *Journal of Phycology*, **43** (6), 1164-1176.
- Lamote, M., & Johnson, L. E. (2008). Temporal and spatial variation in the early recruitment of furoid algae: the role of microhabitats and temporal scales. *Marine Ecology Progress Series*, **368**, 93-102.
- Maxwell, K. & Johnson, G.N. (2000). Chlorophyll fluorescence - a practical guide. *Journal of Experimental Botany*, **51**, 659-668.
- Mota, C.F., Engelen, A.H., Serrão, E.A. & Pearson, G.A. (2015). Some don't like it hot: microhabitat-dependent thermal and water stresses in a trailing edge population. *Functional Ecology*, **29** (5): 640-649.
- Pearson, G.A., Lago-Leston, A. & Mota, C. (2009). Frayed at the edges: Selective pressure and adaptive response to abiotic stressors are mismatched in low diversity edge populations. *Journal of Ecology*, **97**: 450-462.
- Schagerl, M., & Möstl, M. (2011). Drought stress, rain and recovery of the intertidal seaweed *Fucus spiralis*. *Marine biology*, **158** (11), 2471-2479.
- Schonbeck, M.W. & Norton, T.A. (1980). Factors causing the lower limits of furoid algae on the shore. *Journal of Experimental Marine Biology and Ecology*, **12**, 131–150.
- Zaneveld, J.S. (1937). The littoral zonation of some fucaceae in relation to desiccation. *Journal of Ecology*, **12**, 431–468.

5.6 – Acknowledgements

I would like to thank the help of Denise Schrama and Dr. Pedro Rodrigues from Aquagroup at CCMAR, for assistance and use of their equipment for DIGE and the ASSEMBLE staf at SBR, Roscoff for information and help with printing for the field work.

This study was supported by projects UID/Multi/04326/2013, EXCL/AAG-GLO/0661/2012 and fellowship SFRH/BD/74436/2010 of the Portuguese Science Foundation (FCT).

Supporting information

Supporting information to this chapter can be found on the Appendix (digital version)

Table S5.1 – PERMANOVA results of F_v/F_m from field Top and Bottom microhabitats.

Table S5.2 - Top observations on 2sps x 2 sites

Table S5.3 – binomial tests for Top preference (FDR)

Chapter 6

Proteomic profiling of desiccation-related proteins in furoid algae

Chapter 6 –Proteomic profiling of desiccation-related proteins in furoid algae

6.1 – Introduction

Genomic-scale approaches such as transcriptomics and proteomics are becoming more routinely applied in studies of biological processes, such as the basis of tolerance to environmental stressors. Nevertheless, progress in some organismal groups has outpaced others. In particular, although proteomic techniques such as 2DE electrophoresis have been around for decades (O'Farrell 1975), their application to difficult or poorly covered groups such as macroalgae remains in its infancy (reviewed by Contreras-Porcía & López-Cristoffanini, 2012). Within the Phaeophyceae (brown algae) the proteomic literature is even more constrained, both in extent and taxonomic coverage, to the filamentous Ectocarpales and Dictyosiphonales (Contreras *et al.* 2008, 2010; Ritter *et al.* 2010; Fu *et al.* 2014) or kelps of the order Laminariales (Yotsukura *et al.* 2010, 2012).

Related intertidal species within the genus *Fucus* exhibit distinct levels of abiotic stress tolerance, that relate to their position on the shore (Dring and Brown 1982, Davison & Pearson 1996). This offers an attractive system for comparative studies of abiotic stress tolerance, open to evolutionary interpretation in a well-studied group (Serrão *et al.* 1999, Coyer *et al.* 2006, Cánovas *et al.* 2011). The more sensitive species *F. serratus* is usually found in the low intertidal and subtidal, below *F. vesiculosus*, an abundant mid- to high-shore species that is more sensitive to desiccation than the closely related taxa *F. guiryi* and *F. spiralis*. *F. spiralis* locates usually high in the intertidal, just below *Pelvetia* belts.

Desiccation stress is long known to be a key determinant of ecological zonation restricting the upper limit of many species, particularly in furoid algae (Dring and Brown 1982, Davison & Pearson 1996), but the cellular and molecular mechanisms of desiccation tolerance are still largely unexplored. The lack of appropriate markers for desiccation stress limits research into

the ecological role of desiccation in relation to canopy structure and population dynamics of *Fucus* species. Earlier attempts to identify molecular markers related to desiccation and rehydration from expressed sequence tag (EST) libraries were unfruitful (Pearson *et al.* 2010), and the success of current efforts to identify protein expression changes using conventional 2DE analysis was limited in short-term lab-desiccated (unpublished data) and field-desiccated tissues (Chapter 4). These previous studies may indicate that constitutive expression of desiccation-protection proteins and other cellular components is the major mode of protection in furoid algae. This might represent a useful strategy in intertidal species that can experience rapid desiccation when emerged at low tide, by ensuring that the main tolerance mechanisms are always in place. However, it is possible that small but important changes in protein expression are occurring that are technically challenging to detect against a background of individual variability in protein expression. This issue can be addressed by using a larger number of replicates to improve the signal to noise ratio resulting from biological variation, (Valledor & Jorrín 2011), but this increases the required number of gels, making spot matching harder. In DIGE (Difference Gel Electrophoresis) protein samples are labelled with three (size and charge matched) fluorescent markers with non-overlapping spectra, allowing the analysis of two different samples and a common internal standard in the same gel, after separately scanning the three spectra (Ünlü *et al.* 1997). 2DE-DIGE allows the use of more biological replicates in a small number of gels, and the common internal standard improves spot matching between gels and ensuing image analysis, permitting the detection of small expression changes.

Most studies of desiccation tolerance have focused on organisms that face infrequent and extended periods of desiccation (bryophytes, resurrection plants, rotifers, tardigrades), many of which require gradual water loss (during days or weeks) to survive desiccation, and extended recovery periods to repair the damages sustained and resume growth (see reviews by Proctor & Pence 2002, Oliver *et al.* 2005, Rebecchi *et al.* 2007, Charron & Quatrano 2009, Dinakar & Bartels 2013). Even in these taxa, research at the molecular level was initially limited by a lack of genomic resources (reference genomes and transcriptomes), but has expanded in recent years. Studies in bryophytes and resurrection plants highlighted the role of LEA proteins during desiccation, a family of disordered proteins induced during drought and involved in stabilizing proteins and membranes (e.g. Battaglia *et al.* 2008, Graether & Boddington 2014). Other common patterns were induction of transcripts of antioxidant proteins, early light induced proteins (ELIPs), ABA-regulated proteins and many unknown

proteins, often absent in related desiccation-sensitive organisms. Proteomic studies identified proteins involved in ROS scavenging, sucrose accumulation, defense, cell wall remodeling, and proteins with unknown functions, among others (Dinakar & Bartels 2013). Constitutive expression of some LEA-genes and many antioxidant genes was detected in desiccation tolerant plants (*H. rhodopensis*) that were further induced upon drought and desiccation (Dinakar & Bartels 2013). Many of these proteins are also involved in drought-tolerance (on desiccation-sensitive plants).

Lichen and green algae also benefit from growing molecular knowledge in related model organisms (land plants and microalga) and seem to share some desiccation-tolerance features despite faster dehydration. A terrestrial green alga was found to strongly up-regulate mostly unidentifiable transcripts (not similar to known viridiplant proteins) upon strong desiccation for 2.5h. Some known desiccation-related transcripts were also induced (e.g. similar to LEA/late embryogenesis abundant and ERD/early response to desiccation proteins), and transcripts for raffinose-biosynthesis enzymes (osmolyte production), photosynthesis, energy production, reactive oxygen species (ROS) metabolism, and light-harvesting complex proteins (nonphotochemical quenching) psbS and elip (Holzinger *et al* 2014). In the isolated phycobiont *Asterochloris erici* (green alga) dried slowly (5–6 h) or rapidly (<60 min), DIGE only detected increased relative abundance of 11–13 proteins per treatment, involved in glycolysis, cellular protection, cytoskeleton, cell cycle, targeting and degradation or not identified, suggesting constitutive mechanisms (Gasulla *et al.* 2013). Desiccation rate affected recovery as most rapid-dried cells had extensive plasmolysis and cytorrhysis but the alga survived this treatment. After rapid drying expression changes may be smaller in desiccated tissue, but rehydration will induce further changes to repair additional damages (Gasulla *et al.* 2013).

Intertidal algae, like lichens, may face frequent desiccation (they can be emersed twice a day during low tides) and need to resume normal metabolism soon after rehydration to sustain growth in sites that may be emerged for a considerable portion of time.

Previous analysis found little evidence for significant changes in protein expression resulting from a single event of severe desiccation (between controls and desiccation/ rehydration samples, Chapter 4), or after multiple daily cycles of desiccation (comparing intense and mild desiccation, on Top or Bottom of the algal canopy, see Chapter 5). We hypothesised that long-term acclimation may be required to induce or repress desiccation tolerance, or

alternatively that constitutive mechanisms are in place that do not require the expression of new proteins. To detect possible changes in expression resulting from long-term acclimation to desiccating conditions, samples from both extremes of the tidal distribution were compared: low shore (infrequent mild desiccation) and high shore (frequent intense desiccation). At the low-shore edge of the vertical distribution we identified sites where individuals of both *F. serratus* and *F. vesiculosus* remain submerged during most low tides, experiencing emersion only for short periods during spring tide cycles. These individuals are unlikely to have ever experienced severe desiccation. In contrast, high-shore samples were collected at sites where both species were exposed for over six hours on spring tides and experience very frequent intense desiccation.

In case of constitutive mechanisms promoting desiccation tolerance, no differential expression of proteins will be detected by comparing samples exposed or not to desiccation. Even in this scenario it might be possible to identify desiccation-responsive proteins by comparing related algae that are very tolerant to others that are sensitive to desiccation. We compared species possessing different levels of tolerance to identify proteins whose expression correlates with differential desiccation tolerance. Three species were examined; the lower shore, more distantly related, less tolerant *F. serratus* was compared with the intermediate species *F. vesiculosus*, and a second set of samples was used to compare *F. vesiculosus* with the closely related, higher shore and more desiccation-tolerant species *F. spiralis*. Differences in protein profiles may reflect expression-level changes, Post-Translational Modifications (PTMs) and protein sequence variation, and include not only proteins related to desiccation-tolerance, but many other proteins (under selection or neutral variants) unrelated with emersion-tolerance.

The total extractable proteome of *F. vesiculosus* was also characterized, both to illustrate the ability of the methods used to identify a large and representative number of proteins in this brown alga and determine active metabolic pathways, but also to ascertain any bias introduced by these methods on the selection of particular classes of proteins.

6.2 – Materials and methods

Fucus vesiculosus and *F. serratus*; sampling of High shore vs Low shore tissue

Tissue samples of *F. vesiculosus* and *F. serratus* were collected on the 22nd May 2013, around the peak of spring low tide (10:40h) in the intertidal at Roscoff, Brittany, France.

Low shore individuals were selected in the low intertidal, where some sparse *Fucus vesiculosus* and *F. serratus* could be found attached to large rocks, among abundant *Himantalia elongata* stands mixed with other brown, red and green algae. These algae, at the lowest end of the *Fucus* zone, are usually submerged even during low tides, experiencing emersion only for short periods during spring tides (on a semi-lunar cycle, or ca. every 2 weeks). High shore individuals were isolated plants high on the shore, exposed for several (5-6 h) hours every low tide, lacking protection from a dense canopy and therefore expected to desiccate frequently. Apical vegetative tips (n=5 individuals) were flash-frozen in liquid nitrogen after rinsing with ddH₂O and 50mM Tris-HCl, as described previously for proteomic analysis.

Fucus vesiculosus and *F. spiralis*; laboratory desiccation and recovery

Four large individuals of *Fucus vesiculosus* and *F. spiralis* were collected in June, 2014, in Viana do Castelo, Northern Portugal. In the laboratory, fronds were acclimated for seven days at 10°C, immersed in filtered seawater with aeration, with 100 $\mu\text{mol m}^{-2} \text{s}^{-1}$ light on a 12h L-12 h D cycle. Vegetative apical tips from each individual (10-15 tips) were divided in three similar sets (control, desiccation and recovery). Apical tips were dark-adapted for *F_v/F_m* measurements, lightly blotted to remove surface water and weighted to determine fully hydrated weight (hW). Desiccation and recovery treatments were placed to desiccate for 3 hours over a plastic grid, in a climatic chamber (S600, Aralab) at 20°C, $\sim 100 \mu\text{mol m}^{-2} \text{s}^{-1}$ light and control samples were returned to 10°C acclimation conditions. After 3h of emersion at 20°C, tips were weighed (iW) and *F_v/F_m* was measured. Desiccated apical tips were rinsed and frozen for proteomics and recovery tips were returned to acclimation conditions for 2h of rehydration at 10°C. *F_v/F_m* and intermediate weight (iW) was determined after 2h recovery. Recovery and Control tissues were rinsed and frozen for proteomics.

Physiological status (*F_v/F_m*) was determined by chlorophyll fluorescence (Junior-PAM, Walz, Germany) on apical tips dark-adapted for 10-20 min. Desiccation intensity was

determined by tissue water content (TWC), where $TWC (\%) = (iW - DW) / (hW - DW) \times 100$, and Dry Weight (DW) was assumed to be 23% of hW value, based on previous values, since all tips were used for subsequent proteomic analysis. Tissue samples for proteomic analysis (n=4 biological replicates) were flash-frozen in liquid nitrogen after rinsing 2-4 x with ddH₂O and 50 mM Tris-HCl, pH 8.8.

Protein phenol extraction for DIGE

Proteins were extracted by the phenol extraction method A, described in detail in Chapter 3, with some modifications. Since less protein is required for DIGE analysis than for conventional Coomassie staining, extractions were performed in 2 ml tubes, using a total of 0.2-0.4 g of tissue. Proteins were resuspended in a rehydration buffer (RB) specific for DIGE, without DTT and at pH 8.5 to allow effective dye-labelling. Briefly, frozen tissue (0.3 g) was ground in liquid nitrogen, homogenised for 20 min with 0.5 ml Extraction buffer (2 % PVP-40, 0.7 M sucrose, 0.75 M KCl, 0.5 M Tris-HCl pH 7.5, 250 mM EDTA, 0.5 % CHAPS, 2 % DTT, protease inhibitor cocktail) and extracted for 20 min with 2 volumes of phenol (pH 8). Proteins were precipitated from the phenol phase with 5 volumes 0.1 M ammonium acetate in methanol and consecutively washed with 0.1 M ammonium acetate in methanol, 10% TCA in acetone and three times in 80 % acetone. The final protein pellet was dissolved in 85 µl of RB (30 mM Tris pH=8.5, 7 M urea, 2 M thiourea, 4 % CHAPS), spun down to remove any pellet and stored at -80°C.

Protein quantitation and DIGE labelling

Protein concentrations of *Fucus* extracts (1:20 dilutions) were determined using the Quick Start™ Bradford Protein Assay (Bio-Rad), on a Synergy plate reader using BSA standards. Protein concentration was adjusted to 5 mg/ml with RB and the pH was adjusted to 8.5 with diluted NaOH. Protein samples (50 µg of protein) were labeled with either Cy3Dye or Cy5Dye (200pmol) and internal standards (a pool of equal amounts of each experimental sample) with Cy2Dye (Cyanine NHS minimal dyes, Lumiprobe, Germany), according to the manufacturer's instructions, but for 50 min on ice.

DIGE

For each DIGE gel, two labeled protein samples (with Cy3Dye and Cy5Dye) were mixed with 50 µg of Cy2Dye-labelled internal standard, ampholytes (Bio-Lyte 3-10 buffer), DTT,

and DIGE RB. Sample combinations and labeling schema are shown in Table 6.1. The proteins (150 µg) were loaded into a 24 cm Immobiline DryStrip pH 4-7 (GE Healthcare) and 2DE was performed as described in Chapter 4 for large gels. After overnight rehydration, IEF separation was performed on Ettan IPGphor3 (GE Healthcare): 1 h gradient to 500 V, hold at 500 V for 1 h, gradient to 1000 V for 1 h, gradient to 8000 V in 3 h and hold at 8000 V for 5.40 h. Strips were equilibrated 20 min with DTT and 20 min with iodoacetamide, loaded into hand-cast 12 % SDS-PAGE gels and run at 24°C on Ettan DALTsix, with TGS 1x (192 mM glycine; 25 mM Tris-base; 0,1 % SDS) in the lower tank and TGS 2x in the upper tank. Molecular masses were estimated using a co-migrating broad-range standard (Precision Plus Protein Dual X-tra Standards, Bio-Rad). Gel cassettes were then rinsed and scanned on Typhoon TRIO Variable Mode Imager (Molecular Dynamics, GE) at 100 micron resolution, adjusting the voltage to avoid saturation, using the recommended laser/ emission filter pairs for the fluorescent Dyes: Cy2 (Blue) 488/ 520 nm, Cy3 (Green) 532/ 580 nm, Cy5 (Red) 633/ 670 nm.

Table 6.1 – Sample labels and gel loading design of the DIGE experiments. a) Comparisons of field-collected high shore (H) and low shore (L) *F. serratus* (ser) and *F. vesiculosus* (ves), n = 5. b) Laboratory experiment comparing recovery from desiccation (R) versus controls (C) in *F. vesiculosus* (ves) and *F. spiralis* (spir), n = 4.

a)	Cy3	Cy5	Cy2
gel 1	ser 1H	ser 1L	pool ser+ves
gel 2	ves 1H	ves 1L	pool ser+ves
gel 3	ser 2H	ves 3H	pool ser+ves
gel 4	ves 2H	ser 3H	pool ser+ves
gel 5	ser 2L	ves 5L	pool ser+ves
gel 6	ser 3L	ves 4H	pool ser+ves
gel 7	ves 2L	ser 5L	pool ser+ves
gel 8	ves 3L	ser 4H	pool ser+ves
gel 9	ves 5H	ves 4L	pool ser+ves
gel 10	ser 4L	ser 5H	pool ser+ves

b)	Cy3	Cy5	Cy2
gel 1	spirC1	vesC1	pool ves+spir
gel 2	vesR1	spirC3	pool ves+spir
gel 3	spirC2	spirR2	pool ves+spir
gel 4	vesR2	vesC2	pool ves+spir
gel 5	vesC3	spirR1	pool ves+spir
gel 6	spirR3	vesR3	pool ves+spir
gel 7	spirR4	vesR4	pool ves+spir
gel 8	vesC4	spirC4	pool ves+spir

Image analysis and experimental design

Image analysis of the 16-bits DIGE files was performed using Progenesis SameSpots software (NonLinear Dynamics). Gel images (High shore vs Low shore: five biological replicates x four conditions; Laboratory desiccation/rehydration vs controls: four biological replicates x four conditions) were aligned with some manually added vectors using internal

standard images, spot boundaries were defined across all gels and normalized after removing low intensity spots. Across the same DIGE experiment, several designs were analysed, allowing comparison of the same set of aligned spots (across species and treatments). Then it is easy to verify if the same spot presents (expression) changes in more than one design.

Designs used with High shore vs Low shore samples: **1)** High shore x Low shore in *F. serratus* (n=5); **2)** High shore x Low shore in *F. vesiculosus* (n=5); **3)** High shore x Low shore in both species (n=10); **4)** *F. serratus* x *F. vesiculosus* (n=10); **5)** High shore *Fser* x Low shore *Fser* x High shore *Fves* x Low shore *Fves* (four groups, n=5).

For laboratory desiccation/rehydration DIGE experiment, the designs were: **1)** Control x Recovery in *F. spiralis* (n=4); **2)** Control x Recovery in *F. vesiculosus* (n=4); **3)** *F. spiralis* x *F. vesiculosus* (n=8); **4)** *F. spiralis* Control x *F. spiralis* Recovery x *F. vesiculosus* Control x *F. vesiculosus* Recovery (four groups, n=4).

Each design produced a separate list of putative differentially expressed spots, fold-change, *p*-values (ANOVA), *q*-values (false discovery rate adjusted *p*-values) and power of the analysis. To control False Discovery Rate (FDR) at 0.05 confidence level, correction for multiple testing was also performed using the Benjamini & Hochberg approach (Benjamini and Hochberg, 1995).

Protein Identification

A limited set of spots, presenting minor changes ($p < 0.05$, > 1.5 fold between treatments or > 3 fold between species) and clearly detectable on the gel for picking, were retrieved for protein identification (27-40 spots across three species) All visible, retrievable spots from the *F. vesiculosus* field samples from Roscoff were also picked to characterize the total extractable proteome (340 well-defined spots). To retrieve the proteins, preparative gels were run with a larger amount of protein (700 μg of an unlabelled pool of samples), and the protein spots were manually excised from the Coomassie-blue stained gel(s) for mass spectrometry analyses (performed at the DTU Proteomics Core, Technical University of Denmark). At DTU, protein spots were washed with ammonium bicarbonate and acetonitrile, incubated with 45 mM DTT, then with 100 mM iodoacetamide and washed again before trypsin (0.05 $\mu\text{g}/\mu\text{l}$) digestion overnight at 37°C. For LC-MS/MS, peptide containing samples with ammonium bicarbonate were run on a SYNAPT G2 HDMS mass spectrometer (Waters) coupled to a nanoAquity UPLC system (Waters). Each sample was first trapped using a C18

trap column (C18 symmetry, 5 μm , 180 μm x 20 mm, Waters) and subsequently separated using a C18 analyzer nanoanalytical column (BEH130 C18 1.7 μm , 75 μm x 200 mm, Waters) kept at 35°C. During separation the flow rate of the loading pump was 0.3 $\mu\text{l}/\text{min}$, using two mobile phases, A (0.1% formic acid) and B (acetonitrile with 0.1% formic acid). During the 20 min gradient B was increased from 1 to 45%. Data was collected on the mass spectrometer employing the positive ion MS^e acquisition method (cycle time 0.8 s). The resulting data were used as input in the ProteinLynxGlobalServer (PLGS) using three brown algal protein databases; *Ectocarpus siliculosus* (Cock *et al.* 2010, obtained from <https://bioinformatics.psb.ugent.be/gdb/ectocarpus/>), *Fucus vesiculosus* and *F. serratus* predicted open reading frames (unpublished NGS transcriptomic data). Searches were performed assuming the formation of single-charged peptides, carbamidomethylation of cysteine residues, possible oxidation of methionine residues and up to 1 missed cleavage. Mass tolerance was 10 ppm for MS data and 0.5 Da for MS/MS data. LC-MS/MS protein identification independently used the three protein databases indicated above.

Protein identification by MS^E using ProteinLynx Global Server (PLGS) makes use of detailed information from chromatography, peptide mass fingerprinting and peptide ion series to identify and assign a score to a matching sequence, assuming the correct hit is present in the database used. In this study, searches were independently made against three protein databases: from the genome of *Ectocarpus siliculosus* (Esil db) and from NGS transcriptomes of *F. serratus* (Fser db) and of *F. vesiculosus* (Fves db). The only complete proteome (*Ectocarpus*) is phylogenetically distant from furoid algae (Silberfeld *et al.* 2010) and may contain divergent genes and/or gene content, while transcriptomes from the target species may be limited in terms of gene/isoform representation. It is important to note that some proteins may not be accurately identified, even if they produce good-quality MS spectra, because the quality of the database is limiting for successful identification and subsequent functional annotation.

Functional annotation

Functional annotation of the database hits was performed by bioinformatic analysis of the corresponding *Fucus* protein sequences, consisting of searches against the publicly available protein databases SwissProt, NCBI nr and KEGG (BLASTp and KASS searches), conserved domains (Pfam, CDD) and sequences of related *Fucus* species (reciprocal BLASTp searches for the most similar sequence in *F. serratus* and *F. vesiculosus*).

6.3 – Results

High shore versus Low shore analysis

The global analysis of the 10 gels produced a generally good alignment, despite an apparent excess of free dye in some gels (see Fig. 6.1) that reduced the aligned area and the number of identified spots. After excluding some small spots, 1003 were analysed with all designs. Comparing protein profiles of High and Low shore samples in *F. vesiculosus* (n=5), 87 spots showed significant differences (ANOVA $p < 0.05$), of which 44 had more than 1.4-fold changes (Tab. 6.2), and three appear to be true discoveries (FDR test for Rv685, Rv993, Rv1133). Unfortunately these three small spots could not be retrieved from the gel. In *F. serratus* (n=5) 38 spots changed between High and Low shore samples (ANOVA $p < 0.05$ and > 1.4 -fold change), but all failed multiple testing correction (Tab. 6.3). High shore x Low shore was also analysed with both species pooled (n=10), (Table 6.4). One spot was significantly changed (FDR test), but could not be picked from the gel. Several spots had low p -values (< 0.05), high fold-change (> 1.5), and were identified in multiple designs (e.g. spots 668, 224, 227, 752, 1174, 902). For example, spot 668 was the second best hit (in pooled species), with a low probability of being a false discovery (5.2% in pooled species; 14% in Fser; but 25% in Fves; q -values). As some of these spots may have escaped FDR detection because of the low number of replicates and large biological variability, some were selected for protein identification. Since it was not possible to pick very faint spots or spots in some crowded areas, selection was also based on ease of retrieval from the gel.

The remaining designs (*F. serratus* x *F. vesiculosus*, n=10; four groups, n=5) included comparison of both species. As there are abundant differences between these two species, many spots were significantly changed: in “four groups” 567 spots had low p -values (< 0.05) and high fold-change (> 1.5), 562 after multiple testing correction, in “Fser x Fves” this rises to 657 and 623 spots.

Table 6.2 – Protein changes between High and Low shore samples in *Fucus vesiculosus* (n=5). Table of 44 spots showing largest changes in expression (ANOVA; $p < 0.05$, fold-change >1.5).

spot Rv#	Anova (p)	Fold	q Value	Power	Highest Mean	FDR test
1133	3.57E-05	1.6	0.0240	1.0000	High shore	True
685	8.38E-05	2.9	0.0240	1.0000	Low shore	True
993	9.70E-05	1.8	0.0240	1.0000	High shore	True
1289	0.00021057	1.7	0.0391	0.9998	High shore	False
1270	0.00059289	1.5	0.0880	0.9973	High shore	False
775	0.00110474	1.6	0.1343	0.9906	Low shore	False
1154	0.00137553	1.5	0.1343	0.9861	High shore	False
750	0.00188132	1.9	0.1343	0.9770	High shore	False
1011	0.00203325	1.8	0.1343	0.9741	High shore	False
205	0.00231446	1.6	0.1343	0.9687	Low shore	False
989	0.00235034	1.8	0.1343	0.9680	High shore	False
551	0.00268114	1.7	0.1412	0.9615	High shore	False
224	0.00289303	1.7	0.1416	0.9574	Low shore	False
227	0.00414602	2.8	0.1907	0.9330	Low shore	False
69	0.0048969	1.7	0.2014	0.9188	Low shore	False
1149	0.00493606	1.5	0.2014	0.9181	High shore	False
777	0.00591353	1.8	0.2281	0.9004	High shore	False
1025	0.00638686	3	0.2369	0.8921	High shore	False
645	0.00949788	1.8	0.2543	0.8425	High shore	False
682	0.01008098	2.5	0.2543	0.8340	High shore	False
1166	0.01041959	1.6	0.2543	0.8292	High shore	False
1195	0.01130899	1.5	0.2543	0.8169	High shore	False
910	0.01378075	1.8	0.2543	0.7853	High shore	False
229	0.01381653	2.9	0.2543	0.7848	Low shore	False
1171	0.01439391	1.7	0.2543	0.7779	High shore	False
668	0.01475832	2.4	0.2543	0.7737	High shore	False
1076	0.01550277	1.5	0.2645	0.7652	High shore	False
567	0.01677519	1.5	0.2738	0.7512	Low shore	False
57	0.01808723	1.5	0.2818	0.7375	Low shore	False
155	0.01919546	1.6	0.2849	0.7264	Low shore	False
1193	0.01920082	1.6	0.2849	0.7263	High shore	False
486	0.02140475	1.6	0.3078	0.7056	Low shore	False
874	0.02464843	1.5	0.3078	0.6777	High shore	False
84	0.02475486	1.6	0.3078	0.6769	Low shore	False
539	0.0264667	1.5	0.3078	0.6633	Low shore	False
591	0.02882744	1.5	0.3078	0.6457	Low shore	False
721	0.02884044	1.5	0.3078	0.6456	High shore	False
905	0.03013793	3	0.3078	0.6364	High shore	False
935	0.03015174	1.9	0.3078	0.6363	High shore	False
1278	0.03386331	1.6	0.3078	0.6118	High shore	False
1176	0.0357592	1.5	0.3078	0.6001	High shore	False
123	0.03787099	1.8	0.3078	0.5877	Low shore	False
881	0.04063849	1.9	0.3078	0.5724	High shore	False
590	0.04267566	1.6	0.3078	0.5617	High shore	False

Table 6.3 – Protein changes between High and Low shore samples in *Fucus serratus* (n=5). Table of 38 spots showing largest changes in expression (ANOVA<p 0.05, fold-change >1.5).

spot Rs#	Anova (p)	Fold	q Value	Power	Highest Mean	FDR test
409	0.000133	3	0.1137	1.0000	High shore	False
752	0.0002414	2	0.1137	0.9997	High shore	False
361	0.0004198	2.6	0.1313	0.9988	High shore	False
1174	0.0005587	2.8	0.1313	0.9976	High shore	False
381	0.00087	2.7	0.1395	0.9940	High shore	False
668	0.001038	1.8	0.1395	0.9916	High shore	False
556	0.001407	1.9	0.1653	0.9856	High shore	False
900	0.0020772	2.8	0.1952	0.9733	High shore	False
1186	0.0023118	2.8	0.1977	0.9688	High shore	False
1165	0.0041629	1.7	0.3247	0.9326	Low shore	False
842	0.0057081	1.6	0.3624	0.9040	High shore	False
942	0.0061326	2.9	0.3624	0.8965	High shore	False
765	0.0074163	1.7	0.3624	0.8748	Low shore	False
857	0.0078636	7	0.3695	0.8676	High shore	False
1001	0.0102679	3	0.3918	0.8313	High shore	False
1177	0.0104928	3.8	0.3918	0.8281	High shore	False
876	0.011769	2.3	0.3918	0.8107	High shore	False
488	0.0155162	1.9	0.3918	0.7650	High shore	False
551	0.0156698	1.5	0.3918	0.7633	High shore	False
1117	0.0187466	1.9	0.3918	0.7308	High shore	False
505	0.0203871	1.7	0.3918	0.7150	High shore	False
1034	0.022868	1.5	0.3918	0.6927	Low shore	False
241	0.0240073	1.6	0.3918	0.6830	High shore	False
1172	0.0264685	1.9	0.3918	0.6633	High shore	False
669	0.0278512	1.5	0.3918	0.6528	High shore	False
261	0.0292022	1.8	0.3918	0.6430	Low shore	False
1200	0.0312414	1.6	0.3918	0.6289	High shore	False
953	0.0315294	1.7	0.3918	0.6269	High shore	False
946	0.0328531	2.3	0.3918	0.6182	High shore	False
902	0.0351528	1.9	0.3918	0.6038	High shore	False
961	0.0364302	3.3	0.3918	0.5961	High shore	False
1058	0.0367023	1.5	0.3918	0.5945	Low shore	False
1004	0.0371243	1.7	0.3918	0.5920	High shore	False
772	0.0390896	1.6	0.3918	0.5808	High shore	False
614	0.040925	2	0.3918	0.5708	High shore	False
1083	0.0422066	1.5	0.3918	0.5641	Low shore	False
317	0.0429373	1.5	0.3918	0.5603	High shore	False
852	0.0454406	1.5	0.3918	0.5479	High shore	False

Table 6.4 – Protein changes between High and Low shore samples (*Fucus serratus* and *F. vesiculosus*, n=10). Twenty spots with largest changes in expression (ANOVA $p < 0.05$, fold-change > 1.5).

spot R#	Anova (p)	Fold	q Value	Power	Highest Mean	FDR test
551	4.06E-05	1.6	0.04077	0.9991	High shore	True
668	0.00010319	2.1	0.0517	0.9967	High shore	False
752	0.00113188	1.6	0.25943	0.9547	High shore	False
1011	0.00204414	1.6	0.3139	0.9255	High shore	False
227	0.00233357	2	0.3139	0.9172	Low shore	False
905	0.00481805	2.3	0.4818	0.8595	High shore	False
682	0.00864628	1.8	0.56862	0.7955	High shore	False
1172	0.01052141	1.5	0.56862	0.7703	High shore	False
229	0.01143396	1.8	0.56862	0.7591	Low shore	False
224	0.01169492	1.5	0.56862	0.756	Low shore	False
1231	0.01233715	1.5	0.56862	0.7486	High shore	False
277	0.02264041	2.2	0.56862	0.6549	Low shore	False
85	0.02540459	1.6	0.56862	0.6353	Low shore	False
1171	0.03048902	1.5	0.56862	0.6033	High shore	False
645	0.03348127	1.5	0.56862	0.5865	High shore	False
857	0.0409423	4.5	0.56862	0.5493	High shore	False
942	0.04168446	2.6	0.56862	0.5459	High shore	False
1174	0.04284154	1.5	0.56862	0.5408	High shore	False
902	0.04638302	1.6	0.56862	0.5257	High shore	False
669	0.04670477	1.9	0.56862	0.5244	High shore	False

In total 33 spots were retrieved from *F. serratus* gel and 40 from *F. vesiculosus* for protein identification, clearly visible on the gel and with fold-changes ≥ 1.5 between shore levels or ≥ 3 between species. Additionally, 300 more identifiable spots (all the well-visible, defined spots present) were picked from the *F. vesiculosus* gel to characterize the total extractable proteome of *Fucus vesiculosus* (340 spots). A few of these spots were lost during processing (4 Fves + 2 Fser) and 25 (out of 340 Fves spots) had no hits to any database. All 31 *F. serratus* spots had hits to at least one database sequence. NanoUPLC-MSMS is a very sensitive technique that allows the identification of even minor protein components present in a gel spot. Overall the annotation rate was quite high, and many spots apparently contained multiple proteins, although some with very different scores. This may in some cases depend on their relative abundance: a major component has many peptides identified and a high score, while a trace component, e.g. minor streaking from adjacent spots, will have lower scores. In many cases it was not possible to identify a major component, and similar scores may indicate proteins that reside in the same area of the gel (similar charge and mass).

Identification was consistently better with Fser db, possibly indicating larger numbers of partial sequences in Fves db, a result supported by the larger size discrepancies of the Fves db sequences (Fig. 6.2). Most of the functional (bioinformatic) analyses were performed on hits from both Fser db and Fves db, yielding generally similar results.

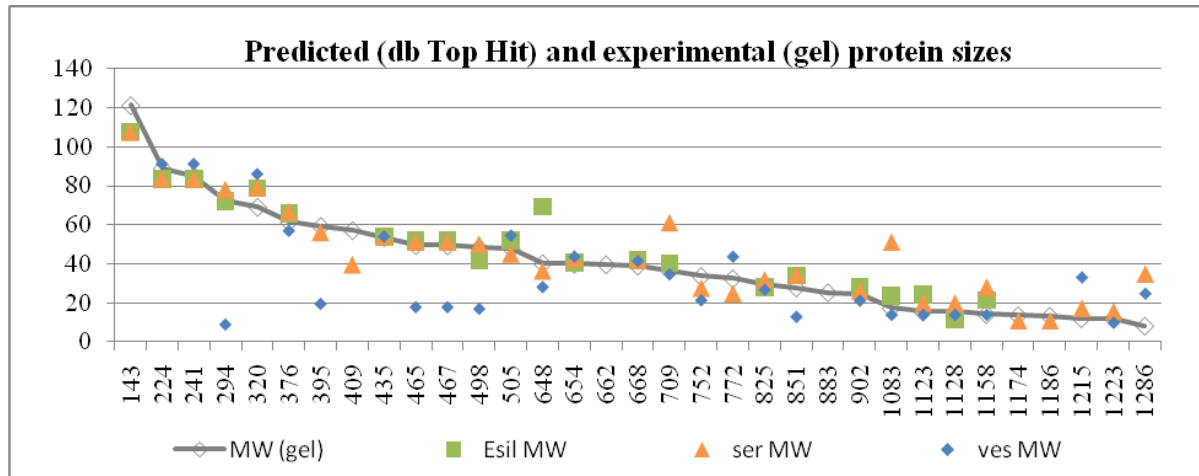


Figure 6.2 – Predicted size of the *F. serratus* proteins and their corresponding db sequences. The spot numbers (ordered from the top of the gel) are shown on the X-axis and the molecular weight (MW, in kDa) of the gel or Top-hit database proteins on the Y-axis. The plot illustrates the correspondence between the apparent size on the gel and the predicted size of the top hit sequence for each database. Note the most divergent blue symbols (Fves db) and two spots without db hits (662+883). *F. vesiculosus* protein spots presented similar trends (not shown).

Looking at some identified proteins from *F. serratus* (Tab. 6.5) we can illustrate some features of the data, like the wide range of PLGS scores and the large number of protein hits that some spots present. This may reflect identification of minor spot components, mostly streaking from adjacent spots.

Some proteins are present in several spots, like metE (involved in amino acid metabolism) in spots Rs224 and Rs241, upregulated in different conditions. PTMs may shift the protein's gel position and modify its activity, and could explain the contrasting regulation. It is also possible that the low score in spot Rs241 results from metE being a minor component of the spot, due to some streaking from nearby spots (like Rs224) and that the major component(s) have not been identified because corresponding sequences were missing from the databases used. A related metE sequence is present in the Esil db, but was not identified, instead both spots had a (very low score) hit to an aconitate hydratase (a similarly sized protein, that was identified in several nearby spots in the equivalent area of the Fves gel, sometimes accompanying metE), pointing to a role of streaking from adjacent spots in the identification

of additional proteins. The data available at this point does not permit the unambiguous identification of the major spot component and, as in any 2DE experiment, a minor component can be responsible for the expression changes detected, so caution must always be taken in the interpretation of protein identification data.

Looking at spot Rs409, not matched to any proteins in the Fves db or Esil db, it has a high score match to a Fser sequence that presents no similarity to any Fves or Esil protein, pfam or other conserved domain (in CDD database) and has weak similarities to a LEA protein. LEA proteins have low sequence conservation (low sequence complexity and repeat motifs), some of which may not be easily identifiable in evolutionary distant organisms. It may be a true LEA-like protein from *Fucus serratus* that is too divergent to be matched to Esil or other species, absent from *F. vesiculosus* or from the Fves db used.

Another common feature, as in spots Rs465 and Rs467, is the presence of a large number of protein hits in some spots. This also occurs in the Fves gel, in Rv465, Rv467 and other adjacent spots, and likely results from two effects: gel streaking and similar domains. The very sensitive nature of nanoUPLC-MSMS is well suited to detect minor components on a protein mixture, particularly on the crowded HMW region of the preparative gel, loaded with a large amount of protein. The identification of similar proteins, two ATPases (atpB chloroplast gene product and F-type H-ATPase beta subunit) and two EF Tu-like sequences (tufA chloroplast gene product) may result from their mixture in the gel spot or from misidentification, either by absence of the true sequence or by presence of duplicated sequences in the database. In this case both Fser db sequence pairs match one single Fves db sequence (by reciprocal Top Blast Hit), so additional analysis of the transcripts would be needed to clarify the source of the differences between the two (male and female) transcripts identified in Fser. In this case a much higher PLGS score indicates the likely major component (chloroplast atpB).

Table 6.5 – Annotation of *Fucus serratus* proteins from High and Low shore samples (Roscoff). Predicted MW of the RS# protein spot (gel) and the database protein (ser seq); PLGS score is the ProteinLynxGlobalServer identification score for the db sequence; description and KEGG annotation result from Blast and KAAS queries. Note that some spots have multiple hits.

Fser spot RS#	gel MW (Da)	spot abundance	ser seq MW (Da)	PLGS score	description (Top Blast Hit of Fser seq)	KEGG
143	121.300	ser >> ves	107.554	808	Glycine dehydrogenase (decarboxylating)	K00281
224	89.126	ves >> ser, low > High	83.606	2796	metE - homocysteine S-methyltransferase	K00549
241	85.202	ves >> ser, High >>low	83.606	274	metE - homocysteine S-methyltransferase	K00549
294	72.727	ser >> ves	78.268	1060	transketolase	K00615
			71.673	192	Molecular chaperones HSP70/HSC70	K03283
320	69.242	ser >> ves	79.176	8222	FtsH protease	K03798
376	61.515	ser >> ves	66.754	2727	chaperonin cpn60	K04077
395	59.394	ser >> ves	56.222	13258	protein disulfide isomerase	K09580
409	57.273	ser >> ves, High >>low	39.703	17967	no info (weak similarity to LEA proteins)	no info
435	53.788	ser >> ves	53.961	8767	atpA (chloroplast) [Fves]	K02111
			46.879	6852	enolase	K01689
			55.078	953	rbcl (chloroplast) [Fves]	K01601
465	49.658	ser >> ves	51.302	73021	atpB (chloroplast) [Fves]	K02112
			44.265	6684	tufA (chloroplast) [Fves]	K02358
			31.319	5109	tufA (chloroplast) [Fves]	K02358
			53.057	2962	F-type H-ATPase beta subunit	K02133
			45.908	844	eukaryotic initiation factor 4A	K03257
			47.564	454	argininosuccinate synthetase	K01940
			17.476	373	no info	no info
			46.394	350	S-Adenosyl-Methionine synthetase	K00789
50.234	328	Phosphoribulokinase	K00855			
467	49.486	ser >> ves	51.302	53970	atpB (chloroplast) [Fves]	K02112
			44.265	14850	tufA (chloroplast) [Fves]	K02358
			31.319	11952	tufA (chloroplast) [Fves]	K02358
			53.057	1782	F-type H-ATPase beta subunit	K02133
			42.973	1333	polyadenylate binding protein	no info
			54.264	808	Phosphoglycerate kinase	K00927
			50.234	777	Phosphoribulokinase	K00855
			45.908	629	eukaryotic initiation factor 4A	K03257
498	48.459	ser >> ves	50.234	3613	Phosphoribulokinase	K00855
			47.084	2691	acetylornithine deacetylase	K01438
			64.797	2665	actin	K05692
			60.082	620	conserved unknown protein	K01689
505	48.116	ser >> ves, High >>low	45.216	2894	Mitochondrial Processing Peptidase beta	K01412
			23.459	345	atpB (chloroplast) [Fves]	K02112
648	40.297	ser >> ves	36.583	3039	predicted protein [P. tricornutum].	K15306
			41.058	1995	Ran-binding protein 1	K15306

Fser spot RS#	gel MW (Da)	spot abundance	ser seq MW (Da)	PLGS score	description (Top Blast Hit of Fser seq)	KEGG
654	40.068	ser >> ves	42.863 37.179 41.695	11404 1080 614	GAPDH precursor GADPH Heat shock protein 40	K00134 K00134 K14002
668	39.155	ves >> ser, High >>low	41.924 34.929 40.665	7273 986 459	fructose-1,6-bisphosphate aldolase ATP synthase gamma chain enoyl-(acyl carrier protein) reductase	K01623 K02115 K00208
709	36.701	ser >> ves	61.253 28.402 40.317	9044 1215 305	sedoheptulose-bisphosphatase lysyl-tRNA ligase conserved unknown protein	K01100 K03232 no info
752	33.733	ser >> ves, High >>low	27.641 49.53	1224 782	esterase L-ascorbate peroxidase	K01070 K00434
772	32.591	ser >> ves, High >>low	24.892	468	expressed unknown protein	no info
825	29.338	ser >> ves	31.788	39749	14-3-3-like protein	K06630
851	27.911	ser >> ves	34.348 32.108 62.448	62958 481 188	oxygen-evolving enhancer protein 26S proteasome beta type 7 subunit conserved unknown protein	K02716 K02739 no info
902	24.526	ser >> ves, High >>low	26.234 31.720 31.788	1238 537 364	putative carbonic anhydrase Mg-protoporphyrin IX methyltransferase, chloroplast 14-3-3-like protein	K00680 K03428 K06630
1083	17.435	ser >> ves, low >>High	51.302	747	atpB (chloroplast) [Fves]	K02112
1123	15.539	ser >> ves	20.001 23.467 11.853	13900 653 558	light harvesting protein lhcf3 cytochrome b6-f complex iron-sulfur sub. no info	K08910 K02636 no info
1128	15.431	ser >> ves	20.001	1963	light harvesting protein lhcf3	K08910
1158	14.214	ser >> ves	28.192 20.001	18671 2280	Peroxyredoxin light harvesting protein lhcf3	K11187 K08910
1174	13.696	ves >> ser, High >>low	10.917	2962	petF (chloroplast) [Fves]	K02639
1186	13.375	ser >> ves, High >>low	10.917	1839	petF (chloroplast) [Fves]	K02639
1215	12.196	ser >> ves	17.225	8532	FKBP-type peptidyl-prolyl cis-trans isomerase 11 (PPIase)	K03773
1223	12.107	ves >> ser	15.653 20.001	15892 596	conserved unknown protein light harvesting protein lhcf3	K05765 K08910
1286	8.307	ser >> ves	34.971	385	glutaredoxin	K03676

Among the putative *F. serratus* High shore x Low shore differentially expressed spots retrieved from the gel and identified, one spot was more abundant in the Low shore samples (RS224 - metE). This metE protein involved in amino acid metabolism is present in spot RS241, more abundant in High shore samples. Either the mobility shift results from a Post-translational modification that modifies enzyme activity, explaining the opposite regulation, or metE is a minor component of Rs241 and another protein is present and upregulated in the High shore.

Another upregulated spot in the more stressful environment (High shore) is RS409 that may encode a LEA-like protein involved in desiccation tolerance (BLAST hit to “Late embryogenesis abundant protein D-29”, Glycine soja, gb|KHN03228.1, expect 2e-07). LEA proteins form a large family of intrinsically disordered proteins in aqueous state, abundant in water stressed plants and described in fungi, bacteria and desiccation-tolerant animals, thought to protect other proteins, membranes and organelles from aggregation and inactivation during desiccation or freezing. Dehydrins, one class of LEA-like proteins, may be constitutively present in Fucooids, where species and stage specific proteins that react to anti-dehydrin antibodies have already been described (Li et al, 1998).

Spots RS1174 and RS1186 both contain ferredoxin and are upregulated in High shore. Ferredoxin is a chloroplast protein that eliminates excess electrons from PSI thus reducing oxidative stress under physiological and stress conditions. In higher plants, ferredoxin cycles electrons from PSI to plastoquinone, in a mechanism that is upregulated in some forms of stress like drought stress (Lehtimäki *et al.* 2010), while ferredoxin transcripts have been found downregulated under drought, cold, or salt stress conditions in Arabidopsis (Noctor & Foyer, 1998). Other Fser spots upregulated in High shore (table 6.5) contain proteins involved in energy metabolism, mostly in photosynthesis and oxidative phosphorylation (ATPases beta and gamma).

Many of the Fser spots identified contain proteins involved in energy metabolism (32), carbohydrate (12), amino acid metabolism (7), folding, sorting and degradation (6), cell growth and death (2) or transport and catabolism (3) and some (24) have no pathway annotation in KEGG. This predominance of energy (298) and carbohydrate (340) metabolism (on a total of 1482 hits, including 165 without pathway annotation) is clear on the collective analysis of all the extractable spots (picked from the Rves gel). This abundance of identified

proteins involved in energy and carbohydrate metabolism may reflect a bias of the analysis method, because they are more abundant and/or more evolutionary conserved (see Tab. 6.6).

Table 6.6 – Pathway and superpathway representation of the total identified proteins. Total hits for all superpath categories, and pathway details for the two most abundant (carbohydrate and energy metabolism). NA (not annotated) includes proteins without KEGG or pathway annotation; some proteins have multiple pathway hits; Rser/Rves – Fser/Fves proteins from the High shore/ Low shore experiment at Roscoff; Vspir/Vves – Fspir/Fves proteins from the laboratory experiment (Viana do Castelo); all RV – total extractable proteome of *F. vesiculosus* (includes all the Rves proteins).

superpath/ paths (KEGG)	Rser	Rves	Vspir	Vves	all RV
Amino acid metabolism	7	6	7	4	54
Biosynthesis of other secondary metabolites	0	0	0	1	8
Cell growth and death	2	2	1	2	11
Cell motility	2	2	0	0	20
Folding, sorting and degradation	6	5	8	5	69
Lipid metabolism	1	2	0	4	23
Metabolism of cofactors and vitamins	2	1	2	5	25
Metabolism of other amino acids	3	6	0	1	16
Metabolism of terpenoids and polyketides	1	1	1	2	12
Nucleotide metabolism	0	2	0	4	6
Signal transduction	0	3	1	0	7
Transcription	1	1	4	2	22
Translation	2	2	0	2	28
Transport and catabolism	3	5	6	3	60
Carbohydrate metabolism	12	22	30	20	340
Ascorbate and aldarate metabolism	1	2	0	1	15
Amino sugar and nucleotide sugar metabolism	0	1	2	0	20
Glycolysis / Gluconeogenesis	6	6	7	7	112
Citrate cycle (TCA cycle)	0	3	3	0	24
Pentose phosphate pathway	2	3	1	3	34
Fructose and mannose metabolism	1	2	4	2	40
Inositol phosphate metabolism	0	0	3	2	15
Pyruvate metabolism	0	0	3	3	18
Glyoxylate and dicarboxylate metabolism	2	5	5	2	40
Propanoate metabolism	0	0	2	0	8
others	0	0	0	0	15
Energy metabolism	32	34	10	14	298
Carbon fixation in photosynthetic organisms	10	8	7	8	133
Oxidative phosphorylation	8	6	1	1	57
Photosynthesis	10	13	1	1	52
Photosynthesis - antenna proteins	0	1	0	0	2
Methane metabolism	4	3	1	2	33
Carbon fixation pathways in prokaryotes	0	3	0	1	6
Nitrogen metabolism	0	0	0	1	12
Sulfur metabolism	0	0	0	0	3
Others	0	0	0	0	4
NA	24	20	10	16	165

Many primary metabolism proteins are abundantly expressed and well conserved, which may facilitate their identification and functional annotation, even if they are not major components of the spot. The high number of KEGG hits (1482, corresponding to 655 protein hits) on only 336 spots analysed shows pathway redundancy, as many enzymes act on multiple pathways, but is also influenced by the repeated identification of proteins that streak into adjacent spots. As could be expected from their relative metabolic importance, sequence conservation and cellular abundance, photosynthesis, carbon and energy metabolism proteins appear to be over-represented in these samples.

Laboratory desiccation with related species

Laboratory desiccation/rehydration experiments were performed with four species but proteomic profiles were only compared between the closely related *F. spiralis* and *F. vesiculosus*, after 2h of recovery from a 3h desiccation treatment (to about 10% TWC) and in non-desiccated controls (n=4). These controlled experiments in climatic chambers decrease the variation from other environmental parameters (temperature, light level, wind) and use isolated tips that should desiccate at very similar rates after the initial removal of outside moisture by gentle blotting. Any differences between the treatments should result therefore from desiccation or rehydration effects.

After 2DE-DIGE the gel images (8 gels) were aligned and the final set of 1385 spots analysed using different experimental designs. As expected, no significant changes were detected between treatments (Control x Recovery) in *F. spiralis* (Tab. 6.7), in *F. vesiculosus* (Tab. 6.8), or both (Tab. 6.9), and few spots changed noticeably even before FDR correction.

Comparing the proteomic profiles of both species (*F. spiralis* x *F. vesiculosus*, n=8) significant changes (after multiple test correction, FDR) were detected on 396 of a total of 1385 spots (28.6%), of which 247 have fold-change >1.5. Similar results were found using a for groups design (*F. spiralis* Control x *F. serratus* Recovery x *F. vesiculosus* Control x *F. vesiculosus* Recovery, n=4, similar top hits and 355 spots with ANOVA p<0.05), but only 207 were considered true discoveries, probably because of fewer replicates. A small set of (easy to pick) spots that differ between species, 31 from Fves and 27 from Fspir, were identified by MSMS as described. Again, annotation success was highest using the Fser db, despite *F. spiralis* being more closely related to Fves. Of 31 Fves spots, two (Vv1792 + Vv1885) could not be annotated to any db, a Rubisco small subunit was only identified in

Fves db, and 28 were matched to Fser db, 25 to Fves db and 17 to Esil db. Similarly two Fspir spots (Vsp1885+ Vsp2239) had no hits, 25 matched Fser db sequences, 23 Fves db and 22 Esil db. Again many spots presented multiple protein hits in all databases and most hits were to proteins involved in carbohydrate and energy metabolism (Tab. 6.6).

Several hits are to conserved proteins of unknown function (Vsp1493-1726-2238), reflecting the still limited levels of functional information on *Ectocarpus*, and brown algal proteins in general. Other spots that may contain novel proteins of interest are those not matching any available database sequences (like 1885, no hits from the *F. spiralis* or the *F. vesiculosus* spots), or those having only low score hits to abundant proteins (present in nearby spots with high scores, that are likely minor components of the spot).

Table 6.7 – Protein changes between Control and Recovery samples in *Fucus spiralis* (n=4). Table of 8 spots showing the largest changes in expression during recovery from desiccation (ANOVA<p 0.05, fold-change >1.5), false discoveries (FDR tests).

spot Vsp#	Anova (p)	Fold	q Value	Power	Highest Mean	FDR test
2887	0.00468	2.3	0.56389	0.95094	Fspir Recovery	False
2173	0.00489	1.6	0.56389	0.94758	Fspir Control	False
1998	0.02491	1.7	0.56389	0.69869	Fspir Control	False
1863	0.02537	1.5	0.56389	0.69465	Fspir Control	False
1948	0.03520	1.5	0.56389	0.62002	Fspir Control	False
2259	0.03539	1.5	0.56389	0.61874	Fspir Control	False
1221	0.03777	2.3	0.56389	0.60348	Fspir Control	False
1933	0.04627	1.9	0.56389	0.55513	Fspir Control	False

Table 6.8 – Protein changes between Control and Recovery samples in *Fucus vesiculosus* (n=4). Table of 4 spots showing the largest changes in expression during recovery from desiccation (ANOVA<p 0.05, fold-change>1.5), false discoveries (FDR tests).

spot Vv#	Anova (p)	Fold	q Value	Power	Highest Mean	FDR test
2475	0.01424	1.7	0.56306	0.8106	Fves Recovery	False
2412	0.01725	1.5	0.56306	0.77491	Fves Control	False
2436	0.0408	2.1	0.56306	0.58514	Fves Control	False
1338	0.05009	1.8	0.56306	0.53608	Fves Control	False

Table 6.9 – Protein changes between Control and Recovery samples (mixed species, n=8). Table of 12 spots showing (non-significant) changes in expression during recovery from desiccation (all ANOVA <math>p < 0.05</math>) in *F. spiralis* + *F. vesiculosus*.

spot V#	Anova (p)	Fold	q Value	Power	Highest Mean	FDR test
187	0.00658	1.2	0.708555	0.842061	Control	False
1834	0.015109	1.2	0.708555	0.730505	Recovery	False
2157	0.024395	1.2	0.708555	0.650598	Control	False
963	0.027974	1.1	0.708555	0.625965	Recovery	False
2436	0.035268	1.5	0.708555	0.582748	Control	False
1877	0.036462	1.3	0.708555	0.576402	Recovery	False
1198	0.041619	1.2	0.708555	0.55086	Control	False
2091	0.041877	1.2	0.708555	0.549659	Recovery	False
1041	0.044831	1.2	0.708555	0.536319	Control	False
470	0.045632	1.5	0.708555	0.532833	Control	False
1200	0.04636	1.6	0.708555	0.529717	Recovery	False
2412	0.046802	1.3	0.708555	0.527843	Control	False

Looking at the five spots containing HSP70 chaperones (761, 765 and 774), one was retrieved just from Fspir (Vsp761 was 1.9-fold upregulated in *F. spiralis*), while the others were picked from both species, and presented similar hits and scores: several HSP70/DnaK proteins were identified, and traces of transketolase (low scores) in some spots. Yet 765 was upregulated in Fves and 774 in Fspir. Are we seeing related proteins with different relative abundances in these species, or a single protein that is differentially regulated by PTMs in Fspir, shifting its position and changing the relative abundances of the spots? Using the Esil db, two HSP70 superfamily members have very similar scores and could be equally similar to the *F. spiralis* protein present in spots 761 and 774, like the single related sequence from Fser db. Without a species-specific database it is not possible to identify specific isoforms, making it harder to interpret such profile shifts. Interestingly, the highest scores come from the Fves db (not shown), for a protein sequence that has <math>< 70\%</math> identity (BLASTp) to other brown algae HSP70s, including Fser sequences and <math>< 50\%</math> identity to dnaK (Fves). Given the high sequence conservation in the HSP70 family, this sequence may represent a novel isoform, with a specific role in the higher shore, more desiccation-tolerant species.

Table 6.10 – Annotations of *Fucus spiralis* proteins from laboratory desiccation. Annotation from the Esil db; description and KEGG annotation from Blastp and KAAS queries of Fser sequences; PLGS - ProteinLynxGlobalServer (identification score).

spot Vsp#	Esil hit annotation	Esil PLGS score	Fser hit (Blastp_nr) description	Fser PLGS score	Fser KEGG no
761	HSP70 HSC70 HSP70 superfamily	4357	HSP70/HSC70, HSP70 superfamily	5631	K03283
	HSP70 HSC70 HSP70 superfamily	4252	dnaK (chloroplast) [Fves].	1240	K04043
	Chaperone protein DnaK	418	Heat shock protein 70	298	K04043
	Heat shock protein 70	62	transketolase	182	K00615
765	HSP70 HSC70 HSP70 superfamily	2034	HSP70/HSC70, HSP70 superfamily	3118	K03283
	Heat shock protein 70	95	Heat shock protein 70	472	K04043
	Heat shock protein 70	95	transketolase	59	K00615
774	HSP70 HSC70 HSP70 superfamily	2695	HSP70/HSC70, HSP70 superfamily	3874	K03283
	HSP70 HSC70 HSP70 superfamily	2656	Heat shock protein 70	692	K04043
	Heat shock protein 70	373	dnaK (chloroplast) [Fves].	169	K04043
941	Dihydrolipoyl dehydrogenase	250	dihydrolipoamide dehydrogenase	643	K00382
	Dihydrolipoyl dehydrogenase	250	phosphoenolpyruvate carboxykinase (ATP)	292	K01610
949	Dihydrolipoyl dehydrogenase	1351	dihydrolipoamide dehydrogenase	3881	K00382
	Dihydrolipoyl dehydrogenase	1351	phosphoenolpyruvate carboxykinase (ATP)	434	K01610
1281	No Hit		Aminomethyltransferase	508	K00605
1360	Aspartyl protease	378	tagatose-6-phosphate kinase-like protein	775	K00917
	Aspartyl protease	378	aspartyl protease	980	K01379
1493	Uncharacterized protein	467	na	13191	na
	Uncharacterized protein	467	Uncharacterized protein	9821	K13158
	Uncharacterized protein	467	conserved unknown protein	201	K12450
1726	Putative uncharacterized protein	601	expressed unknown protein	8634	na
1803	14 3 3 like protein	20941	14-3-3-like protein	29565	K06630
1822	Putative uncharacterized protein	2908	conserved unknown protein	4532	K01834
1885	No Hit		No Hit		
1920	Putative uncharacterized protein	8881	conserved unknown protein	14062	K02726
	Putative uncharacterized protein	8881	conserved unknown protein	358	K01840
1971	Triosephosphate isomerase	365	Triosephosphate isomerase	2545	K01803
1972	Triosephosphate isomerase	441	Triosephosphate isomerase	3505	K01803

spot Vsp#	Esil hit annotation	Esil PLGS score	Fser hit (Blastp_nr) description	Fser PLGS score	Fser KEGG no
1982	Putative uncharacterized protein	685	conserved unknown protein	2555	K01423
	Putative uncharacterized protein	509	conserved unknown protein	675	K03626
1990	Triosephosphate isomerase	321	Triosephosphate isomerase	2484	K01803
			conserved unknown protein	643	K08683
			delta-1-pyrroline-5-carboxylate reductase	141	K00286
2002	Putative uncharacterized protein	421	FKBP-type peptidyl-prolyl cis-trans isomerase 5	3064	K03773
			conserved unknown protein	424	K03626
2008	No Hit		FKBP-type peptidyl-prolyl cis-trans isomerase 5	7344	K03773
2238	No Hit		expressed unknown protein	1162	na
2277	Light harvesting complex protein	1812	light harvesting protein lhcf3	1326	K08910
2575	Cytochrome c 550	8855	psbV (chloroplast) [Fves].	24353	K02720
3001	Peroxyredoxin	5966	Peroxyredoxin	2512	K11187
3002	Peroxyredoxin	4732	Peroxyredoxin	2340	K11187
			NADH dehydrogenase (ubiquinone)	998	K03949
3003	Putative uncharacterized protein	268	rbcS (chloroplast) [Fves]	23754	K01602
3004	Putative uncharacterized protein	358	rbcS (chloroplast) [Fves]	24454	K01602
			NAD synthase (glutamine-hydrolyzing)	422	K01950
			conserved unknown protein	155	na
s2239	No Hit		No Hit		

The proteome of *F. vesiculosus*

The extractable proteome of *F. vesiculosus* (340 protein spots, Tab. 6.6) allowed identification of a large number of proteins. Unfortunately most of the identified proteins are involved in a limited number of pathways (energy and carbohydrate metabolism, Tables 6.6, 6.11), revealing a bias for the identification of a particular set of proteins. This bias does not stem from the database used, since some pathways that are well represented in the transcript data (like translation, folding, replication, amino acid metabolism) are underrepresented in the gel data. There is also much redundancy in this dataset because many proteins are identified in many spots, often because of streaking but also likely due to isoforms or PTMs.

Table 6.11 –KEGG pathway hits from the proteome and the transcriptome of *Fucus*. Fser DB – total KAAS hits from the whole database (Fser transcriptome); gel_redund - data from 1584 total hits from 304 gel spots to Fser DB (270 unique orfs, 131 unique KEGGs); gel_nr - (non-redundant) data from 1584 total hits, removed repeat KEGGs if on the same spot and repeat sequences (orf) on different spots, (267 unique orfs, 181 spots, 131 unique KEGGs).

	gel_redund	gel_nr	Fser DB
Amino acid metabolism	54	28	442
Biosynthesis of other secondary metabolites	8	4	87
Carbohydrate metabolism	339	102	742
Cell growth and death	10	5	243
Cell motility	23	6	88
Energy metabolism	297	66	396
Environmental adaptation	3	2	58
Folding, sorting and degradation	69	28	564
Glycan biosynthesis and metabolism	0	0	170
Lipid metabolism	23	11	302
Membrane transport	0	0	62
Metabolism of cofactors and vitamins	24	13	255
Metabolism of other amino acids	16	6	120
Metabolism of terpenoids and polyketides	12	3	70
Nucleotide metabolism	6	6	337
Replication and repair	0	0	351
Signal transduction (merged)	113	25	691
Transcription	22	5	275
Translation	28	12	637
Transport and catabolism	60	18	438
Xenobiotics biodegradation and metabolism	1	1	84

It is also possible that the high number of non-annotated proteins (not similar to any KEGG entries, thus lacking functional pathway information) includes many other pathway members that could not be identified due to lower sequence conservation, but these sequences would also be missing from the database analysis. Bias can also occur on the transcriptomic data, like the general abundance of ribosomal transcripts that impact the Translation category.

Given the verified high sensitivity of the method chosen for protein identification, loading lower amounts of protein in the gels might have improved results by minimizing contamination from adjacent spots. Still the observed predominance of (presumably very abundant) primary metabolism proteins, from carbon metabolism, biosynthesis of amino acids, carbon fixation and glycolysis/ gluconeogenesis, may have prevented the detection of expression changes in less abundant proteins that overlap in the gels.

From the data available, *Fucus* does not seem to strongly regulate pathway activity during emersion by changes in the protein levels of intermediary enzymes. Protein levels appear quite stable during desiccation-rehydration cycles.

6.4 – Discussion

In order to identify molecular markers associated with desiccation-rehydration, not previously identified in transcriptomic or proteomic analysis of furoid brown algae, differential protein expression was examined using 2DE-DIGE separation, image analysis and LC-MS/MS protein identification using a database from the model alga *E. siliculosus* and two NGS-derived *F. serratus* and *F. vesiculosus* protein databases. Two experimental desiccation setups were used, simultaneously comparing the responses of two species: field sampling at contrasting desiccation environments (High and Low shore) for proteomic changes resulting from long-term acclimation; and short-term laboratory desiccation in controlled conditions (2h Recovery and Controls) to detect immediate effects and repair mechanisms but also to minimize environmental variation when comparing the two species. With over 1000 spots examined per gel, no significantly differentially expressed proteins could be identified between desiccation treatments (except four small spots that differed between High and Low shore but could not be retrieved from the gel for identification). Lack of detectable differences using this sensitive DIGE analysis points to the strong constitutive nature of desiccation tolerance in *Fucus* species.

Intertidal algae face frequent desiccation-rehydration cycles, in contrast to the seasonal desiccation experienced by some plants and animals that require slow desiccation and an extended recovery period to repair cellular damage. It can be difficult to relate slow- or fast-desiccation with metabolic changes, not only because of the wide variety of organisms and desiccation mechanisms but because of lack of consistent protocols and terminology. Fast desiccation can describe cessation of visible metabolism in under one hour (alga, Gasulla et al, 2013) or in around 20 hours for a resurrection plant (Cooper & Farrant, 2002). Comparing slow-drying of 8 days (Cooper & Farrant, 2002) or 5-6 hours (Gasulla et al, 2013) shows the differences between algae and vascular plants, with impermeable cuticles that retard water loss and where “fast” reconstitution of photosynthetic capacity takes several hours. Resurrection plants typically dry over several days or weeks, some disassemble their chloroplast structure and require considerable reassembly and repair upon rehydration, so there is an important role of new transcription and protein synthesis during desiccation.

Intertidal algae and other poikylhydric organisms that desiccate quickly in dry air cannot afford to rely in lengthy induction of desiccation-tolerance, and may rely on constitutive expression of many protective mechanisms to insure survival in adverse environments.

Intertidal *Fucus* usually experience tidal emersion cycles every 12 hours, can dry to under 10% TWC in less than an hour and regain photosynthetic activity within minutes of rehydration, with complete recovery in a few hours. Such swift, potentially frequent and unpredictable desiccation cannot entirely rely on new protein synthesis, and constitutive expression of desiccation-tolerance is supported by the experimental data.

Constitutive markers of desiccation tolerance are hard to detect comparing the profiles of tolerant and sensitive (related) species. Between the well-differentiated species *F. serratus* and *F. vesiculosus*, many spots were significantly changed (56% or 62%, depending on experimental design for image analysis). In the more-closely related species (*F. spiralis* x *F. vesiculosus*) only 29% or 15% of the 1385 spots were significantly changed, but even here most of the differences are probably not related to desiccation-tolerance, including neutral mutations and selection for other functional traits. With over 200 spots changed per species, identifying all the different proteins to later elucidate which might be involved in constitutive desiccation-tolerance would be counterproductive. Despite good annotation rates with the transcriptomic-derived protein databases, a strong bias towards identification of carbon and energy metabolism proteins was detected, that might preclude the identification of other classes of responsive proteins, like membrane transport, replication or repair, biosynthesis of other secondary metabolites or protein processing and degradation.

Nevertheless an induction of antioxidant enzymes and other antioxidant protective molecules in result of desiccation stress has been detected in several intertidal algae (reviewed in Contreras-Porcia & López-Cristoffanini, 2012), and a recent study in the red alga *Pyropia orbicularis* by 2DE and LC-MS/MS (López-Cristoffanini et al. 2015) also detected significant changes in the protein profile under desiccation conditions during low tide. A large number (111) of protein spots were upregulated in naturally desiccated tissue. Half the identified proteins were involved in energy and biomolecule metabolism, and a quarter in antioxidant and defense functions, including chaperones, monodehydroascorbate reductase, manganese superoxide dismutase, phycobiliproteins, and phosphomannomutase. These results in *Pyropia orbicularis* indicate decreased photosynthetic activity and increased antioxidant capacity during low tide, similarly to desiccated resurrection plants and bryophytes.

Given the frequent identification of multiple proteins in a spot and the low scores of many hits it is tempting to believe that some differential expression between High and Low shore samples may be due to novel proteins that were absent from the databases used. Despite it,

we can try to compare some proteins identified in desiccated *Pyropia*: aconitase hydratase increased in *Pyropia* and was identified as a possible minor component, with metE, of Low shore upregulated spots in Fves. Even if this protein is responsible for the differential expression, it would be induced in *Pyropia* and reduced in more exposed *Fucus*. Also SAM synthetase (another enzyme of met recycling) increased in *Pyropia*, but not *Fucus* being more abundant in the lower shore species, like the chaperonine 60, a peptidylprolylisomerase and an oxygen-evolving enhancer protein. This does not seem plausible and other yet unidentified proteins maybe responsible for the differential expression in desiccation.

Recent proteomic profiling of brown algae *Sargassum fusiforme* responding to hyposalinity stress (Qian et al. 2016) identified several ATPases with opposite regulation, identified to the same NCBI accession, with different scores. In one case a 40 kDa protein was hypothesised to be a degradation product of the 80 kDa vacuolar ATP synthase protein, or a regulated truncated variant similar to the *F. vesiculosus* ~70 kDa VHA-A protein and its truncated ~30 kDa variant (Morris et al., 2014). Several proteins were identified from multiple spots, in some cases with low scores (low coverage and few sequenced peptides). Future improvements in brown algal protein databases might allow identification of novel proteins, not present in other organisms and involved in intertidal stress tolerance mechanisms.

Future studies are required to confirm the constitutive nature of desiccation-tolerance in *Fucus* algae, or (and) identify some emersion regulated proteins, with particular focus on those involved in antioxidant defense. These would benefit from reduced gel streaking (avoiding overloading), additional replication, including the use of large pools of individuals per each sample, higher resolution (narrower pH and MW intervals focusing on protein subsets) and also the role of PTMs should be directly addressed, as advances in phosphoprotein detection may reveal changes in phosphorylation status during the tidal cycle.

To improve our ability to detect constitutively expressed proteins involved in desiccation-rehydration tolerance, the use of selected ecotypes (of the same species) with different desiccation-tolerances might reduce the number of candidates relatively to the currently described approach of comparing related species.

6.5 - References

- Battaglia, M., Olvera-Carrillo, Y., Garcarrubio, A., Campos, F., and Covarrubias, A. A. (2008). The enigmatic LEA proteins and other hydrophilins. *Plant Physiol.* 148, 6–24.
- Benjamini, Y. & Hochberg, Y. (1995). “Controlling the false discovery rate: a practical and powerful approach to multiple testing,” *Journal of the Royal Statistical Society, Series B (Methodological)*, 57 (1): 289-300.
- Cánovas, F.G., Mota, C.F., Serrão, E.A. & Pearson, G.A. (2011). Driving south: a multi-gene phylogeny of the brown algal family Fucaceae reveals relationships and recent drivers of a marine radiation. *BMC Evolutionary Biology*, 11: 371.
- Charron, A. J. & Quatrano R.A. (2009). Between a rock and a dry place: the water-stressed moss. *Molecular Plant*, 2 (3): 478 – 486.
- Cock, J. M., Sterck, L., Rouzé, P., Scornet, D., Allen, A. E., Amoutzias, G., ... & Beszteri, B. (2010). The *Ectocarpus* genome and the independent evolution of multicellularity in brown algae. *Nature*, 465 (7298), 617-621.
- Contreras, L., Moenne, A., Gaillard, F., Potin, P., & Correa, J. A. (2010). Proteomic analysis and identification of copper stress-regulated proteins in the marine alga *Scytosiphon gracilis* (Phaeophyceae). *Aquatic Toxicology*, 96 (2), 85-89.
- Contreras, L., Ritter, A., Dennett, G., Boehmwald, F., Guitton, N., Pineau, C., ... & Correa, J. A. (2008). Two-dimensional gel electrophoresis analysis of brown algal protein extracts. *Journal of Phycology*, 44(5), 1315-1321.
- Contreras-Porcía, L., & López-Cristoffanini, C. (2012). *Proteomics in seaweeds: Ecological interpretations*. INTECH Open Access Publisher.
- Cooper, K., & Farrant, J. M. (2002). Recovery of the resurrection plant *Craterostigma wilmsii* from desiccation: protection versus repair. *Journal of Experimental Botany*, 53 (375), 1805-1813.
- Coyer, J.A., Hoarau, G., Oudot-Le Secq, M.P., Stam, W.T. & Olsen, J.L. (2006). A mtDNA-based phylogeny of the brown algal genus *Fucus* (Heterokontophyta; Phaeophyta). *Molecular Phylogenetics and Evolution*, 39: 209–222.
- Davison, I.R. & Pearson, G.A. (1996). Stress tolerance in intertidal seaweeds. *Journal of Phycology*, 32, 197-211.
- Dinakar, C. & Bartels, D. (2013) Desiccation tolerance in resurrection plants: new insights from transcriptome, proteome, and metabolome analysis. *Frontiers in Plant Science*. 4:482.
- Dring MJ & Brown FA (1982). Photosynthesis of intertidal brown algae during and after periods of emersion: A renewed search for physiological causes of zonation. *Marine Ecology Progress Series*, 8, 301-308.
- Fu, G., Nagasato, C., Oka, S., Cock, J. M., & Motomura, T. (2014). Proteomics analysis of heterogeneous flagella in brown algae (Stramenopiles). *Protist*, 165 (5), 662-675.
- Gasulla, F., Jain, R., Barreno, E., Guera, A., Balbuena, T. S., Thelen, J. J., & Oliver, M. J. (2013). The response of *Asterochloris erici* (Ahmadjian) Skaloud et Peksa to desiccation: a proteomic approach. *Plant, cell & environment*, 36 (7), 1363-1378.

- Graether, S.P. & Boddington, K.F. (2014.) Disorder and function: a review of the dehydrin protein family. *Frontiers in Plant Science*, 5:576.
- Holzinger, A., Kaplan, F., Blaas, K., Zechmann, B., Komsic-Buchmann, K., et al. (2014) Transcriptomics of desiccation tolerance in the streptophyte green alga *Klebsormidium* reveal a land plant-like defense reaction. *PLoS ONE* 9 (10): e110630.
- Lehtimäki, N., Lintala, M., Allahverdiyeva, Y., Aro, E. M., & Mulo, P. (2010). Drought stress-induced upregulation of components involved in ferredoxin-dependent cyclic electron transfer. *Journal of plant physiology*, 167 (12), 1018-1022.
- Li, R., Brawley, S.H. & Close, T.J. (1998). Proteins immunologically related to dehydrins in fucoid algae. *Journal of phycology* 34.4: 642-650.
- López-Cristoffanini, C., Zapata, J., Gaillard, F., Potin, P., Correa, J. A. & Contreras-Porcia, L. (2015). Identification of proteins involved in desiccation tolerance in the red seaweed *Pyropia orbicularis* (Rhodophyta, Bangiales). *Proteomics*, 15: 3954–3968.
- Noctor, G., & Foyer, C. H. (1998). Ascorbate and glutathione: keeping active oxygen under control. *Annual review of plant biology*, 49(1), 249-279.
- O'Farrell, P. H. (1975). High resolution two-dimensional electrophoresis of proteins. *Journal of biological chemistry*, 250(10), 4007-4021.
- Oliver, M.J., Velten, J. & Mishler, B.D. (2005). Desiccation tolerance in bryophytes: a reflection of the primitive strategy for plant survival in dehydrating habitats ? *Integrative and Comparative Biology*; 45 (5): 788-799.
- Pearson, G. A., Hoarau, G., Lago-Leston, A., Coyer, J. A., Kube, M., Reinhardt, R., ... & Olsen, J. L. (2010). An expressed sequence tag analysis of the intertidal brown seaweeds *Fucus serratus* (L.) and *F. vesiculosus* (L.) (Heterokontophyta, Phaeophyceae) in response to abiotic stressors. *Marine Biotechnology*, 12(2), 195-213.
- Proctor, M.C.F. & Pence, V.C. (2002). Vegetative tissues: bryophytes, vascular resurrection plants and vegetative propagules. In: Black M, Pritchard HW (eds) *Desiccation and survival in plants: drying without dying*. CABI, Wallingford, pp 207.
- Qian, W-G, Li, N., Lin, L-D., Xu, T., Zhang, X. Wang, L-H, et al. (2016). Parallel analysis of proteins in brown seaweed *Sargassum fusiforme* responding to hyposalinity stress, *Aquaculture*, 465, 189-197.
- Rebecchi L., Altiero, T. and Guidetti, R. (2007). Anhydrobiosis: the extreme limit of desiccation tolerance. *Invertebrate Survival J.* 4, 65-81
- Ritter, A., Ubertini, M., Romac, S., Gaillard, F., Delage, L., Mann, A., ... & Potin, P. (2010). Copper stress proteomics highlights local adaptation of two strains of the model brown alga *Ectocarpus siliculosus*. *Proteomics*, 10(11), 2074-2088.
- from nrDNA-ITS. *Journal of Phycology*, 35: 382–394.
- Serrão, E.A., Alice, L.A. & Brawley, S.H. (1999). Evolution of the Fucaceae (Phaeophyceae) inferred
- Silberfeld, T., Leigh, J. W., Verbruggen, H., Cruaud, C., De Reviers, B., & Rousseau, F. (2010). A multi-locus time-calibrated phylogeny of the brown algae (Heterokonta, Ochrophyta, Phaeophyceae): Investigating the evolutionary nature of the “brown algal crown radiation”. *Molecular phylogenetics and evolution*, 56(2), 659-674.

- Ünlü, M., Morgan, M. E. and Minden, J. S. (1997), Difference gel electrophoresis. A single gel method for detecting changes in protein extracts. *Electrophoresis*, 18: 2071–2077.
- Valledor L., Jorrín J. (2011). Back to the basics: maximizing the information obtained by quantitative two dimensional gel electrophoresis analyses by an appropriate experimental design and statistical analyses. *J. Proteomics* 74, 1–18.
- Yotsukura, N., Nagai, K., Kimura, H., & Morimoto, K. (2010). Seasonal changes in proteomic profiles of Japanese kelp: *Saccharina japonica* (Laminariales, Phaeophyceae). *Journal of applied phycology*, 22(4), 443-451.
- Yotsukura, N., Nagai, K., Tanaka, T., Kimura, H., & Morimoto, K. (2012). Temperature stress-induced changes in the proteomic profiles of *Ecklonia cava* (Laminariales, Phaeophyceae). *Journal of applied phycology*, 24(2), 163-171.

6.6 – Acknowledgements

I would like to thank the help of Denise Schrama and Dr. Pedro Rodrigues from Aquagroup at CCMAR, for assistance and use of their equipment for DIGE and Tune Wulff, at the DTU Proteomics Core, Technical University of Denmark for protein identification (LC-MS/MS).

This study was supported by projects UID/Multi/04326/2013, EXCL/AAG-GLO/0661/2012 and fellowship SFRH/BD/74436/2010 of the Portuguese Science Foundation (FCT).

Supporting information

Supporting information to this chapter can be found on the Appendix (digital version)

Table S6.1 – Identification of *Fucus vesiculosus* proteins from High and Low shore (Roscoff).

Table S6.2 – Identification of *Fucus serratus* proteins from High and Low shore (Roscoff).

Table S6.3 – Identification of *Fucus vesiculosus* proteins from Control and Recovery (VC).

Table S6.4 – Identification of *Fucus spiralis* proteins from Control and Recovery (VC).

Chapter 7

Final conclusions and future directions

Chapter 7 – Final conclusions and future directions

7.1 – Global overview

The distribution of intertidal species is controlled by both biotic and abiotic factors, demographic history and dispersal, and no simple model is applicable to all species, or even to all populations within one species. Chapter 2 describes how different populations from a species can have distinct thermal stress responses on northern (trailing) and southern (rear) edges. Such variation in stress resilience, whether due to local adaptation or genetic drift, will impact responses to climate changes and must be taken into account for accurate modelling of distribution shifts. To predict critical points for population persistence or colonization both stress intensities and resilience (temperature shifts and thermal limits, when temperature is the controlling factor) are required. Distinct thermal stress responses were detected between the two distributional edges that have large environmental differences, for the intertidal species *F. vesiculosus* and the subtidal *Z. marina*. *F. vesiculosus* was impacted at water temperatures (28 - 32°C) unlikely to be reached in seawater, but possible in shallow waters on southern edges or during aerial emersion at low tide. *Z. marina* was slightly less impacted on the southern edge.

Chapter 3 similarly determines thermal limits in another southern edge population of *F. vesiculosus* but compares the heat stress response *in situ* and in laboratory conditions. The stress response reflects the microhabitat temperatures, while meteorological data does not accurately represent the conditions experienced by intertidal organisms, since local features and algal canopies create particular microhabitats where temperatures can diverge considerably. Desiccation may be a protective mechanism, as swift and intense desiccation on the most thermally stressful microhabitat suppressed the stress response. To further explore the impacts of desiccation on resilience and population persistence it is important to understand the metabolic costs of desiccation and its limits. Molecular markers for

desiccation stress in *Fucus* would facilitate measuring its impact but could not be identified in EST libraries.

New methods were optimized to investigate changes in protein expression in these brown algae, for future discovery of desiccation markers and of the processes involved in desiccation tolerance. Chapter 4 describes the development of a protein extraction method for *Fucus* algae, to search for differentially expressed desiccation-related proteins. Furoid brown algae contain abundant secondary metabolites that can precipitate proteins and interfere with subsequent analysis. The optimized protocol produced protein extracts suitable for reproducible 2DE separation, but no significant protein expression changes were detected with this method after intense desiccation and 1h of rehydration in the field, maybe due to low detection power (few replicates and large variation between samples) or to the constitutive nature of desiccation tolerance in *Fucus*.

Another open question from chapter 3 was the cumulative impact of sequential sub-lethal stress exposures, to high temperature and to desiccation. Chapter 5 addresses this question, by examining the physiological impact on photosynthesis of different levels of desiccation during sequential days of daytime emersion. By contrasting desiccation intensity, temperature and physiological impact across two canopy microhabitats during several days, a clear effect of microhabitat was detected. The Top of the canopy presented intense desiccation, higher tissue temperatures and more photodamage than the canopy Bottom, demonstrating the importance of canopy microhabitat. Large daily variation in multiple conditions (temperature, light, rain, etc) affect the physiological impact (hydration status and photodamage) on similar tips, but under the mild conditions examined no cumulative effects were apparent. To examine the impact of this cumulative stress on protein expression, these contrasting microhabitats were compared after five days of exposure, using a more sensitive method (DIGE) and additional replicates. Again no significant changes were detected, pointing to constitutive protection mechanisms.

To confirm the constitutive nature of desiccation-protection mechanisms, two other setups were examined in Chapter 6. To exclude any effects of previous acclimation, that the short exposure period could not eliminate, samples that had life-long exposure to desiccating conditions (High shore site of frequent and intense desiccation) were compared to those kept hydrated during most tidal cycles (Low shore site). Four putatively regulated proteins could not be identified, but other spots (marginally significant, $p < 0.05$) were identified from two

Fucus species. Another approach to minimise the effect of natural environmental variability between replicates, desiccation in laboratory controlled conditions, compared *F. vesiculosus* and *F. spiralis*. Proteomic profiles during recovery from desiccation were undistinguishable from those of hydrated controls for both species, and were pooled to compare the two species. Between the closely related *F. vesiculosus* and *F. spiralis*, 18% of the total spots changed over 1.5-fold, compared to 62% between *F. vesiculosus* and *F. serratus*.

In order to obtain functional information about the expressed proteins some spots were identified by LC-MS/MS and compared with the total extractable proteome. Most proteins were involved in carbohydrate and energy metabolism, and several in amino acid metabolism, folding, sorting and degradation, and signal transduction. Despite the large identification success allowed by LC-MS/MS, some of the identified proteins may not be those responsible for the differential expression detected, as many minor spot components are often identified and protein databases for *Fucus* species are still far from complete.

7.2 – Conclusions

Stress tolerance studies require a measure of the detrimental impact of the environmental factor (stress) that is not necessarily the same for different species or individuals. In *F. vesiculosus*, populations from the distributional edges (Greenland and Portugal) present very distinct thermal tolerances, unlike the populations of *Zostera marina*. To accurately determine thermal stress a measure of the damage is required, since temperature impacts will depend on the species, genetic background, life stage, nutritional status, among others.

The use of molecular markers allows the analysis of a large number of field-collected samples and the determination of some forms of stress. Lack of molecular markers responsive to desiccation stress prevents the evaluation of its impact in *Fucus* populations.

The algal canopy modulates environmental stress, creating microhabitats exposed to particular temperature and desiccation conditions that impact population growth and survival. The Top of the algal canopy is a thermally stressful microhabitat where some tissues may escape heat-stress by fast and intense desiccation, but its negative impact cannot be easily evaluated. The Bottom of the canopy is more sheltered from high temperatures, light and desiccation, but in very hot days may be more impacted as tissues stay hydrated and exposed to high temperatures for longer times. The importance of microhabitat was highlighted by the profound difference in desiccation levels and tissue temperature between Top and Bottom of the canopy, but the impact of sequential exposure was not revealed under mild experimental conditions.

Current efforts failed to identify protein markers regulated by desiccation stress in *Fucus* tissue, nonetheless identified a number of potentially responsive proteins and improved our knowledge on the proteomic profile of *F. vesiculosus*.

Even comparing individuals from the extremes of shore vertical distribution (and associated emersion frequency), the protein profiles of all samples were very similar, pointing to a constitutive desiccation-tolerance in this intertidal species.

7.3 – Future directions

The present work contributed to the research on desiccation tolerance mechanisms in intertidal brown algae, still many questions were left unanswered and could benefit from additional efforts. Continued work in intertidal alga, and growing number of complete protein sequences in a large set of intertidal and subtidal macroalgae will improve detection and functional characterization of proteins involved in desiccation-tolerance.

On the effect on sequential desiccation stress, additional data under more extreme conditions, and determination of the rate of desiccation might address the cost/ benefit ratio of fast desiccation. Additional manipulation of other co-occurring stressors could help elucidate individual impacts on algal metabolism and recovery. Monitoring canopy positions and frond survival during heat waves in distinct canopies could illustrate an ecological role for the distinct morphologies. In dense canopies, Bottom tissues remain hydrated, but can experience heat stress, while Top tissues desiccate quickly even in cool weather. Simultaneous growth monitoring during cumulative exposure might confirm our hypothesis that swift desiccation limits growth to hydrated periods, while sheltering is detrimental during extremely hot days. Complex canopy structure may be an optimized strategy for diverse and variable environments, where hot, cold or dry periods might impact and destroy a portion of the fronds, while another portion (from a sheltered microhabitat) recovers and may re-grow after the extreme event.